CalVal Jason

Jason-1 validation and cross calibration activities

Contract No 60453/00 - lot2.C

Reference : CLS.DOS/NT/10-332

Nomenclature : SALP-RP-MA-EA-21903-CLS

Issue : 1rev 1

Date : July 22, 2011

CLS - 8-10 Rue Hermès - Parc Technologique du Canal - 31520 Ramonville St-Agne - FRANCE
Telephone 33 5 61 39 47 00 / Fax 33 5 61 75 10 14

Chronology Issues :		
Issue :	Date :	Reason for change :
1.0	28/01/2011	Created
1.1	22/07/2011	Revision, taking into account remarks from N. Picot

People involved in this issue :				
	AUTHORS	**COMPANY**	**DATE**	**INITIALS**
Written by:	G. Valladeau S. Philipps M. Ablain	CLS CLS CLS		
Checked by:	S. Dalessio	CLS		
Approved by:	JP. Dumont M. Ablain	CLS CLS		
Application authorised by:				

Index sheet :	
Context	
Keywords	Jason-1, Calval, orbits, 59-day signal
hyperlink	

Distribution:		
Company	Means of distribution	Names
CLS/DOS	electronic copy	G.DIBARBOURE V.ROSMORDUC J.DORANDEU
CNES	electronic copy	thierry.guinle@cnes.fr nicolas.picot@cnes.fr aqgp_rs@cnes.fr dominique.chermain@cnes.fr delphine.vergnoux@cnes.fr

List of tables and figures :

List of Tables

List of Figures

List of items to be defined or to be confirmed :

Applicable documents / reference documents :

Contents

1. Introduction

This document presents the synthesis report concerning validation activities of Jason-1 GDRs under SALP contract (N° 60453/00 Lot2.C) supported by CNES at the CLS Space Oceanography Division. It is divided into several parts concerning mainly CAL/VAL Jason-1 activities, but when useful, results from Topex/Poseidon and Jason-2 are also shown for comparison.

Since the beginning of the mission, Jason-1 data have been analyzed and monitored in order to assess the quality of Jason-1 GDR products (AVISO and PODAAC User handbook, [74]) for oceanographic applications. This report is basically concerned with long-term monitoring of the Jason-1 altimeter system, from all GDR data available to date, that is for almost 9 years of data (cycles 1 to 324, corresponding to period from January 2002 to october 2010). This includes careful monitoring of all altimeter and radiometer parameters, performance assessment, geophysical evaluation and cross-calibration with T/P measurements (as long as T/P data were available). For comparison and cross-calibration with Jason-2 data, see [73]. For comparison and cross-calibration with Envisat data, see [67].

This work is routinely performed at CLS and in this frame, besides continuous analyzes in terms of altimeter data quality, Jason-1 GDR Quality Assessment Reports (e.g. Ablain et al. 2010 [11]) are produced and associated to data dissemination. Even if only low order statistics are mainly presented here, other analyzes including histograms, plots and maps are continuously produced and used in the quality assessment process.
The work performed in terms of data quality assessment also includes cross-calibration analyzes mainly with the T/P mission until November 2005 (end of the T/P mission). Even if T/P mission is finished, cross-calibration analyzes are useful for the reprocessing activities in order to study the sea state bias or the SSH bias for instance. Cross-calibration analyzes with Jason-2 are also performed, but shown in annual report of Jason-2 (see [73]).
Indeed, it is now well recognized that the usefulness of any altimeter data only makes sense in a multi-mission context, given the growing importance of scientific needs and applications, particularly for operational oceanography. One major objective of the Jason-1 mission is to continue the T/P high precision altimetry and to allow combination with other missions (ENVISAT, Jason-2). This kind of comparisons between different altimeter missions flying together provides a large number of estimations and consequently efficient long term monitoring of instrument measurements. Of course, other sources of comparisons are also needed, using independent datasets (e.g. Queffeulou et al. 2004 [77], Ray and Beckley 2003 [80], Arnault et al. 2004 [14], Provost et al. 2004 [75],Durrant et al. 2009 [38], Abdalla et al. 2010 [1]). [97] and [55] show comparisons between altimeter data and in-situ data (respectively tide gauges measurements and T/S profiles).

2. Processing status

2.1. IGDR, GDR and CAL/VAL Processing

To date, the whole mission of Jason-1 (GDR products) is available in version "c" of CMA ground processing software. The purpose of this document is to report the major features of the data quality from the Jason-1 mission. Moreover, the document is associated with comparison results from T/P GDRs. All these cycle reports are available on AVISO website: http://www.jason.oceanobs.com. In addition to these reports, several meeting (CAVE, OSTST) have been performed to inform the Jason-1 GDR's users about the main results and the studies in progress.

2.1.1. Models and Standards History

Three versions of the Jason-1 Interim Geophysical Data Records (IGDRs) and Geophysical Data Records (GDRs) have been generated to date. These three versions are identified by the version numbers "a", "b" and "c" in the name of the data products. For example, version "a" GDRs are named "JA1_GDR_2Pa", version "b" GDRs are named "JA1_GDR_2Pb", and version "c" GDRs are named "JA1_GDR_2Pc". All versions adopt an identical data record format as described in Jason-1 User Handbook and differ only in the models and standards that they adopt. Version "a" I/GDRs were the first version released soon after launch. Version "b" I/GDRs were first implemented operationally from the start of cycle 140 for the IGDRs and cycle 136 for the GDRs. Reprocessing to generate version "b" GDRs for cycles 1-135 were performed in 2006 and 2007 in order to generate a consistent data set. Version "c" I/GDRs were first operationally implemented from mid cycle 237 for the IGDRs and cycle 233 for the GDRs. Reprocessing to generate version "c" GDRs for cycles 1-232 were performed from June 2008 to January 2010 in order to generate a consistent data set. Table 1 below summarizes the models and standards that are adopted in these three versions of the Jason-1 I/GDRs. More details on some of these models are provided in Jason-1 User Handbook document ([74]).

Model	Product Version "a"	Product Version "b"	Product Version "c"
Orbit	JGM3 Gravity Field	EIGEN-CG03C Gravity Field	EIGEN-GL04S with time-varying gravity
	DORIS tracking data for IGDRs	DORIS tracking data for IGDRs	DORIS tracking data for IGDRs
	DORIS+SLR tracking data for GDRs	DORIS+SLR+GPS tracking data for GDRs	DORIS+SLR+GPS tracking data for GDRs with increased weight of D/L
.../...			

Model	Product Version "a"	Product Version "b"	Product Version "c"
Altimeter Retracking	MLE3 + 1st order Brown model (mispointing estimated separately)	MLE4 + 2nd order Brown model : MLE4 simultaneously retrieves the 4 parameters that can be inverted from the altimeter waveforms: epoch, SWH, Sigma0 and mispointing angle. This algorithm is more robust for large off-nadir angles (up to 0.8°).	Identical to version "b"
Altimeter Instrument Corrections	Consistent with MLE3 retracking algorithm.	Consistent with MLE4 retracking algorithm.	Identical to version "b". A new correction is available in the product to account for the apparent datation bias (field 28). Users are advised to add this correction to the Ku-band altimeter range, as it is not a component of the net instrument correction that has already been applied to the provided Ku-band range
Jason Microwave Radiometer Parameters	Using calibration parameters derived from cycles 1-30.	Using calibration parameters derived from cycles 1-115.	Using calibration parameters derived from cycles 1-227
Dry Troposphere Range Correction	From ECMWF atmospheric pressures.	From ECMWF atmospheric pressures and model for S1 and S2 atmospheric tides.	From ECMWF atmospheric pressures and model for S1 and S2 atmospheric tides. Uses new ECMWF delivery to correct for spurious oscillation effects.
Wet Troposphere Range Correction from Model	From ECMWF model	From ECMWF model.	Identical to version "b"
			.../...

Model	Product Version "a"	Product Version "b"	Product Version "c"
Back up model for Ku-band ionospheric range correction.	Derived from DORIS measurements.	Derived from DORIS measurements.	Derived from JPL's Global Ionosphere Model (GIM) maps
Sea State Bias Model	Empirical model derived from cycles 19-30 of version "a" data.	Empirical model derived from cycles 11-100 of MLE3 altimeter data with version "b" geophysical models.	Empirical model derived from cycles 11-100 of MLE4 altimeter data with version "c" geophysical models"
Mean Sea Surface Model	GSFC00.1	CLS01	Identical to version "b"
Along Track Mean Sea Surface Model	None (set to default)	None (set to default)	None (set to default)
Geoid	EGM96	EGM96	Identical to version "b"
Bathymetry Model	DTM2000.1	DTM2000.1	Identical to version "b"
Mean Dynamic Topography	None (was a spare)	None (was a spare)	Rio 2005 solution
Inverse Barometer Correction	Computed from ECMWF atmospheric pressures	Computed from ECMWF atmospheric pressures after removing model for S1 and S2 atmospheric tides.	Identical to Version "b" but using new ECMWF delivery to correct for spurious oscillation effects
Non-tidal High-frequency De-aliasing Correction	None (set to default)	Mog2D ocean model on GDRs, none (set to default) on IGDRs. Ocean model forced by ECMWF atmospheric pressures after removing model for S1 and S2 atmospheric tides.	High resolution Mog2D model for both IGDR and GDR products
Tide Solution 1	GOT99	GOT00.2 + S1 ocean tide . S1 load tide ignored.	Identical to version "b"
Tide Solution 2	FES99	FES2004 + S1 and M4 ocean tides. S1 and M4 load tides ignored.	FES2004 + S1 and M4 ocean tides. S1, K2 and loading tides have been updated
			.../...

Model	Product Version "a"	Product Version "b"	Product Version "c"
Equilibrium long-period ocean tide model.	From Cartwright and Taylor tidal potential.	From Cartwright and Taylor tidal potential.	Identical to version "b"
Non-equilibrium long-period ocean tide model.	None (set to default)	Mm, Mf, Mtm, and Msqm from FES2004.	Identical to version "b"
Solid Earth Tide Model	From Cartwright and Taylor tidal potential.	From Cartwright and Taylor tidal potential.	Identical to version "b"
Pole Tide Model	Equilibrium model	Equilibrium model.	Identical to version "b"
Wind Speed from Model	ECMWF model	ECMWF model	Identical to version "b"
Altimeter Wind Speed	Table derived from TOPEX/POSEIDON data.	Table derived from version "a" Jason-1 GDR data.	Identical to version "b"
Rain Flag	Derived from TOPEX/POSEIDON data.	Derived from version "a" Jason-1 GDRs.	Derived from version "b" Jason-1 GDRs using the AGC instead of sigma naught values
Ice Flag	Climatology table	Climatology table	New flag based on the comparison of the model wet tropospheric correction and of a radiometer bi frequency wet tropospheric correction (derived from 23.8 GHz and 34.0 GHz), accounting for a backup solution based on climatologic estimates of the latitudinal boundary of the ice shelf, and from altimeter wind speed.

Table 1: *M*odels and standards adopted for the Jason-1 product version "a", "b", and "c"

2.1.2. Differences in editing procedure for the different GDR product versions

For GDR version "c" the same editing criteria and thresholds like in GDR version "b" should be used. Since GDR version "b" the MLE4 retracking algorithm is used. It is based on a second-order altimeter echo model and is more robust for large off-nadir angles (up to 0.8 degrees). For product version "a" (CMA version 6.3), the maximum threshold on square off-nadir angle proposed in Jason-1 User Handbook document was set to 0.16 deg^2. Since GDR version "b", this threshold is too restrictive and has to be set to 0.64 deg^2.

However, this editing criteria had the side effect of removing some bad measurements impacted by rain cells, sigma0 blooms or ice. With the new threshold (0.64 deg^2), these measurements are not rejected anymore.

2.1.3. Impact of product versions

The main changes between GDRs version "a" and "b" were the new orbit, the retracking of the wave forms with MLE4 algorithm, and new geophysical corrections. This had not only an impact on editing procedure, but also on crossover performances. For version "c", the main changes are the new orbit, new JMR calibration and new sea state bias. For information concerning reprocessing in version "b", please refer to [71] or [7]. Concerning reprocessing in version "c", please refer to [26] or [98].

2.2. CAL/VAL status

2.2.1. Missing measurements

This section presents a summary of major satellite events that occurred from cycle 1 to 324. Table 2 gives a status about the number of missing passes (or partly missing) for GDRs version "c" and the associated events for each cycle.
Gyro calibration, Star Tracker unavailability and ground processing issues were the main events which produced missing data from cycle 1 to 64 (2002 and 2003).
During year 2004 (cycle 65 to 109), 2 safe hold mode incidents have produced 15 days of missing data due to a wheel anomaly. As result of this incident, only 3 wheels have been available but this has had no impact on scientific applications.
During year 2005 (110-146), most of incidents are due to SEU. The altimeter was reinitializied automatically without C-band. Few passes have only been impacted each time, and they are rejected because of the lack of C-band data, and therefore lack of dual-frequency ionospheric correction.
During year 2006 (cycles 147 - 183) Jason-1 experienced a safe hold mode (cycle 177 to 179) producing 17 days of missing data due to mass memory error. In addition 2 altimeter SEU occurred. It also happened that small data gaps occur (less than one minute duration).
During 2007 (cycles 183 to 220) Jason-1 had experienced several altimeter SEU. In 2008 (cycles 221 to 256), there were two major events : the altimeter switch-off in May, due to the close encounter with drifting TOPEX/Poseidon, and a safehold mode in August.
During 2009 (cycles 257 to 293), Jason-1 was moved from its original groundtrack to its new interleaved groundtrack from 26th January to 14th February 2009. During most of this time, no altimeter or radiometer data is available. Furthermore, the satellite experienced a safehold mode in September 2009 producing 10 days of missing data.
During 2010 (cycles 294 to 324) Jason-1 was particularly impacted by degraded performances of its Star Trackers and Gyro wheels, especially when the satellite is in yaw fix mode. This lead to high mispointing, which caused sometimes altimeter lost of track and altimeter incidences. To avoid the possibility of a spacecraft safe hold, Jason-1 swaped on 14th of April 2010 from Gyro wheel 1 to redundant Gyro wheel 3. Furthermore, during cycle 315 (July 2010), Jason-1 performed several out of plane maneuvers in order to deplete fuel (to reduce risk of explosion in case of loss of control). Groundtrack departed up to 7 km from nominal groundtrack. For further information of events occured during 2010 see also section 8.4.

Jason-1 Cycles	Number of completely missing passes	Number of partly missing passes	Events
001	2	7	Science telemetry unavailability
002	14	3	On board Doris anomaly
003	0	2	Gyro-calibration
004	2	5	Gyro-calibration and Science telemetry unavailability
			.../...

Jason-1 Cycles	Number of completely missing passes	Number of partly missing passes	Events
006	1	4	Altimeter echo data unavailability
007	0	2	Science telemetry unavailability
008	2	5	Ground processing issue
009	3	4	Poseidon-2 altimeter SEU and Gyro-calibration
010	0	2	Gyro-calibration
015	0	1	Ground processing issue
019	0	1	Ground processing issue
021	0	1	Star tracker unavailability
023	0	1	Ground processing issue
026	0	2	Gyro-calibration
027	0	2	Gyro-calibration
031	0	1	Star tracker unavailability
038	0	4	Ground processing issue
039	0	1	Gyro-calibration
042	5	2	Poseidon-2 altimeter SEU
045	0	3	Gyro-calibration
046	0	1	Poseidon-2 altimeter SEU
048	0	1	Gyro-calibration
062	0	1	Ground processing issue
064	0	2	Exceptional calibrations
075	4	0	Poseidon-2 altimeter SEU
077	69	0	Safe hold mode (15/02/04 to 21/02/04)
078	82	0	Safe hold mode (15/02/04 to 21/02/04)
080	0	1	Calibration over ocean
082	54	1	Failure in module 3 of PLTM2
087	0	1	Calibration over ocean
			.../...

Jason-1 Cycles	Number of completely missing passes	Number of partly missing passes	Events
091	2	4	DORIS instrument switch to redundancy and altimeter incident (no C band information)
094	0	1	Altimeter incident or star tracker unavailability
099	0	1	Altimeter incident or star tracker unavailability
101	0	1	Altimeter incident or star tracker unavailability
102	1	0	Altimeter SEU (no C band information)
103	0	2	Altimeter SEU (no C band information)
104	0	1	No data between 21:29:18 and 21:30:07 on November 8th pass 189
106	3	2	Altimeter SEU (no C band information)
108	0	2	Altimeter SEU (no C band information)
114	3	1	Altimeter SEU (no C band information)
115	0	4	2 altimeter SEU incidents (C band) and altimeter initialization procedure.
118	6	2	Altimeter SEU (no C band information)
131	0	7	TRSR2 "elephant packets" anomaly
132	0	1	Altimeter SEU (no C band information)
133	0	2	Altimeter SEU (no C band information)
136	104	2	Altimeter SEU (no C band information), Platform incident (20/09/05 to 28/09/05)
			.../...

Jason-1 Cycles	Number of completely missing passes	Number of partly missing passes	Events
137	91	2	Platform incident (20/09/05 to 28/09/05)
161	0	5	TRSR elephant packets
165	0	1	(planned) Poseidon calibration (board filter)
173	0	3	Altimeter SEU (no C band information)
177	141	1	Safehold mode (30/10/2006 to 16/11/2006)
178	254	0	Safehold mode (30/10/2006 to 16/11/2006)
179	45	1	Safehold mode (30/10/2006 to 16/11/2006)
181	5	2	Altimeter SEU
185	0	3	calibration over ocean
191	0	2	Altimeter SEU
192	0	1	calibration over ocean
198	1	1	Altimeter SEU
200	0	3	calibration over ocean
206	0	2	Altimeter SEU
219	2	0	Missing telemetry
222	0	2	calibrations over ocean
231	0	1	erroneous command sent by JTCCS
233	142	2	altimeter switch off (TP/J1 close encounter)
234	0	1	calibration
242	84	1	safehold mode
243	254	0	safehold mode
254	1	1	Altimeter SEU
260	254	0	Jason-1 moves to its new interleaved ground-track
			.../...

Jason-1 Cycles	Number of completely missing passes	Number of partly missing passes	Events
261	254	0	Jason-1 moves to its new interleaved ground-track
262	12	4	Jason-1 moves to its new interleaved ground-track + calibrations over ocean
263	0	4	calibrations over ocean
276	0	2	calibrations over ocean
283	26	1	safehold mode (2009-09-15 to 2009-09-24)
284	233	0	safehold mode (2009-09-15 to 2009-09-24)
290	0	2	Altimeter SEU
301	0	3	Altimeter SEU + restart
304	0	42	Due to on-orbit degradation of star trackers and gyro wheel performances, altimeter lost track
305	0	5	Due to on-orbit degradation of star trackers and gyro wheel performances, altimeter lost track
		2	calibrations over ocean
306	0	3	Altimeter SEU + restart
310	39	53	Due to on-orbit degradation of star trackers performances, altimeter lost track + altimeter incidents + reinits
312	0	3	Altimeter SEU + restart
315	12	28	Due to on-orbit degradation of star trackers performances, altimeter lost track + altimeter incidents
316	0	5	calibrations + missing PLTM (probably linked to high mispointing)
318	0	2	calibrations over ocean
319	1	2	calibrations over ocean
324	0	2	calibrations over ocean
			.../...

Jason-1 Cycles	Number of completely missing passes	Number of partly missing passes	Events

Table 2: *M*issing pass status

2.2.2. Edited measurements

Table 3 indicates the cycles which have a larger amount of removed data due to editing criteria (see section 3.2.1.). Most of the occurrences correspond to dual-frequency ionospheric correction at default value (altimeter SEU) or missing radiometer wet troposphere correction (following safehold modes).
Notice that since cycle 78, the satellite operates with only 3 wheels: the maneuver impact (burn maneuver, yaw transition) is greater than before on the attitude control. Consequently, some measurements could be edited due to higher mispointing values when a maneuver occurs, until improvements in ground retracking algorithm have been set up and applied since the GDR "b" release, and improvements on Star Tracker behaviour have been performed in 2006. Therefore only few measurements were edited by mispointing criterion.
Following Star Tracker and Gyro wheel performance degradation combined with bad beta angle environment, Jason-1 experienced high mispointing for several cycles in 2010, leading in some cases to edited measurements or even altimeter loss of tracking. This is described in more details in section 8.4..

Jason-1 Cycles	Comments
001	Passes 252 to 254 are edited due to radiometer wet troposphere correction at default value.
006	Pass 56 (in the Pacific ocean) is partly edited due to the bad quality of data. Indeed, the altimetric parameters values are out of the thresholds.
008	All the altimetric parameters are edited for 10% of pass 252 due to the bad quality of all the altimetric parameters as a result of a Star Tracker incident leading to a quite high off nadir angle.
009	Passes 004 and 005 partly edited by dual-ionospheric correction at default value (no c-band information).
021	Small part of pass 210 is edited after checking the square of the mispointing angle criterion.
069	Passes 209 to 211 are edited due to the radiometer wet troposphere correction at default value. This is linked to the safe hold mode on cycle 69 : the JMR has been set on 2 hours after the altimeter.
078	Passes 83 to 85 are edited due to the radiometer wet troposphere correction at default value. This is linked to the safe hold mode on cycle 88 : the JMR has been set on 2 hours after the altimeter.
	.../...

Jason-1 Cycles	Comments
091	Passes 126, 127 and partly 130 are edited by dual-ionospheric correction at default value (no c-band information).
102	Passes 187, 188 and partly 189 are edited by dual-ionospheric correction at default value (no c-band information).
103	Passes 29 to 31 are edited by dual-ionospheric correction at default value (no c-band information).
108	Passes 16 and 17, as well as part of passes 15 and 18 are edited by dual-ionospheric correction at default value (no c-band information).
115	Passes 19 to 21 and 29 to 31 are edited by dual-ionospheric correction at default value (no c-band information).
133	Pass 13 is partly edited due to dual-ionospheric correction at default value (no c-band information).
137	Passes 92, 93 and partly 94 are edited by radiometer wet tropospheric correction, since the radiometer was later switched on than the other instruments.
173	Due to an altimeter upset (no c-band information), the dual-frequency ionospheric correction is partially missing for passes 65 and 68 and fully for passes 66 and 67.
175	Pass 9 is partly edited by mispointing criterion out of threshold (probably aberrant quaternion).
179	As radiometer was only switch on later, passes 046 to 058, as well as part of pass 059 are edited by radiometer wet troposphere correction at default values.
181	Pass 247 is partly edited by dual-frequency ionosphere at default value (no C-band information).
198	Pass 073 is partly edited by dual-frequency ionosphere at default value (no C-band information).
212	Pass 187 is entirely edited: one half by altimetric parameters at default value, other half by apparent squared mispointing values out of thresholds. Pass 186 is partly edited by apparent squared mispointing values out of thresholds.
220	Pass 189 is partly edited by altimetric parameters at default value.
224	Passes 30 and 163 are partly edited by altimetric parameters at default value. Just before and after these parts, they are edited by outbounded apparent squared mispointing values.
	.../...

Jason-1 Cycles	Comments
256	On passes 003 and 111 a portion is edited by several altimetric parameters at default value due to high mispointing (probably related to maneuver burn and yaw flip).
262	Passes 116 to 120 are completely edited by SLA out of thresholds (related to the last orbit change maneuvers).
279	On passes 241 and 242 a portion is edited by several altimetric parameters at default value due to high mispointing (probably related to yaw flip maneuver).
284	As radiometer was only switch on later after safehold, passes 234 to 236, as well as part of pass 237 are edited by radiometer wet troposphere correction at default values.
292	Pass 137 is partially edited by apparent squared mispointing out of threshold (related to Yaw flip maneuver).
301	Following altimeter reinit on 2010-03-04 at 04:40, though measurements are available since 04:53:11, they are edited till 07:03:27 as due to high off-nadir angles all altimeter parameters are at default values (passes 007, 008 and most of pass 009).
304	Due to high off-nadir angles, several passes are partly edited as altimeter parameters are at default values or mispointing are out of thresholds.
305	Due to high off-nadir angles, several passes are partly edited as altimeter parameters are at default values or mispointing are out of thresholds.
306	Following both altimeter reinit on 2010-04-26 at 09:57:03 and 11:22:13, though measurements are available since 10:00:49, they are edited till 11:43:09 as all altimeter parameters are at default values (passes 100, 101 and part of pass 102 over North America).
310	Apparent squared mispointing is very high for passes 62 to 216 (period between yaw flip and yaw ramp), leading to edited (altimeter parameters at default values) or missing measurements on many passes during this period .
312	Following altimeter reinit on 2010-06-28 at 17:03:26, though measurements are available since 17:07:00, they are edited till 17:27:42 as all altimeter parameters are at default values (pass 198 over North Atlantic).
315	Several passes are completely edited by SLA out of thresholds (2,27,29,54,57,182,183) or SLA pass statistics out of thresholds (3,4,28,53,55,136,160). Furthermore several passes are partly edited by SLA out of threshold. This is caused by the maneuvers. Several passes are completely (123,151,178,191,198,204,221,230,233) and several partly edited by altimeter parameters at default values. This is causes by high mispointing (too high for MLE4 algorithm).
	.../...

Jason-1 Cycles	Comments
	Passes 177 and 178 are partly edited by radiometer wet troposphere correction at default value.
316	Part of pass 1 is edited by the square of the off-nadir angle. Several part of passes (2, 3, 8, 10, 12, and 217) are edited as altimetric parameters are at default value (degraded star tracker performances).

Table 3: *E*dited measurement status

3. Data coverage and edited measurements

3.1. Missing measurements

3.1.1. Over ocean

Determination of missing measurements relative to the theoretically expected orbit ground pattern is used to detect missing telemetry in Jason-1 datasets due to altimetry events for instance. This procedure is applied cycle per cycle and leads to results plotted on the left figure 1. It represents the percentage of missing measurements relative to the theory, when limited to ocean surfaces. The mean value is about 3.8% but this figure is not significant due to several events where the measurements are missing. All these events are described on table 2. Moreover, events which occured during 2010 are also indicated by colored lines and stripes on bottom part of figure 1.
On figure 1 on the right, the percentage of missing measurements is plotted without taking into account the cycles where instrumental events or other anomalies occurred. Moreover shallow waters and high latitudes have been removed. This allows us to detect small data gaps in open ocean. The mean value is about 0.03%. This weak percentage of missing measurements is mainly explained by the rain cells, ice sea or sigma0 blooms. These sea states can disturb significantly the Ku band waveform shape leading to a non significant measure.
Another reason for these small data gaps in open ocean are datation gaps, which occur occasionally.

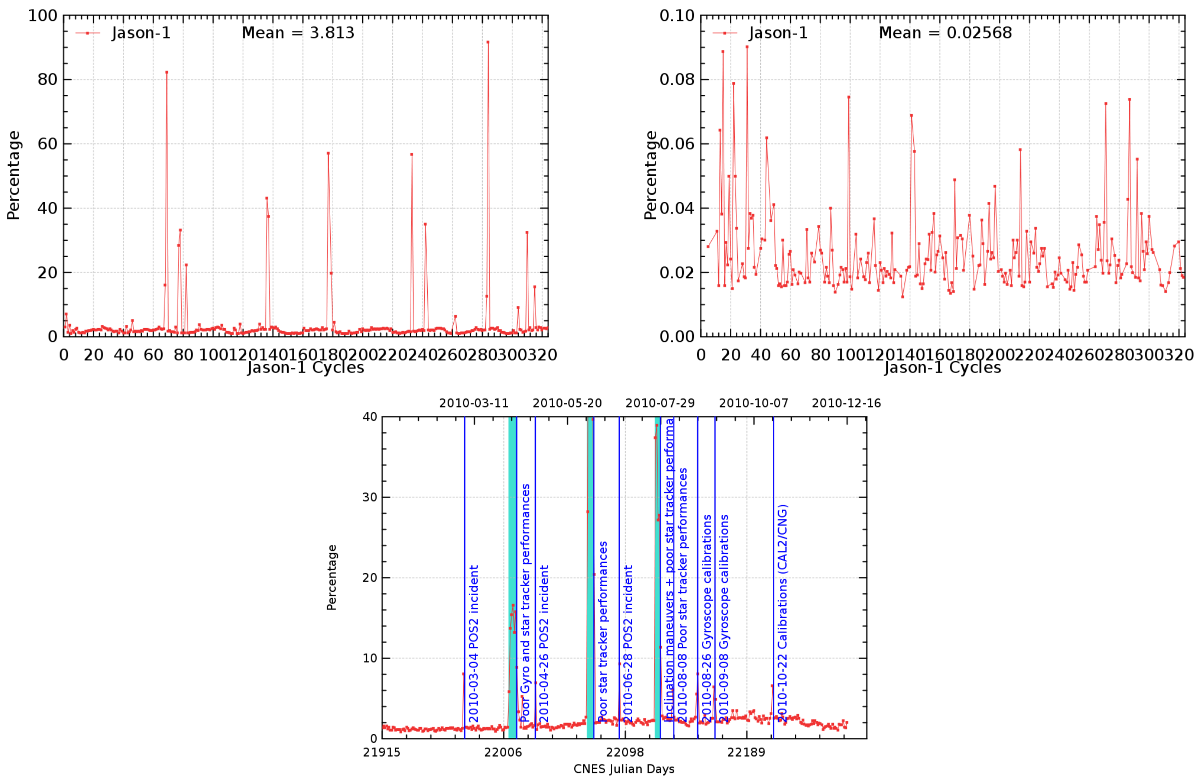

Figure 1: *Percentage of missing measurements over ocean on cyclic basis over the whole mission period (top) and on a daily basis for 2010 (bottom).*

3.1.2. Over land and ocean

Figure 2 shows the percentage of missing measurements for Jason-1 and T/P (all surfaces) computed with respect to a theoretical possible number of measurements. Due to differences between tracker algorithms, the number of data is greater for T/P (excepted when T/P experienced problems, especially since the tape recorders were no longer in service (T/P cycle 444, Jason-1 cycle 101)) than for Jason-1. Differences appear on land surfaces as shown in figure 3.

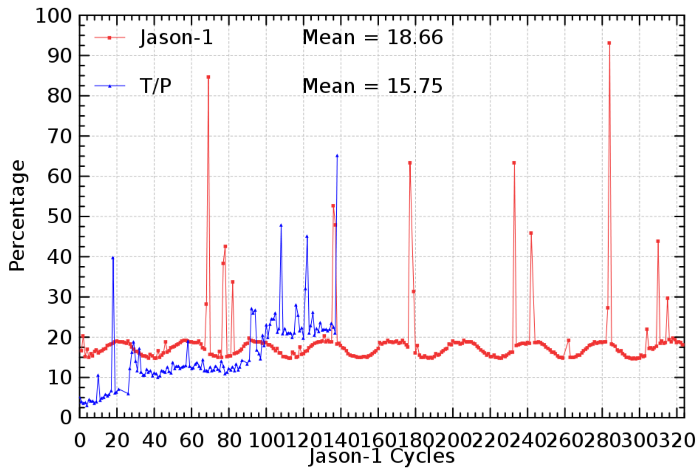

Figure 2: *Percentage of missing measurements over ocean and land for J1 and T/P*

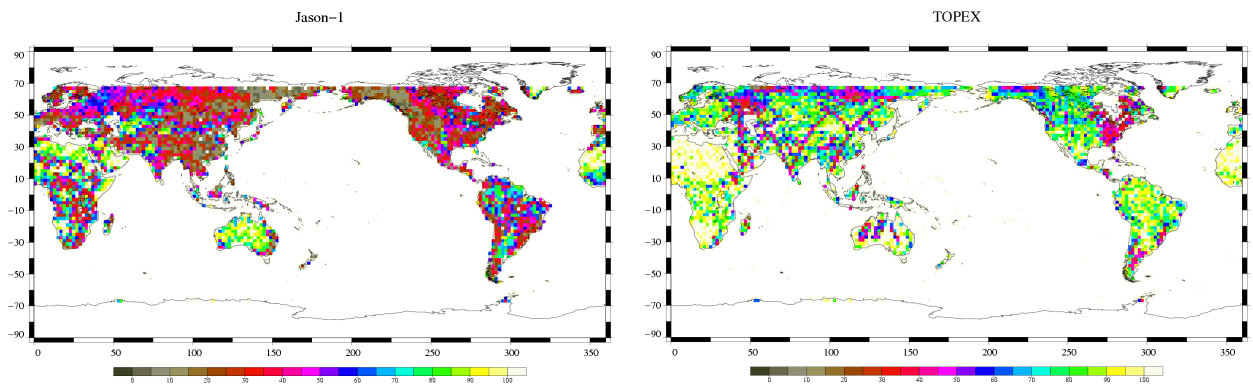

Figure 3: *Map of percentage of available measurements over land for Jason-1 on cycle 61 (left) and for TOPEX on cycle 404 (right)*

3.2. Edited measurements

3.2.1. Editing criteria definition

Editing criteria are used to select valid measurements over ocean. The editing process is divided into 4 parts. First, only measurements over ocean and lakes are kept (see section 3.2.2.). Second, the quality criteria concern the flags which are described in section 3.2.3. and 3.2.4. Then, threshold criteria are applied on altimeter, radiometer and geophysical parameters and are described in table 4. Moreover, a spline criterion is applied to remove the remaining spurious data. These criteria are also defined in AVISO and PODAAC User handbook. For each criterion, the cycle per cycle percentage of edited measurements has been monitored. This allows detection of anomalies in the number of removed data, which could come from instrumental, geophysical or algorithmic changes.

Parameter	Min thresholds	Max thresholds	mean edited
Sea surface height	$-130\,m$	$100\,m$	0.95%
Sea level anomaly	$-10\,m$	$10.0\,m$	1.21%
Number measurements of range	10	*Not applicable*	1.31%
Standard deviation of range	$0\,m$	$0.2\,m$	1.49%
Square off-nadir angle	$-0.2\,deg2$	$0.64\,deg2$	0.69%
Dry troposphere correction	$-2.5\,m$	$-1.9\,m$	0.00%
Inverted barometer correction	$-2.0\,m$	$2.0\,m$	0.00%
JMR wet troposphere correction	$-0.5m$	$-0.001\,m$	0.15%
Ionosphere correction	$-0.4\,m$	$0.04\,m$	1.28%
Significant waveheight	$0.0\,m$	$11.0\,m$	0.72%
Sea State Bias	$-0.5\,m$	$0.0\,m$	0.64%
Number measurements of Ku-band Sigma0	10	*Not applicable*	1.30%
Standard deviation of Ku-band Sigma0	$0\,dB$	$1.0\,dB$	1.82%
Ku-band Sigma0 [1]	$7.0\,dB$	$30.0\,dB$	0.68%
Ocean tide	$-5.0\,m$	$5.0\,m$	0.06%
Equilibrium tide	$-0.5\,m$	$0.5\,m$	0.00%
Earth tide	$-1.0\,m$	$1.0\,m$	0.00%
Pole tide	$-15.0\,m$	$15.0\,m$	0.00%
			.../...

Parameter	Min thresholds	Max thresholds	mean edited
Altimeter wind speed	$0\ m.s^{-1}$	$30.0\ m.s^{-1}$	1.09%
All together	-	-	3.23%

Table 4: *E*diting criteria

3.2.2. Selection of measurements over ocean and lakes

In order to remove data over land, a land-water mask is used. Only measurements over ocean or lakes are kept. Indeed, this allows us to keep more data near the coasts and then detecting potential anomalies in these areas. Furthermore, there is no impact on global performance estimates since the most significant results are derived from analyzes in deep ocean areas. Figure 4 (left) displays the cycle per cycle percentage of measurements eliminated by this selection. It shows a seasonal signal which is due to the varying number of measurements available in the GDRs and varies not only over ocean but also over land. After removing the annual signal, there is no trend noticeable (see figure 4 (right)).

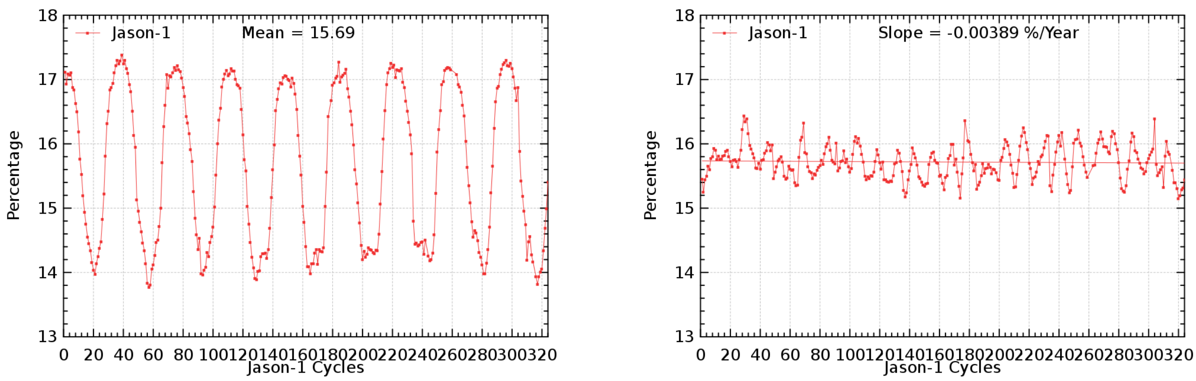

Figure 4: *Cycle per cycle percentage of eliminated measurements during selection of ocean/lake measurements (left). Trend of eliminated measurements after removing annual signal (right).*

[1]The thresholds used for the Ku-band Sigma0 are the same than for T/P, but the sigma0 bias between Jason-1 and T/P (about 2.4 dB) is applied.

3.2.3. Flagging quality criteria: Ice flag

The ice flag is used to remove the sea ice data. Figure 5 shows the cycle per cycle percentage of measurements edited by this criterion. No anomalous trend is detected (figure 5 right) but an annual cycle is visible. Indeed, the maximum number of points over ice is reached during the northern fall. As Jason-1 takes measurements between 66° north and south, it does not detect thawing of sea ice (due to global warming), which takes place especially in northern hemisphere beyond 66°N. For some cycles (304, 310 and 315), the percentage of edited edited measurements by ice flag is increased. This is not related to real sea ice. It is related to high mispointing (number of elementary range measurements used in computation of ice flag is zero due to high mispointing). The ice flag edited measurements are plotted in Figure 6 for one cycle.

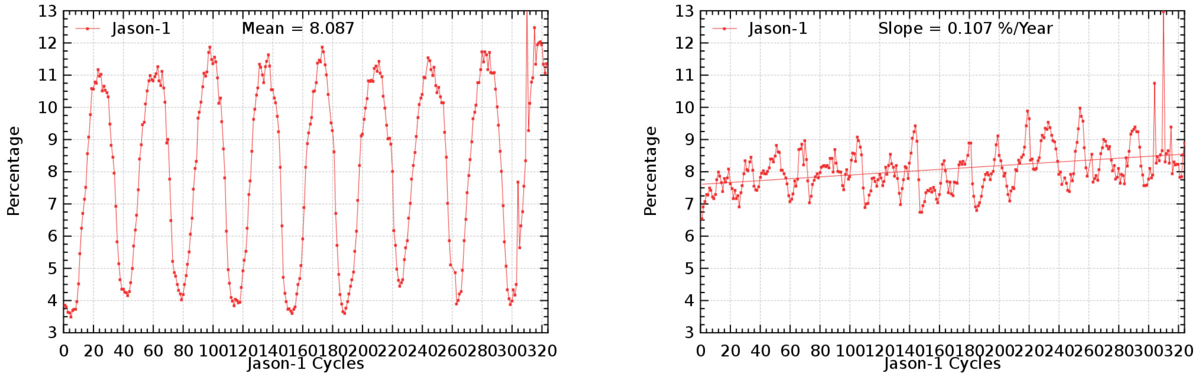

Figure 5: *Cycle per cycle percentage of edited measurements by ice flag criterion (left), after subtracting annual signal (right).*

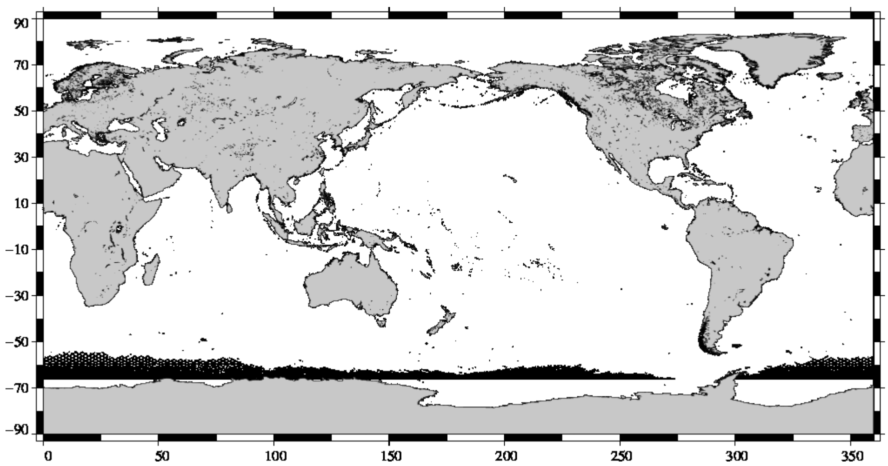

Figure 6: *Map of edited measurements by ice flag criterion on cycle 324*

3.2.4. Flagging quality criteria: Rain flag

The rain flag is not used for data selection since it is quite restrictive. It is thus recommended not to be used by users. The rain flag has changed in version "c", making it even more restrictive. The percentage of rain edited measurements is plotted in figure 7 over cycles 276 to 313 (covering 12 month). It shows that measurements are especially edited near coasts, but also in the equatorial zone and open ocean. The rain flag seems to be too strict, using it would lead to editing 9.3% of additional measurements.

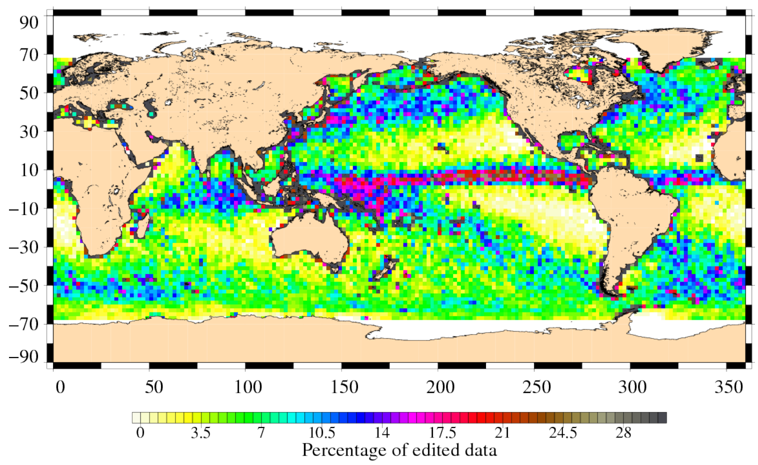

Figure 7: *Map of percentage of edited measurements by rain flag criterion over a 12-month period (cycles 276 to 313).*

3.2.5. Threshold criteria: Global

Instrumental and geophysical parameters have also been analyzed from comparison with thresholds, after selecting only ocean/lake measurements and applying flagging quality criteria (ice flag). Note that no measurements are edited by threshold criteria on the following corrections : dry troposphere correction, inverted barometer correction, equilibrium tide, earth and pole tide, which are all model corrections. Indeed these parameters are only verified in order to detect data at default values, which might happen during a processing anomaly.

The percentage of measurements edited by each criterion has been monitored on a cycle per cycle basis (figure 8). The mean percentage of edited measurements is about 3.2%. An annual cycle is visible due to the seasonal sea ice coverage in the northern hemisphere. Indeed most of northern hemisphere coasts are without ice during its summer. Consequently some of these coastal measurements are edited by the thresholds criteria in summer instead of the ice flag in winter. This seasonal effect visible in the statistics is not balanced by the southern hemisphere coasts due to the shore distribution between both hemispheres.
Note that for some cycles, especially cycles 69, 179 and 284, the percentage of edited measurements is higher than usual. This is mostly due to the lack of radiometer wet troposphere correction, as after safehold modes radiometer is usually swichted on some time after the altimeter, see also section 3.2.10.
For cycles 304, 310 and 315, edited measurements are partly due to mispointing out of thresholds. As during 2010 squared off-nadir angle got for several cycles very high, MLE4 retracking could sometimes no longer retrieve altimeter parameters, they are therefore at default value and edited (see also section 8.4.). In the following sections, all altimeter parameters show an increased percentage of edited measurements for the period of cycles 304 to 316, and especially for cycles 304, 310 and 315.

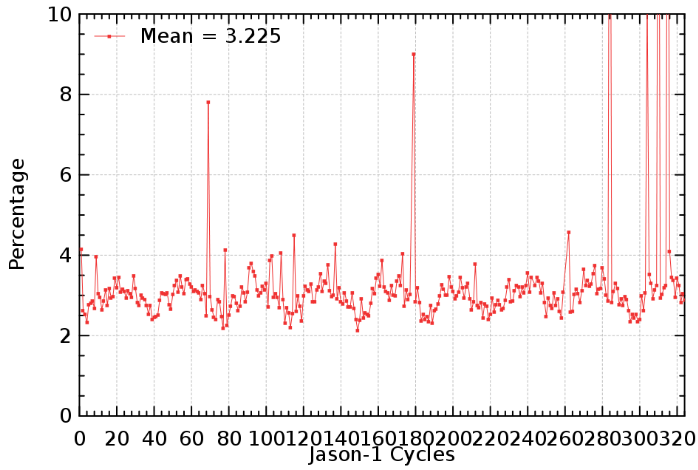

Figure 8: *Cycle per cycle percentage of edited measurements by threshold criteria*

3.2.6. Threshold criteria: 20-Hz measurements number

The percentage of edited measurements because of a too low number of 20-Hz measurements is represented on left side of figure 9. Neither a trend nor any anomaly has been detected, except for cycle 212 and period between cycles 304 and 315.
Indeed during cycle 212, about half of a pass had all altimetric parameters set at default values, due to satellite off-pointing, avoiding the retrieval of altimetric parameters. During 304 to 316, several portions of passes were concerned.

The map of measurements edited by the 20-Hz measurements number criterion is plotted on the right panel of figure 9 and shows correlation with heavy rain, wet areas as well as coastal regions. Indeed the waveforms are distorted by rain cells, which makes them often unexploitable for SSH calculation. In consequence edited measurements due to several altimetric criteria are often correlated with wet areas. Furthermore the sections of passes with altimeter parameters at default values due to very high mispointing are noticeable.

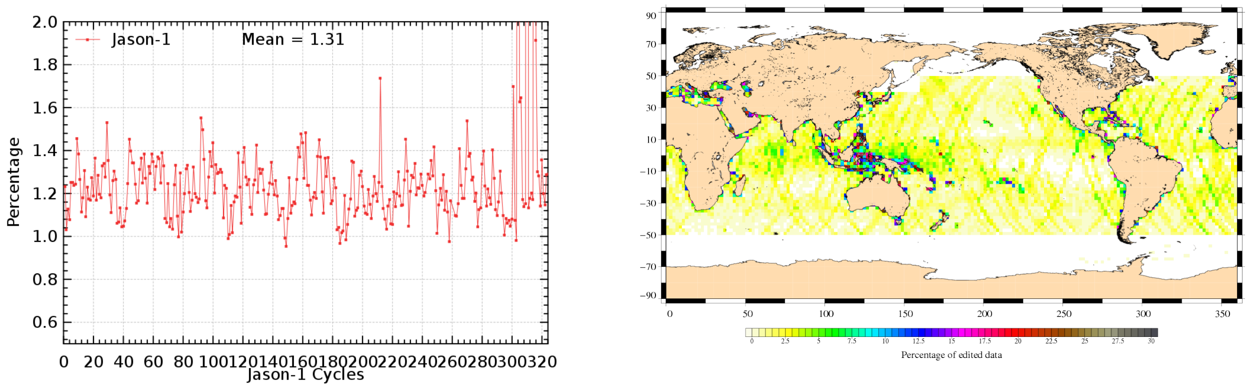

Figure 9: *Cycle per cycle percentage of edited measurements by 20-Hz measurements number criterion (left). Right: Map of percentage of edited measurements by 20-Hz measurements number criterion over an one-year period (cycles 276 to 313).*

3.2.7. Threshold criteria: 20-Hz measurements standard deviation

The percentage of edited measurements due to 20-Hz measurements standard deviation criterion is shown in figure 10. The observed annual signal (left) is linked to the seasonal variability associated with ice coverage. After removing the annual signal and not taking into account cycles which were impacted by very high mispointing (figure 10 right), no trend is visible.

Figure 11 shows a map of measurements edited by the 20-Hz measurements standard deviation criterion. Besides editing due to measurements at default value (see 8.4.), edited measurements are mainly correlated with wet areas.

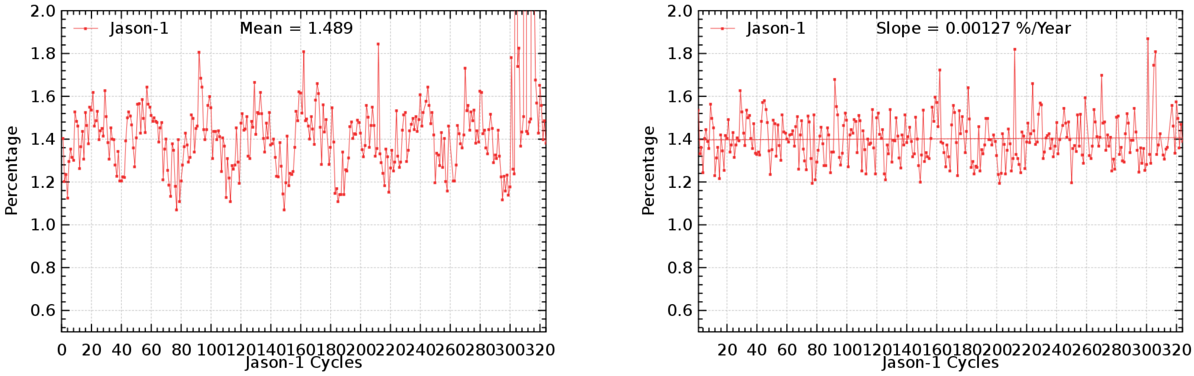

Figure 10: *Cycle per cycle percentage of edited measurements by 20-Hz measurements standard deviation criterion (left); after removing annual signal (right).*

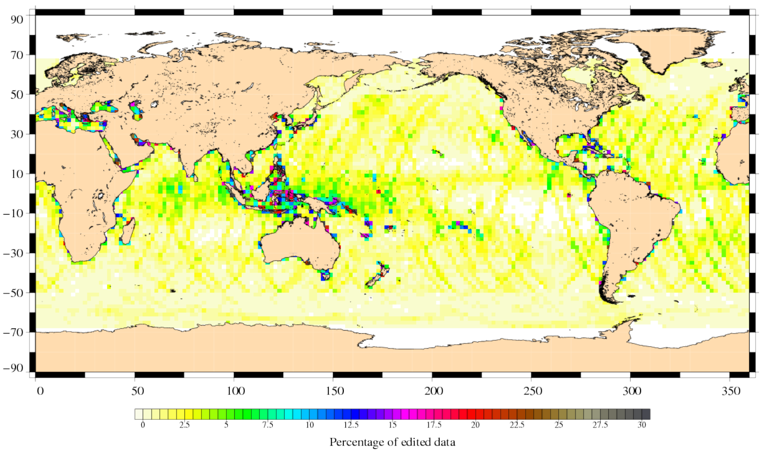

Figure 11: *Map of percentage of edited measurements by 20-Hz measurements standard deviation criterion over an one-year period (cycles 276 to 313).*

3.2.8. Threshold criteria: Significant wave height

The percentage of edited measurements due to significant wave height criterion is represented in figure 12. It is about 0.72%. No drift has been detected over the Jason-1 period. Peaks visible for cyles 304 to 316 are due to altimeter parameters at default values caused by very high mispointing (see section 8.4.). Smaller peaks visible for cycles 212 and 224 are also due to a portion of a pass at default values. The effect is barely visible on the global rejected measurements figure 8 for cycle 212, and unseen for cycle 224, because of the weak impact of the SWH criterion with regard to the global rejection criteria. Figure 12 (right part) shows that measurements edited by SWH criterion are especially found near coasts in the equatorial regions.

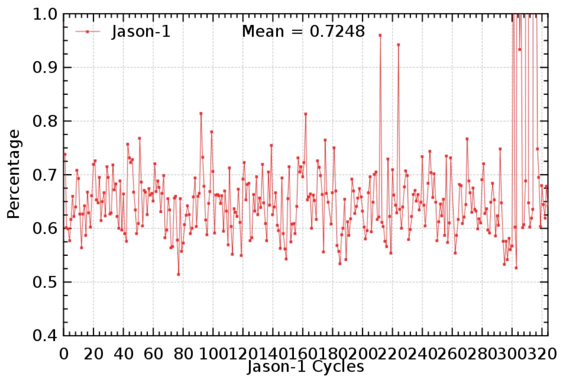

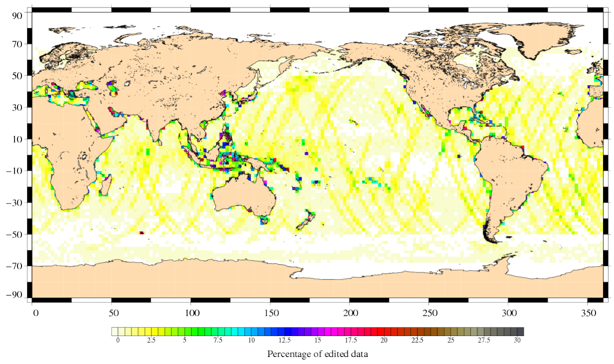

Figure 12: *Left: Cycle per cycle percentage of edited measurements by SWH criterion. Right: Map of percentage of edited measurements by SWH criterion over an one-year period (cycles 276 to 313).*

3.2.9. Backscatter coefficient

The percentage of edited measurements due to backscatter coefficient criterion is represented in figure 13. It is about 0.68% and shows no drift. The peaks visible for cycles 212 and 224 are due to a portion of a pass at default values. This is also the case for the peaks of cycles 304 to 316 (see section 8.4.). The right part of figure 13 shows that measurements edited by backscatter coefficient criterion are especially found near coasts in the equatorial regions, besides of passes with altimeter parameters at default values.

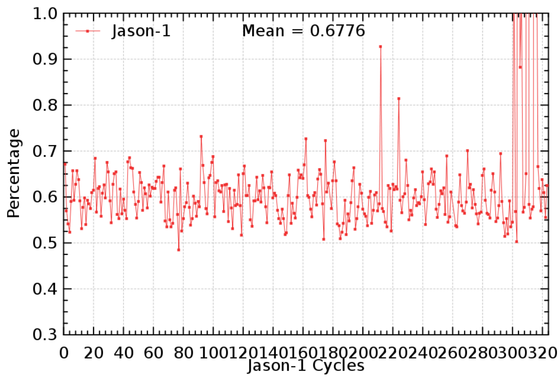

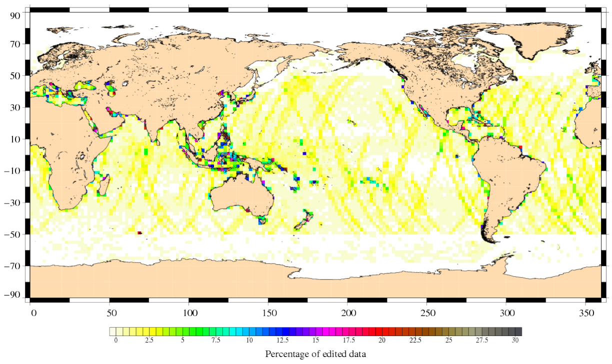

Figure 13: *Cycle per cycle percentage of edited measurements by Sigma0 criterion (left). Right: Map of percentage of edited measurements by Sigma0 criterion over an one-year period (cycles 276 to 313).*

3.2.10. Radiometer wet troposphere correction

The percentage of edited measurements due to radiometer wet troposphere correction criterion is represented in figure 14. It is about 0.15%. When removing cycles which experienced problems, percentage of edited measurements drops to 0.04%. The figure shows irregular oscillations which are not correlated to annual cycle. The map 14 shows that only few measurements are edited by radiometer wet troposphere correction criterion, besides a couple of passes after the safehold mode from cycle 283/284.

Notice that for some cycles the percentage of edited measurements is higher than usual. This is often linked to the Jason safe hold mode on some of these cycles (69, 78, 137, 179, and 284): the radiometer has been set on 2 hours later than the altimeter. As a result, the radiometer wet troposphere correction has been set to default value during this period and these measurements have been edited.
For cycles 1 and 2, radiometer wet troposphere correction is missing for passes which were absent in previous GDR product versions.

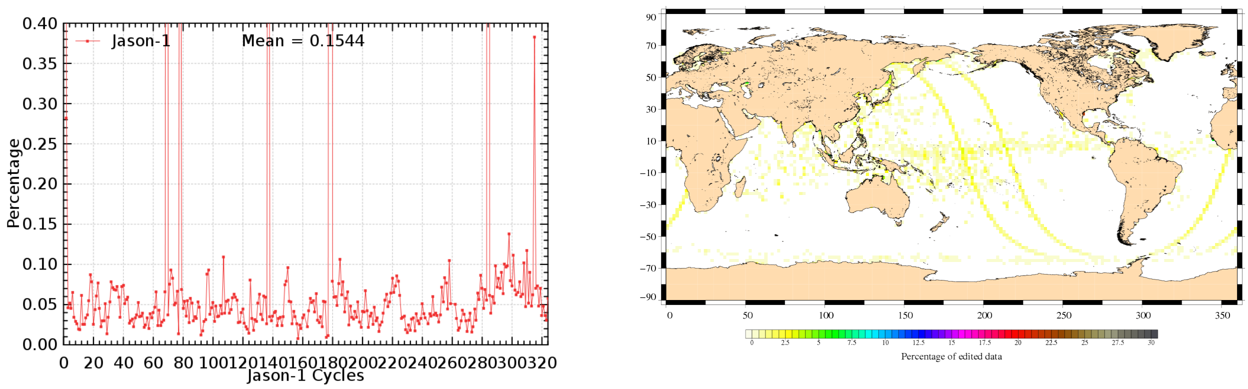

Figure 14: *Cycle per cycle percentage of edited measurements by radiometer wet troposphere criterion (left). Map of percentage of edited measurements by radiometer wet troposphere criterion over an one-year period (cycles 276 to 313).*

3.2.11. Dual frequency ionosphere correction

The percentage of edited measurements due to dual frequency ionosphere correction criterion is represented in figure 15. It is about 1.28% and shows no drift. The map 15 shows that measurements edited by dual frequency ionosphere correction are mostly found in equatorial regions. Notice that for cycles 9, 91, 102, 103, 108, 115, 133, 173, 198, 212, 301, 304-306, 310, 315 and 316 the percentage of edited measurements is higher than usual. Till cycle 198, this is linked to an altimeter SEU occurred on these cycles. The dual frequency ionospheric correction is not available during a few hours following the altimeter incidents (lack of C-band parameters requirering ground TC to resume nominal configurations). Peaks from cycle 212 onwards are mostky due to altimeter parameters at default value related to very high mispointing (see section 3.2.6. and 8.4.).

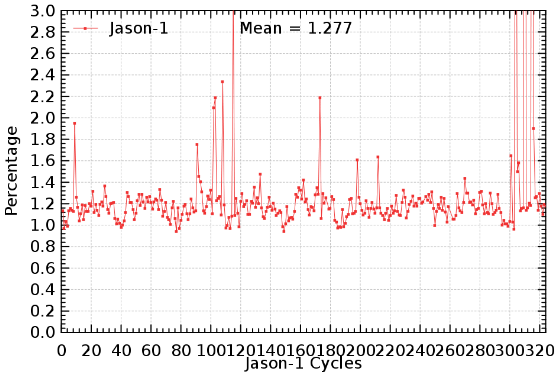

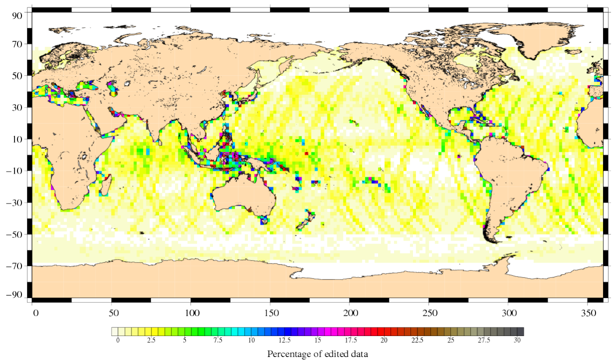

Figure 15: *Cycle per cycle percentage of edited measurements by dual frequency ionosphere criterion (left). Map of percentage of edited measurements by dual frequency ionosphere criterion over an one-year period (cycles 276 to 313).*

3.2.12. Square off-nadir angle

The percentage of edited measurements due to square off-nadir angle criterion is represented in figure 16. It is about 0.69%. During 2010, Jason-1 experienced very high off-nadir angles due to low star tracker and gyro performances, especially for period between cycles 304 and 316. This is shown in more detail in section 8.4.. The map 16 shows that besides periods of low star tracker performances, edited measurements are mostly found in coastal regions.

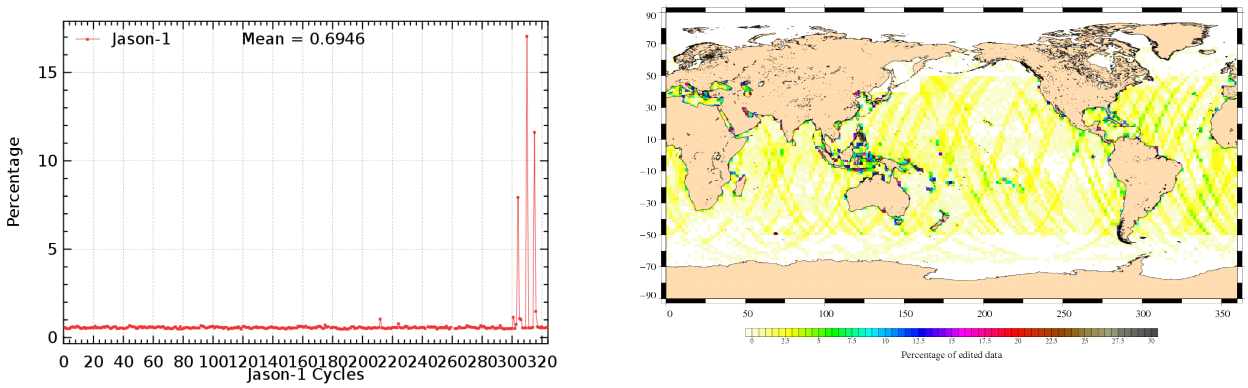

Figure 16: *Cycle per cycle percentage of edited measurements by square off-nadir angle criterion (left). Right: Map of percentage of edited measurements by square off-nadir angle criterion over an one-year period (cycles 276 to 313).*

3.2.13. Altimeter wind speed

The percentage of edited measurements due to altimeter wind speed criterion is represented in figure 17. It is about 1.09% and shows no drift. Measurements are generally edited, because they have default values, as happened due to very high mispointing for period between cycles 304 to 316. Otherwise, this is the case when sigma0 itself is at default value, or when it shows very high values (higher than 25 dB), which occur during sigma bloom and also over sea ice. The annual cycle is probably due to sea ice, which was not detected by the ice flag.

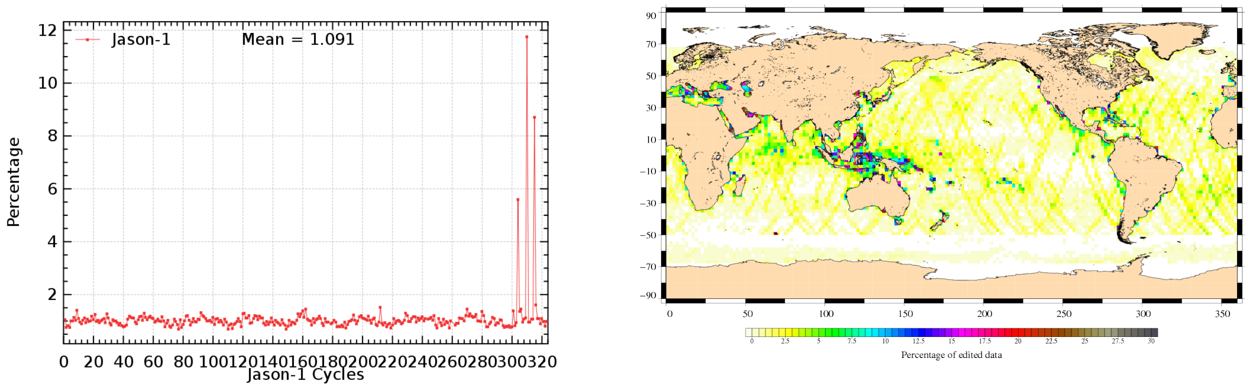

Figure 17: *Cycle per cycle percentage of edited measurements by altimeter wind speed criterion (left). Right: Map of percentage of edited measurements by altimeter wind speed criterion over an one-year period (cycles 276 to 313).*

3.2.14. Sea state bias correction

The percentage of edited measurements due to sea state bias correction criterion is represented in figure 18. The percentage of edited measurements is about 0.69% and shows no drift. But as other parameters, it was impacted by altimeter parameters at default values during period between cycles 304 and 316. The map 18 (right side) shows that edited measurements are mostly found in equatorial regions near coasts.
The map 18 showing percentage of measurements edited by sea state bias criterion is highly correlated with the map 17.

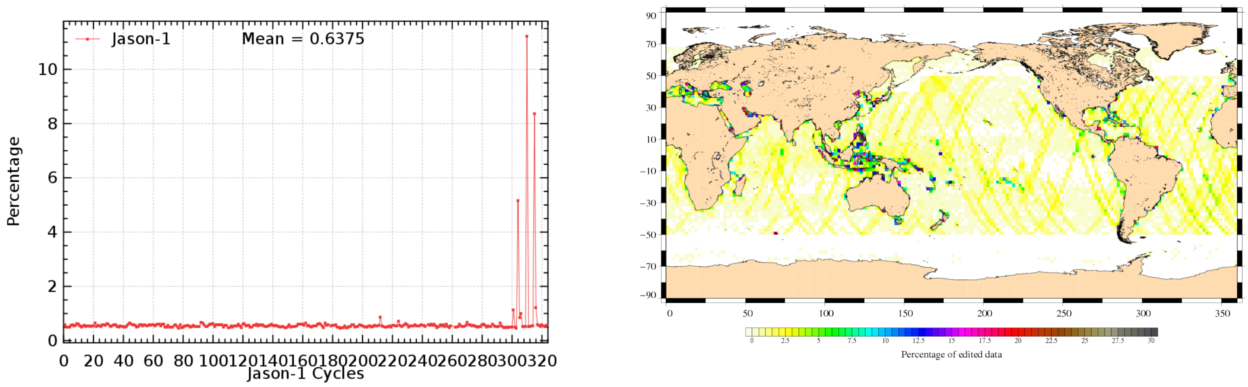

Figure 18: *Cycle per cycle percentage of edited measurements by sea state bias criterion (left). Right: Map of percentage of edited measurements by sea state bias criterion over an one-year period (cycles 276 to 313).*

3.2.15. Ocean tide correction

The percentage of edited measurements due to ocean tide correction criterion is represented in figure 19. It is about 0.06% and shows no drift. The ocean tide correction is a model output, there should therefore be no edited measurements. Indeed there are no measurements edited in open ocean areas, but only very few near coasts or in lakes or rivers (see map 19). These measurements are mostly at default values.
Generally approximatively the same amount of measurements is edited by ocean tide correction for each cycle. The small annual signal visible in figure 19 comes from the seasonal fluctuation of available ocean data (due to seasonal fluctuation of sea ice coverge).

A slight decrease in edited measurements is visible since cycle 262 (change of Jason-1 groundtrack). This is related to the new ground track, which no longer overflows the same areas.

3.2.16. Sea surface height

The percentage of edited measurements due to sea surface height criterion is represented in figure 20. It is about 0.95% and shows no drift. There is however an annual signal visible. For the peaks see section 3.2.12.
Besides anomalies due to poor star tracker and gyro performances, the measurements edited by sea surface height criterion are mostly found near coasts in equatorial regions (see map 20).

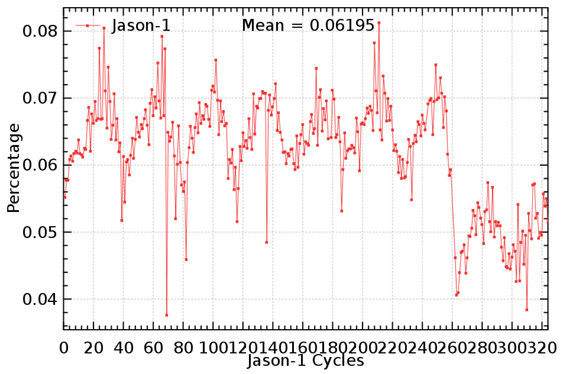

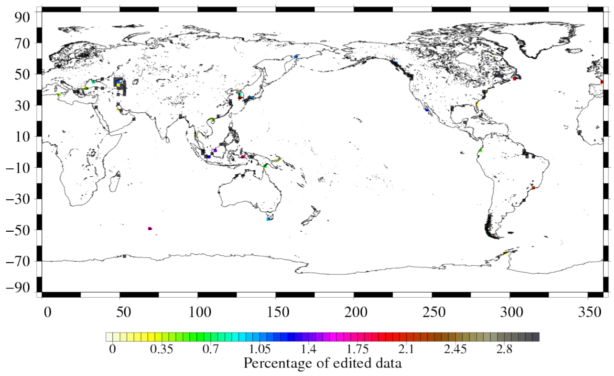

Figure 19: *Cycle per cycle percentage of edited measurements by ocean tide criterion (left). Right: Map of percentage of edited measurements by ocean tide criterion over an one-year period (cycles 276 to 313).*

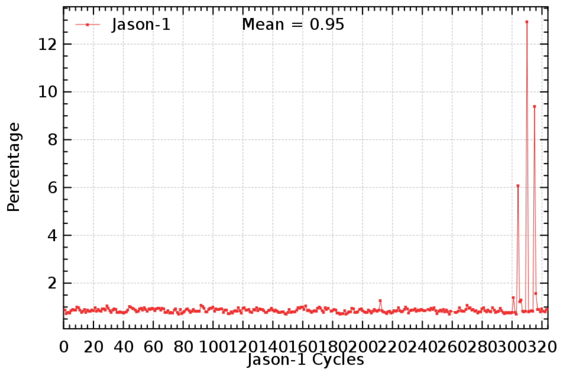

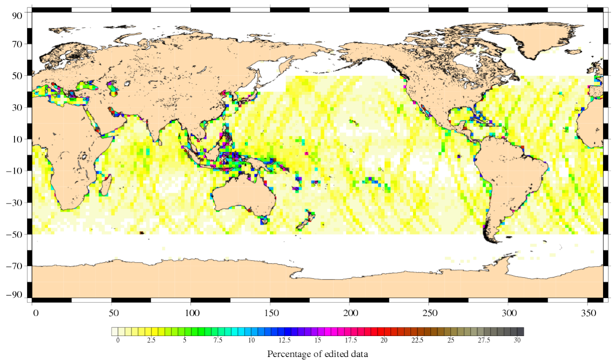

Figure 20: *Cycle per cycle percentage of edited measurements by sea surface height criterion (left). Right: Map of percentage of edited measurements by sea surface height criterion over an one-year period (cycles 276 to 313).*

3.2.17. Sea level anomaly

The percentage of edited measurements due to sea level anomaly criterion is represented in figure 21. It is about 1.21% and shows no drift. The graph is quite similar to the one in figure 8 (showing the percentage of measurements edited by all the threshold criteria), as the SLA clip contains many of the parameters used for editing.
Whereas the map in figure 21 allows us to plot the measurements edited due to sea level anomaly out of thresholds (after applying all other threshold criteria). These are generally only very few measurements.

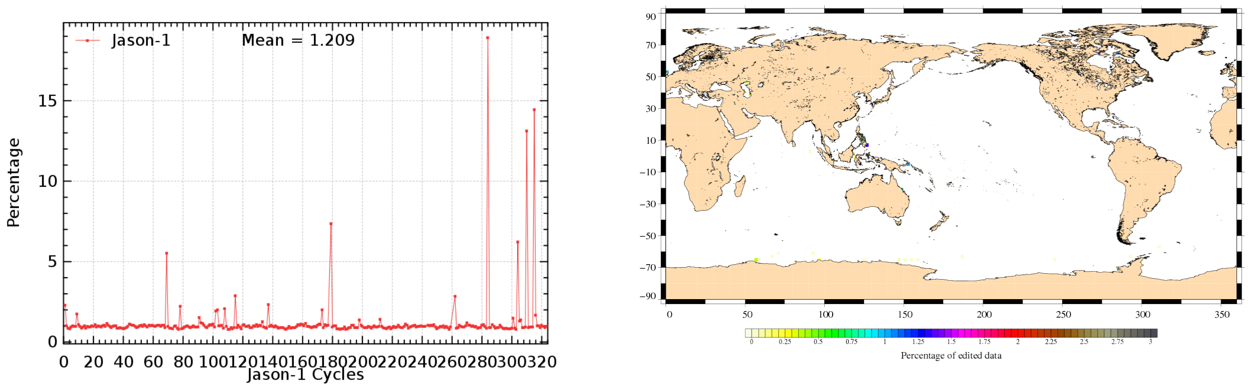

Figure 21: *Cycle per cycle percentage of edited measurements by sea level anomaly criterion (left). Right: Map of percentage of edited measurements by sea level anomaly criterion (after applying all other threshold criteria) over an one-year period (cycles 276 to 313).*

4. Monitoring of altimeter and radiometer parameters

4.1. Methodology

Both mean and standard deviation of the main parameters of Jason-1 have been monitored since the beginning of the mission. Moreover, a comparison with T/P parameters has been performed: it allows us to monitor the bias between the parameters of the 2 missions. The comparison is done till the end of scientific mission of T/P, which occurred during Jason-1 cycle 138. Two different methods have been used to compute the bias:

- During the verification phase, Jason-1 and T/P are on the same ground track and are spaced out about 1 minute apart. The mean of the T/P − Jason-1 differences can be computed using a point by point repeat track analysis.
- From cycle Jason-1 22 (Cycle T/P 365), the 15th of August 2002, a maneuver sequence was conducted over 30 days to move T/P to the new Tandem Mission orbit : further on T/P was located one half of the TP/Jason-1 track spacing to the West of Jason-1. Geographical variations are then too strong to directly compare Jason-1 and T/P parameters on a point by point basis. Therefore cycle per cycle differences have been carried out to monitor Jason-1 and T/P differences, but data gaps on both satellites have been taken into account.

For comparison between Jason-1 and Jason-2 please see annual Jason-2 report ([73]).

4.2. 20 Hz Measurements

The monitoring of the number and the standard deviation of 20 Hz elementary range measurements used to derive 1 Hz data is presented here. These two parameters are computed during the altimeter ground processing. Before a regression is performed to derive the 1 Hz range from 20 Hz data, a MQE criterion is used to select valid 20 Hz measurements. This first step of selection thus consists in verifying that the 20 Hz waveforms can be effectively approximated by a Brown echo model (Brown, 1977 [16]) (Thibaut et al. 2002 [88]). Through an iterative regression process, elementary ranges too far from the regression line are discarded until convergence is reached. Thus, monitoring the number of 20 Hz range measurements and the standard deviation computed among them is likely to reveal changes at instrumental level.

4.2.1. 20 Hz measurements number in Ku-Band and C-Band

Figure 22 shows the cycle per cycle mean of 20-Hz measurements number in Ku-Band (on the left) and C-Band (on the right). A very weak seasonal signal is visible, furthermore a weak negative trend is visible for C-Band.

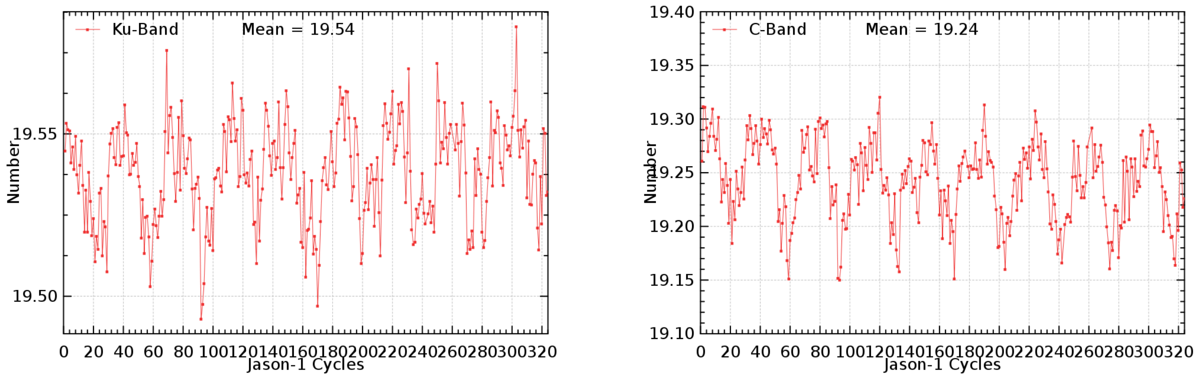

Figure 22: *Cycle per cycle mean of 20-Hz measurements number in Ku-Band (left) and C-Band (right)*

4.2.2. 20 Hz measurements standard deviation in Ku-Band and C-Band

Figure 23 shows the cycle per cycle standard deviation of the 20 Hz measurements in Ku-Band (on the left) and C-Band (on the right). Apart from a weak seasonal signal, neither trend nor any anomaly has been detected. Moreover, since integration is done over less waveforms, values of C-Band standard deviation of the 20 Hz measurements are higher than those of Ku-Band, which leads to an increased noise.

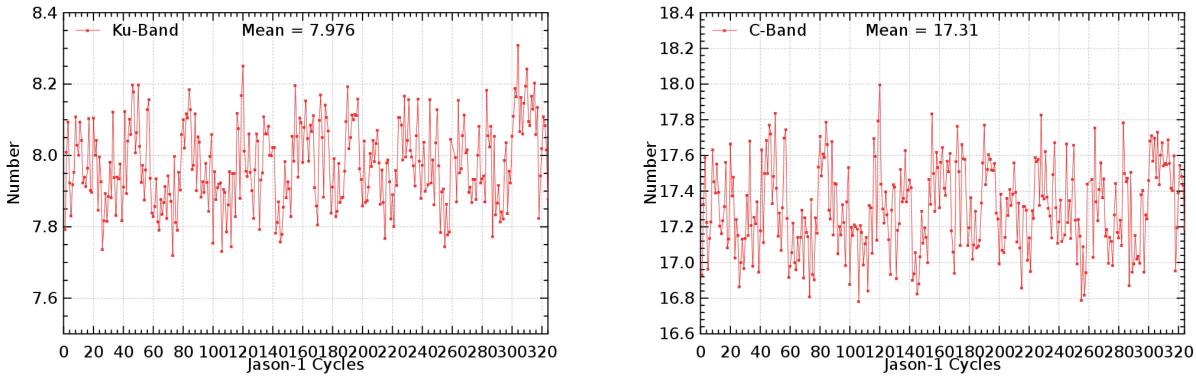

Figure 23: *Cycle per cycle mean of 20-Hz measurements standard deviation in Ku-Band (left) and C-Band (right)*

4.3. Off-Nadir Angle from waveforms

The off-nadir angle is estimated from the waveform shape during the altimeter processing. The square of the off-nadir angle, averaged in a one-cycle basis, has been plotted in figure 24. The mean values are slightly positive. This mean value is not significant in terms of actual platform mispointing. In fact squared attitude is what is retrieved from waveforms, not attitude. During the first third of the mission off-nadir angles are low and quite stable, except for cycle 69 related to a platform safehold mode. Between cycles 100 and 200, the off-nadir angle slightly increases and reaches more often strong values and since cycle 200 it is disturbed with one half of very strong values. Indeed, there are periods where the combination of low Beta angles and Sun glint or Moon in field of view significantly reduces the tracking performance of both star trackers, especially during fixed-yaw. Previously, in GDR version "a", when the off-nadir angle was larger than the 0.2 degree specification, error was introduced in the altimeter parameters as the off nadir was not taken into account in the ground processing (Vincent et al., 2003). Thus, an improvement of the retracking algorithm was made since GDR version "b" ([12]), to correct for estimations of altimeter parameters for mispointing angle errors up to 0.8 deg. (Amarouche et al. 2004 [13]).

During years 2008 and 2009, the satellite has experienced several severe mispointing cases, although the mispointing values remained within the threshold editing criteria (-0.2 to 0.64deg^2). This feature has been repeatedly pointed out, especially after maneuvers. Neither specific geographic pattern nor ascending/descending tracks systematisms are observed. The high mispointing values are related to low star tracker availability and gyro wheels behavior. During 2010, off-nadir angles were particularly high, leading even to altimeter lost of track. Section 8.4.1. gives more details on these events.

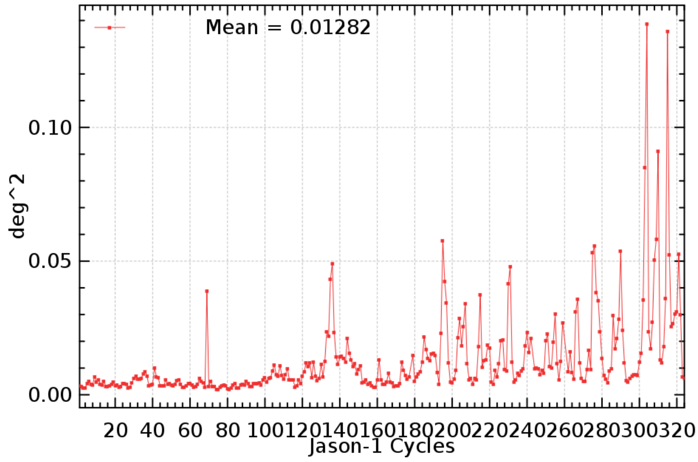

Figure 24: *Cycle mean of the square of the off-nadir angle deduced from waveforms (deg^2).*

4.4. Significant wave height

4.4.1. Ku-band SWH

Jason-1 and T/P Ku SWH are compared in terms of global statistics in figure 25: cycle means and standard deviations of both missions are presented in a cycle basis, as well as mean differences between T/P and Jason-1. Global variations of the SWH statistics are the same on the two missions. A weak annual signal is visible. Jason-1 SWH shows almost no drift on the whole altimeter time period. The (TOPEX - Jason-1) SWH bias is about 5.4 cm. The estimate of the (Poseidon-1 - Poseidon-2) SWH difference is about 12 cm for Poseidon-2 cycle 18 not plotted here.
The standard deviation of Ku-band SWH shows an annual signal for both Jason-1 and T/P data.

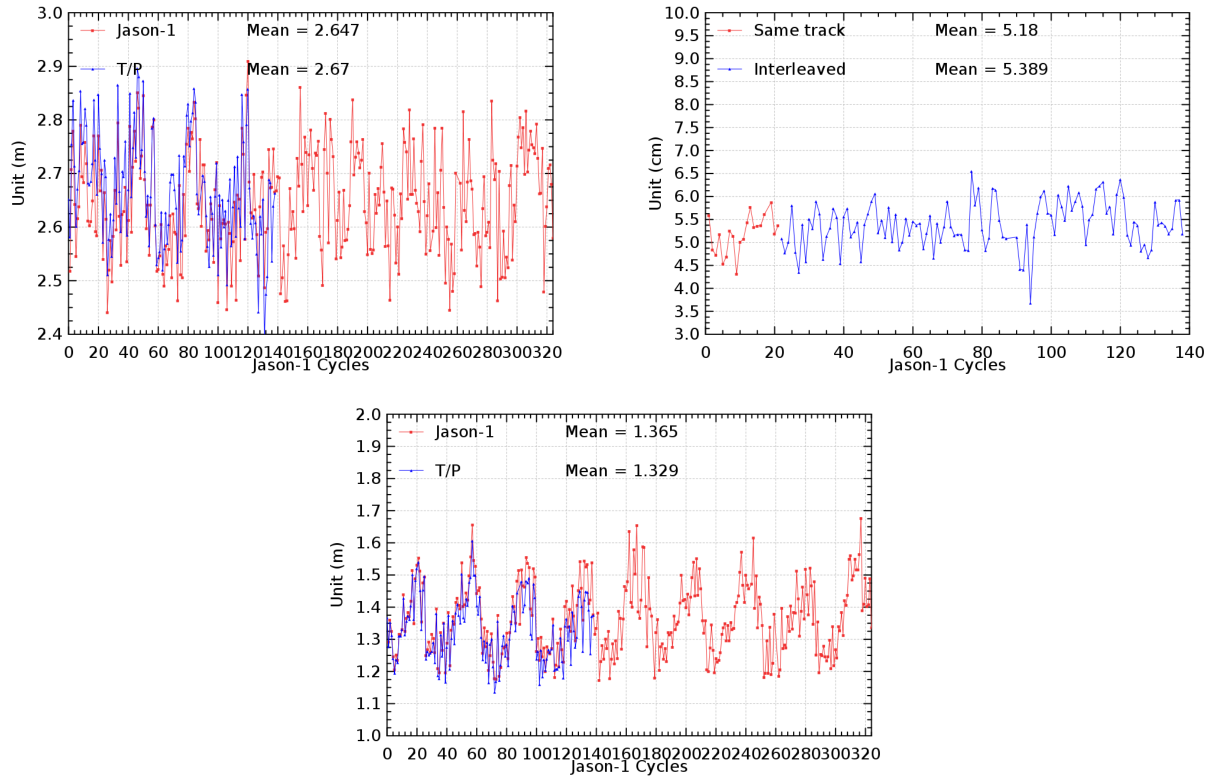

Figure 25: *Cycle per cycle mean (left), T/P−Jason mean differences (right), and standard deviation (bottom) of Ku-band SWH*

4.4.2. C-band SWH

Figure 26 shows global statistics of Jason-1 and T/P C-band SWH. The cycle per cycle mean of both missions shows a small annual signal (figure 26 top left). Jason-1 and T/P values are quite similar. The (TOPEX - Jason-1) C-band SWH mean bias is about 8 cm (figure 26 top right), with a drift of about -2 mm/yr. Moreover, the standard deviation of the C-band SWH is quite similar on both missions, showing an annual signal.

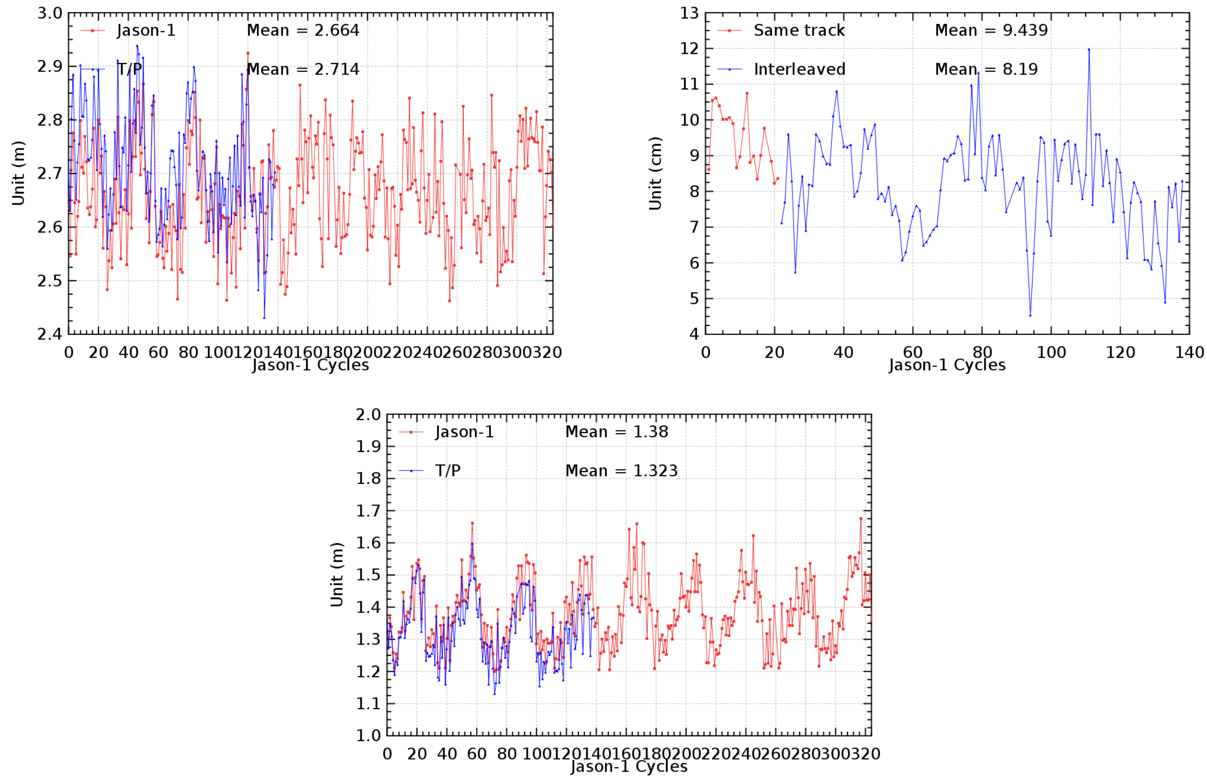

Figure 26: *Cycle per cycle mean (left), T/P−Jason mean differences (right), and standard deviation (bottom) of C-band SWH*

4.5. Backscatter coefficient

4.5.1. Ku-band Sigma0

The cycle per cycle mean (figure 27: top panel on the left) for Jason-1 (red curve) Ku-band sigma0 is coherent with the TOPEX mean (blue curve). In order to compare both parameters and keep a significant dynamic scale, TOPEX Ku-Sigma0 is biased by a 2.26 dB value to align TOPEX with the Jason-1 uncalibrated Sigma0. The bias between the two corrections (figure 27: top panel on the right) is quite stable about -2.5 dB.

Besides, the absolute bias is higher than usual from T/P cycle 433 to 437 (J1 cycles 90 to 94) by 0.1 dB : this is due to the TOPEX Sigma0. Indeed, the satellite attitude was impacted by a pitch wheel event linked to the T/P safe-hold mode occurred on cycle T/P 430 (see electronic communication : T/P Daily Status (26/07/2004)). This anomaly has probably biased the TOPEX sigma0 during this period. Jason-1 and T/P curves on bottom panel, showing the standard deviation differences, are very similar .

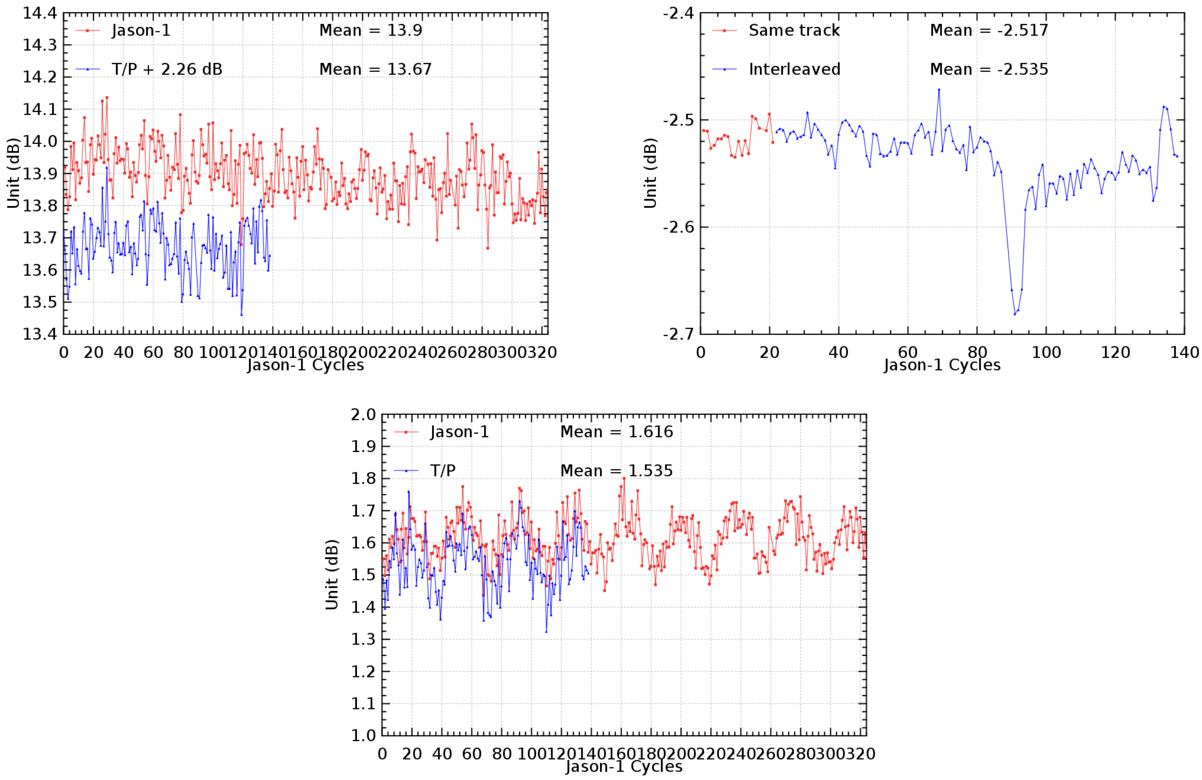

Figure 27: *Cycle per cycle mean (left), T/P−Jason mean differences (right), and standard deviation (bottom) of Ku-band SIGMA0*

4.5.2. C-band Sigma0

The cycle per cycle mean (figure 28: top panel on the left) for Jason-1 (red curve) Ku-band sigma0 is coherent with the TOPEX mean (blue curve). The bias between the two corrections (figure 28: top panel on the right) decreases from -0.6 dB to -0.8 dB. This is due to the T/P C-band Sigma0 (Ablain et al. 2004 [4]).
Note that in science processing software a bias of approximately -0.28 dB is applied to the provided C-Band Sigma0 for any geophysical algorithms that require use of sigma0. Standard deviation of C-band sigma0 (figure 28: bottom) has similar values for both missions and shows an annual signal.

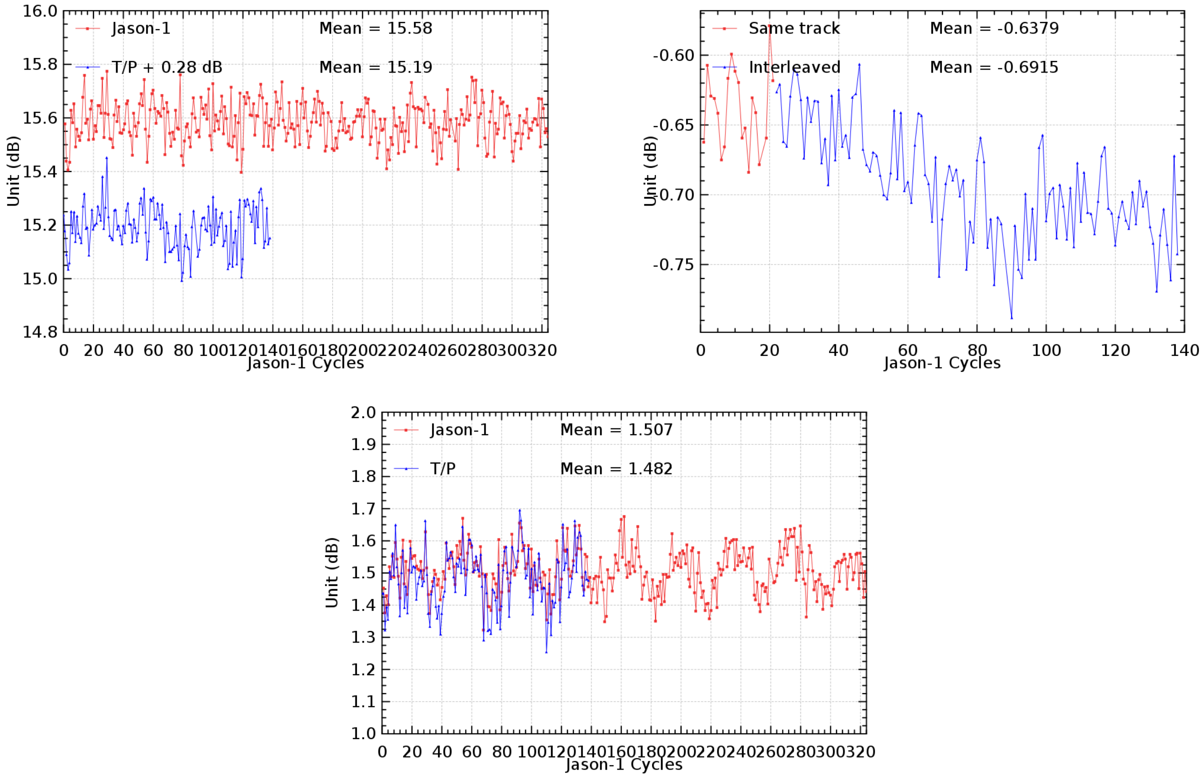

Figure 28: *Cycle per cycle mean (left), T/P−Jason mean differences (right), and standard deviation (bottom) of C-band SIGMA0*

4.6. Dual-frequency ionosphere correction

The dual frequency ionosphere corrections derived from the TOPEX and Jason-1 altimeters have been monitored and compared in the same way (figure 29). The mean difference between TOPEX and Jason-1 estimates is about 1.5 mm, with cycle to cycle variations lower than 2 mm. There is nevertheless a small visible drift of 0.3 mm/yr. Both corrections are very similar and vary according to the solar activity. Note that, as for TOPEX (Le Traon et al. 1994 [58]), it is recommended to filter the Jason-1 dual frequency ionosphere correction before using it as a SSH geophysical correction (Chambers et al. 2002 [22]). A low-pass filter has thus been used to remove the noise of the correction in all SSH results presented in the following sections. Note that in GDR-C product, the DORIS ionospheric correction is no longer available. It has been replaced by the GIM ionospheric correction (model), which displays better metrics than the DORIS' one.

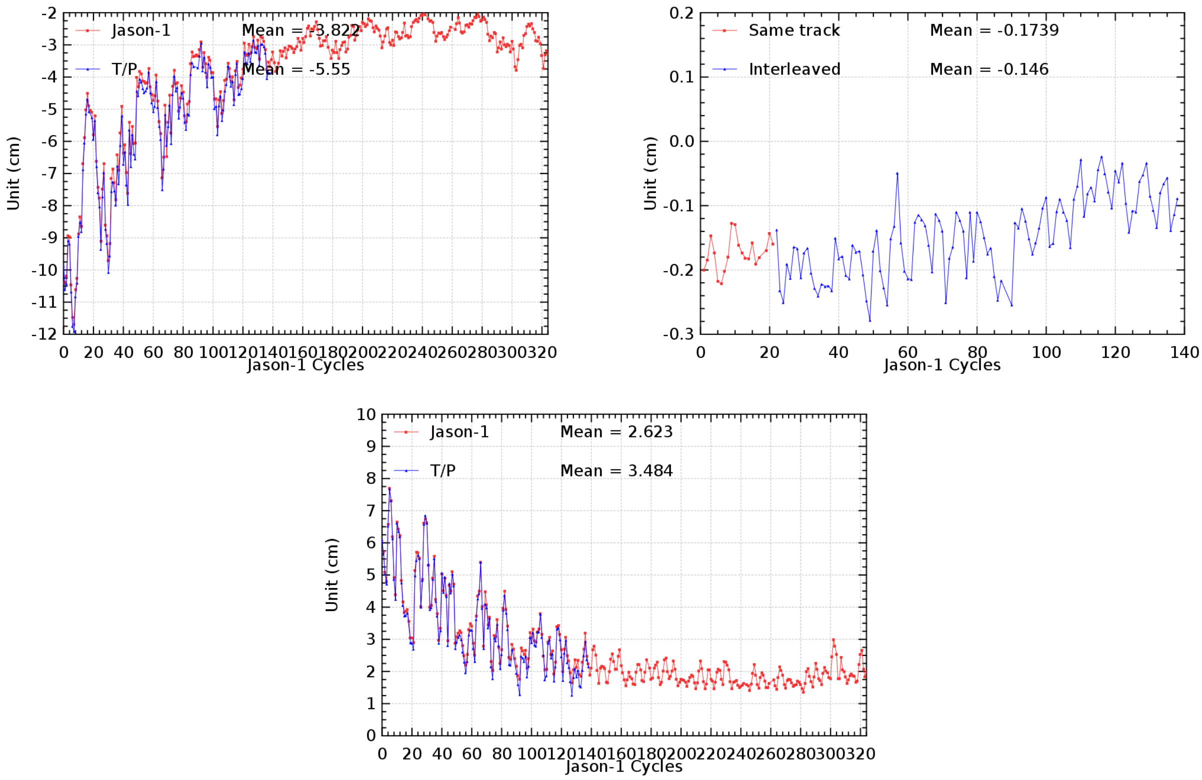

Figure 29: *Cycle per cycle mean (left), T/P−Jason mean differences (right), and standard deviation (bottom) of dual frequency ionosphere correction*

4.7. JMR Wet troposphere correction comparison with ECMWF model

Wet troposphere correction is a very important variable for mean sea level trend calculation (see also [65]). Jason-1 satellite has beside the altimeter also a microwave radiometer (JMR) onboard in order to compute the radiometer wet troposphere correction. Furthermore ECMWF model wet troposphere correction is available in GDR products. Both corrections can be subject to jumps or drifts. Comparing both (as well as other radiometer corrections from e.g. Jason-2 or Envisat missions), can help to detect anomalies.
JMR is subject to jumps, or oscillations especially when thermal environment changes, such as after altimeter switch offs. Right side of figure 30 shows for instance oscillations of up to 7 mm just after August 2008 safe hold. These anomalies are generally corrected when GDR products are reprocessed. In the meanwhile, a JMR replacement product is available ([17]) which corrects for these instabilites. Furthermore, JMR continues to be sensitive to yaw maneuvers. Right side of figure 30 shows the daily monitoring of radiometer minus ECMWF model wet troposphere correction over 2010. In second half of 2010, difference between radiometer and model shows an increase during periods where the satellite is in fixe mode (gray stripes).
On the other hand, ECMWF model is also suject to evolutions, which have an impact on wet troposphere correction. These evolutions are indicated by green lines in figure 30. A jump of several mm occured after model version change of January 2002. The most recent ECMWF model version change (9th November 2010), induced a small jump of about 2 mm.

The improvements of the ECMWF model standards are visible on the standard deviation of wet troposphere correction difference (between radiometer and ECMWF model) which is shown on 30, left panel. At the beginning of 2003 standard deviation decreases from 1.4 cm to 1.1 cm. This corresponds to a model evolution. In the following, it continues to decrease. In 2009, an increase in standard deviation of radiometer minus ECMWF model wet troposphere differences (of about 0.1 cm) is noticeable. This corresponds to a model evolution on 10th March 2009 (see http://www.ecmwf.int/products/data/operationalsystem/evolution/evolution2009.html#10March2009). The most recent model evolution (9th November 2010) caused again a decrease of the standard deviation.

Behavior of wet troposphere correction is therefore continually monitored and comparison of the different radiometer and model wet troposheric corrections are regularly done (see [56]).

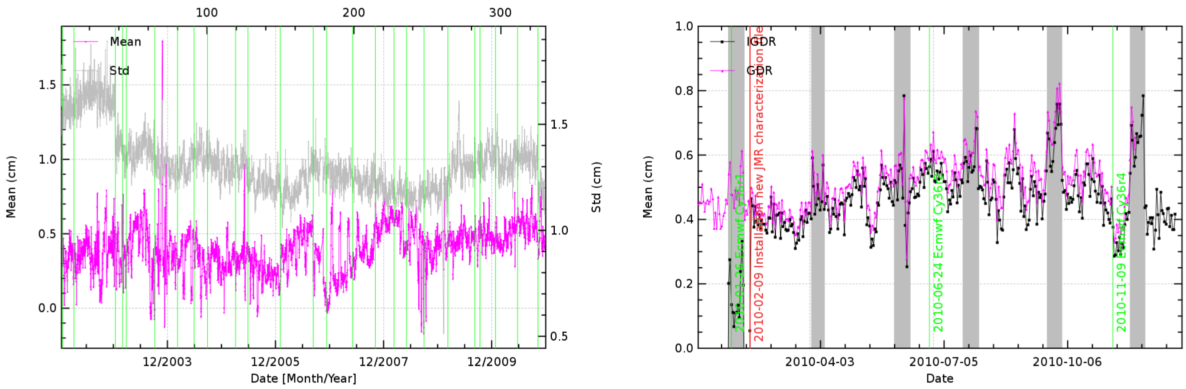

Figure 30: *Difference of radiometer and model wet tropospheric corrections. Left: daily mean and standard deviation over whole Jason-1 mission period. Right: Daily mean during 2010. Green lines indicate ECMWF model version changes, gray stripes indicate periods, where Jason-1 is in fixe mode.*

5. Crossover analysis

Crossover differences are systematically analyzed to estimate data quality and the Sea Surface Height (SSH) performances. Furthermore, T/P crossover performances (as long as they were available) have been monitored in order to compare both performances. SSH crossover differences are computed on a one cycle basis, with a maximum time lag of 10 days, in order to reduce the impact of ocean variability which is a source of error in the performance estimation. The main SSH calculation for Jason-1 and T/P are defined below. For TOPEX, Jason-1 standards have been used for the tidal and atmospheric corrections.

$$SSH = Orbit - Altimeter\ Range - \sum_{i=1}^{n} Correction_i$$

with $Jason-1\, Orbit = POE\, CNES\, orbit$ and

$$\begin{aligned}
\sum_{i=1}^{n} Correction_i \quad = \quad & Dry\, troposphere\, correction : new\, S1\, and S2\, atmospheric\, tides\, applied \\
+ \quad & Combined\, high\, resolution\, dynamical\, atmospheric\, correction \\
+ \quad & Radiometer\, wet\, troposphere\, correction \\
+ \quad & Filtered\, dual\, frequency\, ionospheric\, correction \\
+ \quad & Non\, parametric\, sea\, state\, bias\, correction \\
+ \quad & Geocentric\, ocean\, tide\, height,\ GOT\ 2000:\ S1\, atmospheric\, tide\, is\, applied \\
+ \quad & Solid\, earth\, tide\, height \\
+ \quad & Geocentric\, pole\, tide\, height
\end{aligned}$$

5.1. Mean crossover differences

The mean of crossover differences represents the average of SSH differences between ascending and descending passes. It should not be significantly different from zero. More importantly, special care is given to the geographical homogeneity of the mean differences at crossovers. The map of the Jason-1 crossover differences averaged over the whole period of available GDR (cycle 1 to 324) has been plotted in figure 31 (on the left). It is quite homogeneous. Nevertheless some geographically correlated patterns are visible (as it is also the case for Jason-2 [73]). Note that this map is now totally computed with GDR version "c". As in GDR version "c" products are computed thanks to a new empirically correction, called pseudo_datation_bias_corr_ku is available, no more bias between northern and southern hemisphere is observable. Recently, the origin of this pseudo time tag bias was found by CNES [15].

The cycle mean of Jason-1 SSH crossover differences is plotted for the whole Jason-1 period in figure 31 (right). Though slightly negative, the monitoring is homogeneous on the whole Jason-1 period, as expected with GDR version "c" reprocessing.

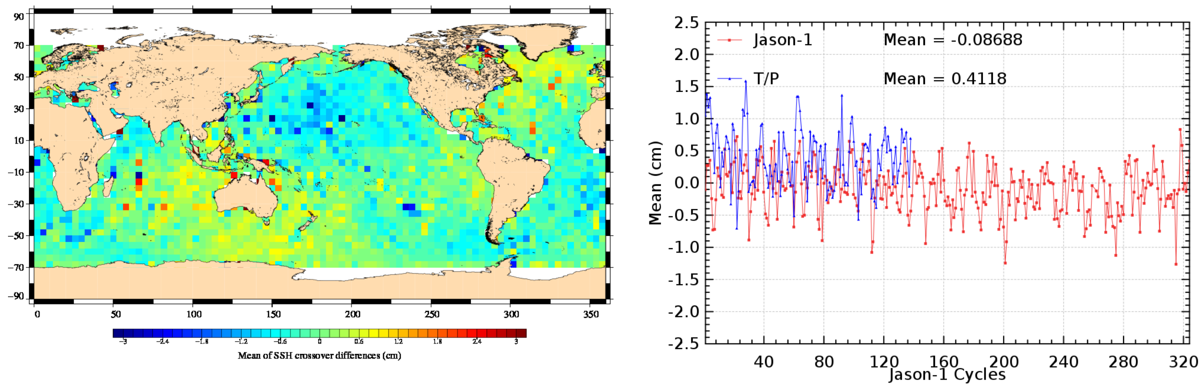

Figure 31: *Map of mean crossovers for Jason cycle 1 to 324 and cycle per cycle mean crossovers (right)*

5.2. Standard deviation of crossover differences

The cycle per cycle standard deviation of crossover differences are plotted in figure 32 (on the left) according to different crossover selections. 3 selections are applied:

- Red curve: no selection is applied. The mean value is 6.3 cm. It shows an annual signal linked to the sea ice extension variations in the Northern Hemisphere.
- Blue curve: shallow waters have been removed (bathy$\leq -1000m$). The previous annual signal has been removed by this selection even though a signal probably due to seasonal ocean variations remains.
- Green curve: the last selection allows monitoring the Jason-1 system performance. Indeed, areas with shallow waters (1000 m), of high ocean variability ($\geq 20cm$) and of high latitudes ($abs(lat) \geq 50$ degrees) have been removed. The standard deviation then provides reliable estimates of the altimeter system performances. In that case, no trend is observed in the standard deviation of Jason-1 SSH crossovers: good performances are obtained, with a standard deviation value of about 5.1 cm all along the mission.

Note that standard deviation of SSH crossover differences is higher than usual for cycle 315. This is related to degraded orbit quality following several out of plan maneuvers (see also section 8.4.2.). The map of standard deviation of crossover differences overall the Jason-1 period, in figure 32 (on the right) shows usual results with high variability areas linked to ocean variability.

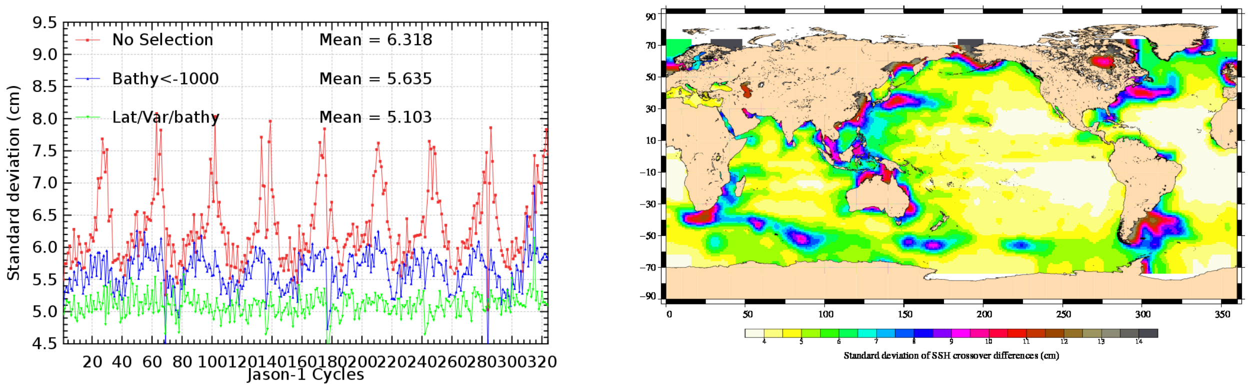

Figure 32: *Cycle per cycle standard deviation crossovers with different selections and map of Jason-1 standard deviation crossovers*

6. Along-track analysis

This analysis is used to compute Sea Level Anomalies (SLA) variability and thus to estimate data quality; it is used to determine the SSH bias between Jason-1 and T/P and the trend in the Mean Sea Level (MSL).

6.1. Along-track performances

6.1.1. Along-track performances on sea level anomaly

Along track analyzes are also used to assess the altimeter system performances, by computing Sea Level Anomalies (SLA). The SLA variance gives an estimate of the errors of the system, even though the ocean variability fully contributes in this case. A comparison between Jason-1 and T/P has been performed computing the variance of SLA relative to the MSS (CLS01). This allows global and direct calculations.
The SLA standard deviation is plotted in left side of figure 33 for Jason-1, Jason-2 and T/P. It exhibits similar and good performances for the satellites. After flight formation phases, SLA standard deviation increases for the satellite which is put on the interleaved ground track (T/P in 2002, Jason-1 in 2009). For TOPEX this is less visible, as its ground processing is different from the Jason's. Dorandeu et al. 2004 ([37]) shows that a clear increase in SLA standard deviation is visible for T/P interleaved ground-track when looking at wavelength shorter than 500km. This SLA standard deviation increase is due to the use of MSS CLS01 ([48]), as errors of this MSS are higher outside the historical T/P-Jason ground track ([37],[8]). Using a newer MSS, such as CNES/CLS 2010 ([85]) which also used data from the interleaved ground track, decreases Jason-1 SLA standard deviation significantly for interleaved period.

During summer and fall 2010 (around cycle 320), the SLA standard deviation has increased, not only for Jason-1, but also for Jason-2 and Envisat (not shown here). This is probably related to "La Niña" episode occuring in Pacific ([95]). Focus on Pacific Ocean data (right side of figure 33) shows indeed an increase in SLA standard deviation. This is under investigation.

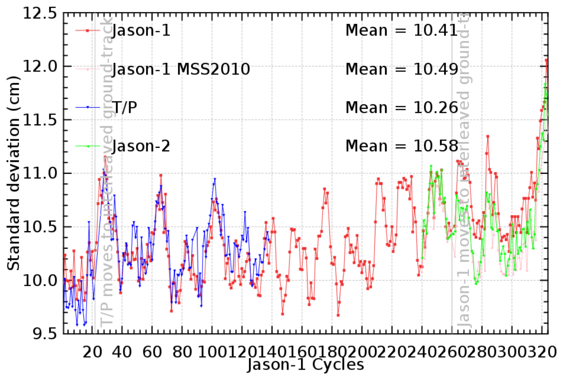

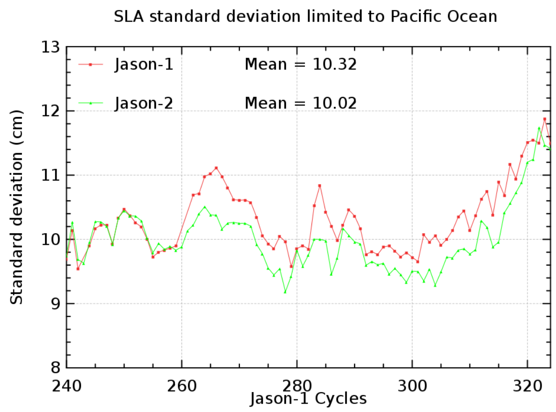

Figure 33: *Cycle per cycle SLA standard deviation. Left: showing T/P, Jason-1 and Jason-2 over whole Jason-1 period. Right: showing Jason-1 and Jason-2 over Jason-2 period and only for Pacific Ocean.*

6.2. Jason-1 Mean sea level

6.2.1. Sea surface height estimate

The assessment of the mean sea level trend is important for climate change studies. MSL estimation from Jason-1 and T/P are plotted in figure 34 (on the left), after reduction of the relative bias between the two time series.
Several error sources can influence MSL evolution, one of them is the choice of wet troposphere correction. On the one hand ECMWF model wet troposphere correction might be influenced by model evolutions, on the other hand radiometer wet troposphere correction is influenced by yaw mode transitions or thermal instabilities after altimeter switch-off. Therefore MSL calculated with radiometer correction (red curve) and with model correction (green curve) are shown in figure 34. The results are obtained after area weighting (Dorandeu and Le Traon 1999 [32]). The figure shows good agreement between the two missions and demonstrates that the Jason-1 mission ensures continuous precise MSL monitoring as it was done for more than a decade by the T/P mission. On both missions, seasonal signals are observed, because the combined dynamic atmospheric correction (which includes inverse barometer) has been applied in the SSH computation (Dorandeu and Le Traon 1999 [32]). Moreover, almost 60-day signals are also detected on Jason-1 and T/P series, with nearly the same amplitude. A source of error could be from the largest tidal constituents at twice-daily periods which alias at periods close to 60 days for Jason-1 and T/P (Marshall et al. 1995 [61]). Orbit errors in T/P altimeter series used to compute the tide solutions could also have contaminated these models (Luthcke et al. 2003 [60]). In this way, a study on the 58.74-day signal observed on the MSL derived from Jason-1&2 and TOPEX data has been performed in 2010 (see part 8.1.). Moreover, using JMR or model wet troposphere correction has a slight impact on the slope of about 0.2 mm/year.

On figure 34 (right panel), annual and semi-annual signals have been adjusted. This allows to decrease the adjustment formal error for both satellites. The global MSL slopes are almost the same for Jason-1 and T/P (close to 2.6 mm/year), but for Jason-1, the shown time period is more than four years longer than for T/P. Also, the MSL slope of Jason-1 shows a flattening at the end of 2006 and during 2007 (between cycles 183 and 219). Calibration with in-situ data (see section 7.5.1. and more detailed in annual reports [97] and [55]) shows no drift of altimetric MSL. Therefore this flattening might be due to "La Niña" active during this period.

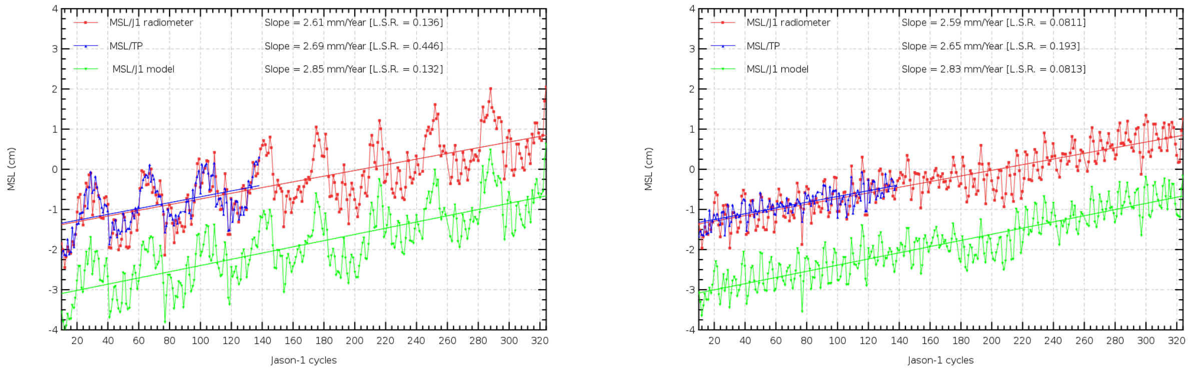

Figure 34: *Jason-1 and T/P mean sea level (on the left) with annual and semi-annual adjustment (on the right)*

The shown MSL trends were computed using as well ascending and descending passes, but when computing Jason-1 MSL slope separately for ascending and descending passes, differences are noticed. Figure 35 shows SLA slopes using Jason-1 GDRs (with ECMWF model wet troposphere correction) and T/P MGDRs.

Jason-1 SLA slopes are similar:

- 2.7 mm/yr using descending passes
- 2.9 mm/yr using ascending passes

Indeed, this represents a difference of 0.2 mm/yr, which is in agreement with T/P even if the time period considered is quite different (see 35 right). For Envisat data, difference of SLA slope between ascending and descending passes is about 0.4 mm/yr, as demonstrated in the Envisat 2010 report, between odd and even tracks.

Although differences between ascending and descending passes are weaker than before, this is no explanation concerning this behavior.Indeed, ascending and descending passes cover the same geographical regions, so there is no reason why SLA slope should rise differently. A study using several orbit solutions showed, that use of different orbits has an impact on difference of SLA slope noticed between ascending and descending passes. Further investigations will be led in 2011.

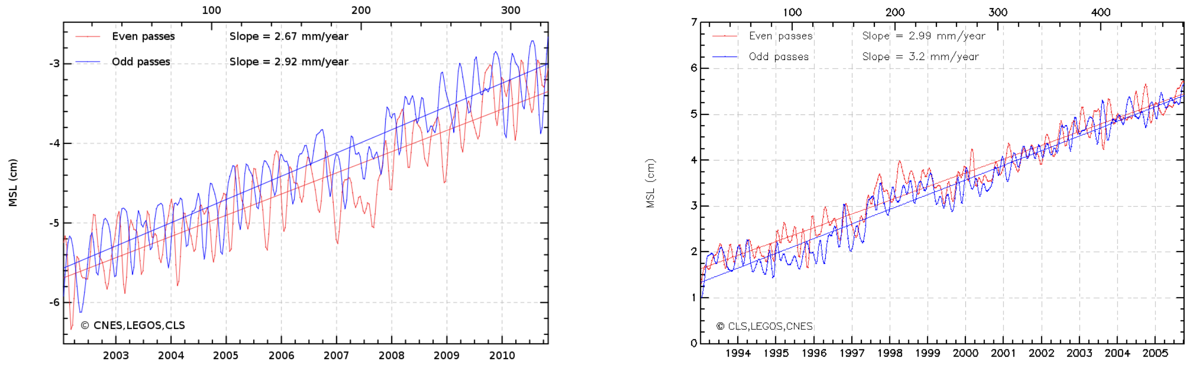

Figure 35: *J1 (left) and T/P (right) SLA slopes using only ascending (odd) or descending (even) passes.*

6.2.2. SSH bias between Jason-1 and T/P

6.2.2.1. Temporal evolution of SSH bias between Jason-1 and T/P

The ECMWF wet troposphere correction is also used in figure 36 which represents the temporal evolution of the SSH bias between T/P and Jason-1. This prevents from errors due to radiometer biases, as the model correction is the same for the two missions. When using radiometer wet troposphere correction, the bias differs by 7 to 8 mm. The impact of all geophysical corrections is also displayed in the figure. Results differ by 1.3 cm when applying or not corrections but signals seem to be homogeneous all over the time period. Notice that present results have been obtained using a dedicated TOPEX SSB estimation. Apart from higher variability for Jason-1 cycle 18 (Poseidon-1 was switched on for T/P cycle 361), the T/P to Jason-1 SSH bias nearly remains constant through the Jason-1 mission period.

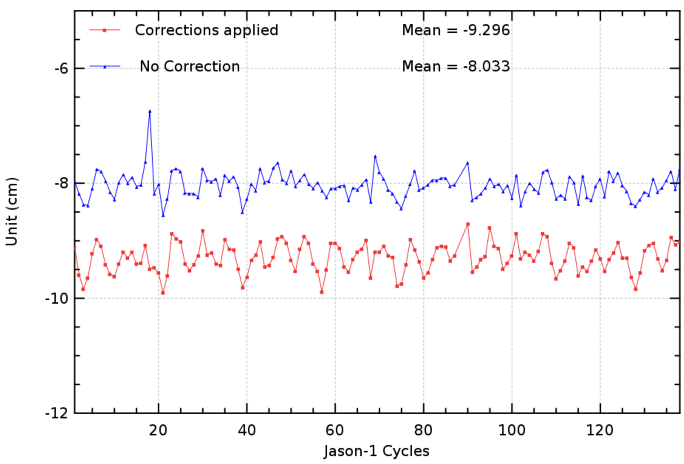

Figure 36: *Cycle per cycle mean of (T/P−Jason-1) SSH differences*

6.2.2.2. Spatial distribution of SSH bias between Jason-1 and T/P

Jason-1 and T/P have not been on the same track from cycle 21 onward. Consequently, the SSH differences can not be obtained directly as a result of the ocean variability. Thus, the map of the SSH differences between Jason-1 and T/P is obtained at the Jason-T/P crossovers in figure 37. The figure was generated using Jason-1 GDR version "c" (cycle 1 to 138) and updated corrections on T/P (GSFC orbit, Sea State Bias, ionospheric bias). The global map is much more homogeneous with these new standards, though there are still some visible structures, they are now much more consistent and have less amplitudes (generally less than ± 1 cm).
Using MGDR T/P standard, large differences were also visible, when looking on the verification phase of Jason-1 (cycles 1 to 21) (figure 38, left panel). Both satellites (T/P and Jason-1) were on the same ground track, which makes direct measurement comparison possible. For OSTST meetings in 2006 and 2007 retracked (new range,...) TOPEX cycles of the Jason-1 verification phase were already available. They contained also on orbit based on GRACE gravity model. This reduces the differences, as visible on figure 38 (right panel). The data of both missions are much more homogeneous, when looking at global maps. Indeed, when separating ascending and descending passes during computing T/P - Jason-1 SLA differences, large hemispheric biases appear (see figure 39).

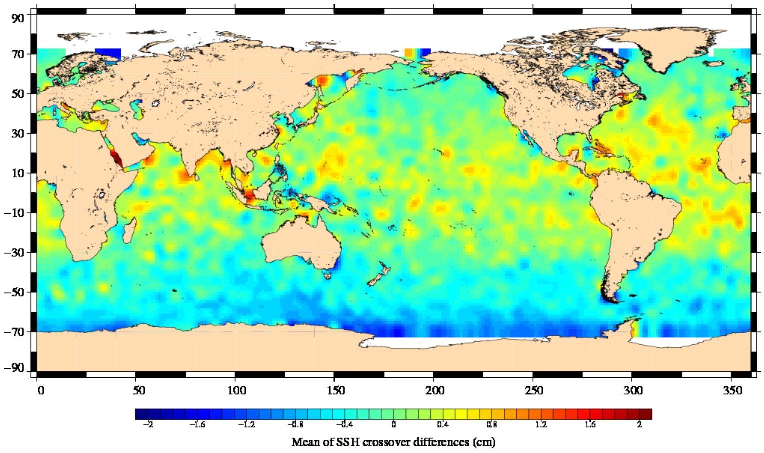

Figure 37: *Map of (T/P−Jason-1) SSH differences for Jason-1 GDR version "c" (cycles 1 to 138).*

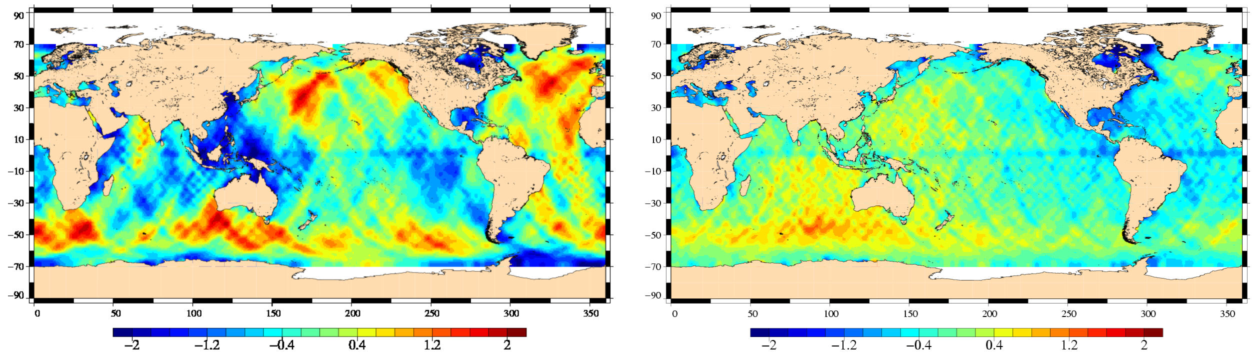

Figure 38: *Map of (T/P−Jason-1) SSH differences for Jason-1 cycles 1 - 21, using orbit of MGDR (left) and GSFC orbit based on GRACE gravity model (right) for T/P.*

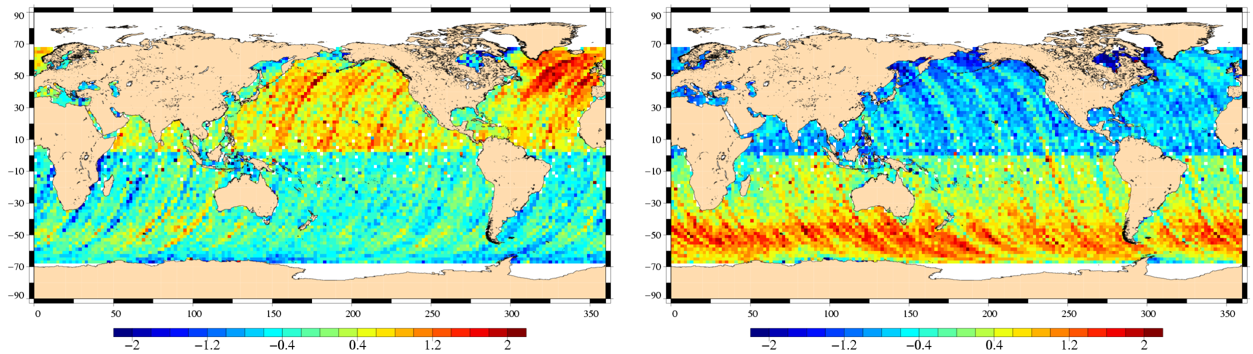

Figure 39: *Map of (T/P−Jason-1) SSH differences separating ascending and descending passes for cycles 1 - 21, using orbit based on GRACE gravity model for T/P.*

Finally new SSB corrections have been computed on cycles 1-21 for TOPEX using RGDR, with the collinear method. For J1 the Venice SSB was used ([53]). These new TOPEX and J1 SSB models are now much closer than before. When applying them in the SLA calculation in addition to the new orbits and the new ranges (Figure 40), the discrepancies between J1 and T/P are reduced. However, an East/West patch (< 1cm) remains, but it is not correlated with SWH. The origin of this signal is explained by CNES and GSFC orbit, used respectively for J1 and TOPEX. Indeed, using GSFC orbit for Jason-1 similar to those used in RGDR TOPEX data, allows to remove this East/West signal (see [6]).

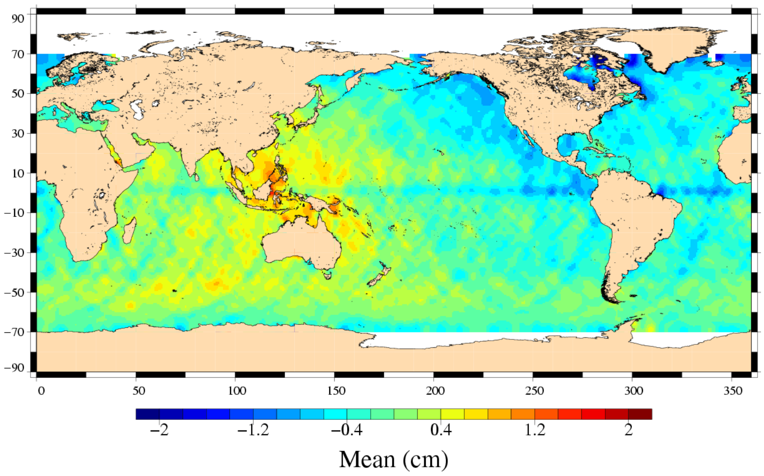

Figure 40: *Map of (T/P−Jason-1) SSH differences for Jason-1 cycles 1 - 21, using GSFC orbit based on GRACE gravity model for T/P, as well as recomputed Sea State Bias.*

6.2.2.3. Hemispheric SSH bias between Jason-1 and T/P

In order to further investigate hemispheric (T/P−Jason-1) SSH biases, its temporal evolution is presented in figure 41. It shows hemispheric differences between T/P and Jason-1, when separating northern and southern hemisphere. From the northern hemisphere to the southern hemisphere the (T/P−Jason-1) SSH bias estimates can thus differ by up to 1.5 cm. These hemispheric differences seem consistent from one cycle to another. The use of more homogeneous altimeter standards between Jason-1 and T/P has considerably lowered the difference between northern and southern hemisphere on the whole time period. Indeed, using orbits with ITRF 2005 reference system for both Jason-1 and T/P reduced these hemispheric differences.

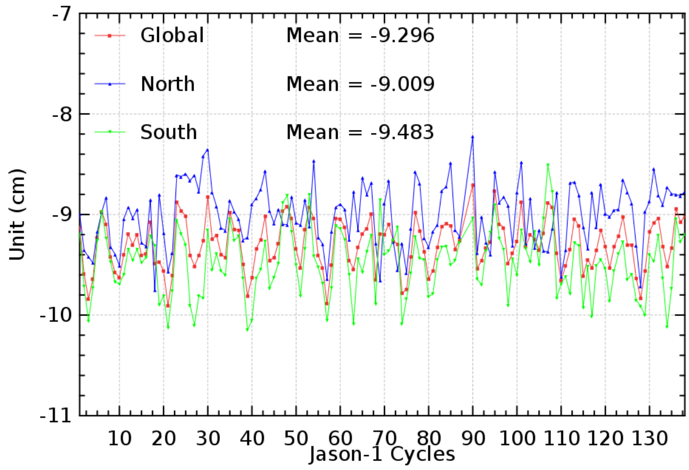

Figure 41: *Cycle per cycle mean of (T/P−Jason-1) SSH differences by hemisphere*

6.3. Sea level seasonal variations

From Sea Level Anomalies computed relative to the Mean Sea Surface CLS 2001 (Hernandez et al, 2001), the surface topography seasonal variations have been mapped from figure 42 to 50 for the overall Jason-1 data set. Major oceanic signals are showed clearly by these maps: it allow us to assess the data quality for oceanographic applications. The most important changes are observed in the equatorial band with the development of an El Niño in 2002-2003. The event peaked in the fourth quarter of 2002, and declined early in 2003. Conditions indicate an event of moderate intensity that is significantly weaker than the strong 1997-1998 El Niño (McPhaden,2003, [70]). End of 2007, a La Niña event is visible in Eastern Pacific on figure 47. It lasted till the mid 2008 (see [93]). From mid 2009 to spring 2010 a moderate El Niño event occured (see [94]). In second half of 2010 a moderate to strong La Niña event developped (see [96]).

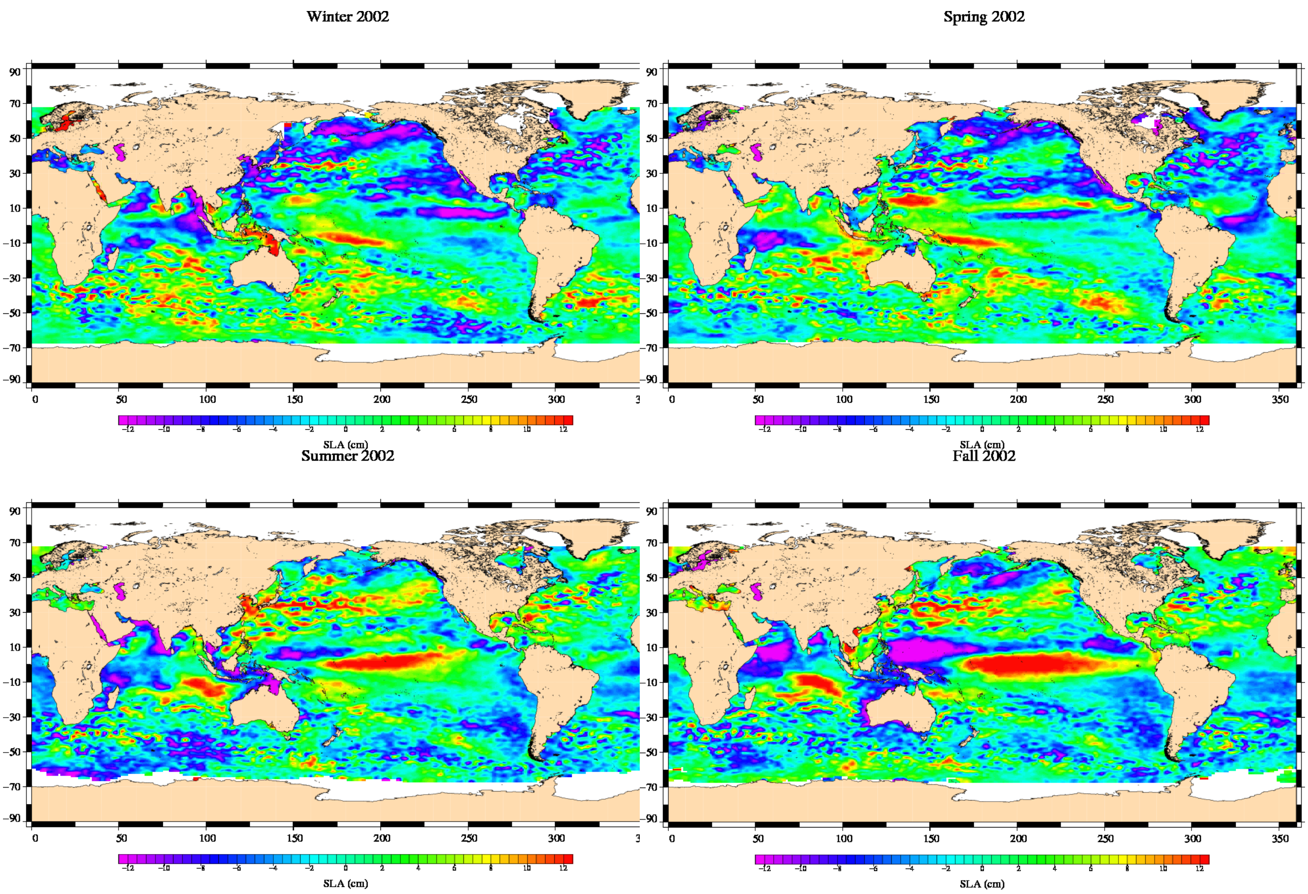

Figure 42: *Seasonal variations of Jason SLA (cm) for year 2002 relative to a MSS CLS 2001*

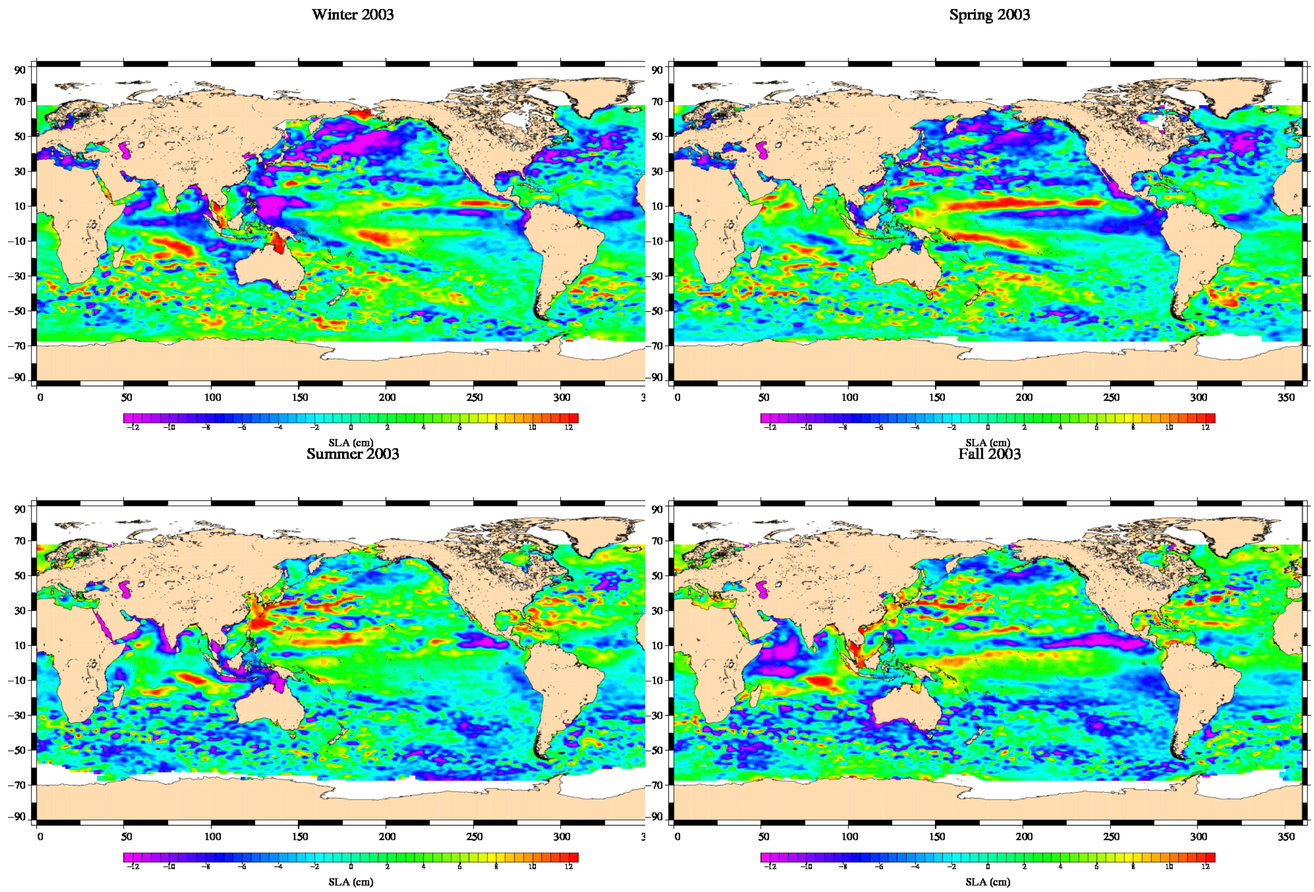

Figure 43: *Seasonal variations of Jason SLA (cm) for year 2003 relative to a MSS CLS 2001*

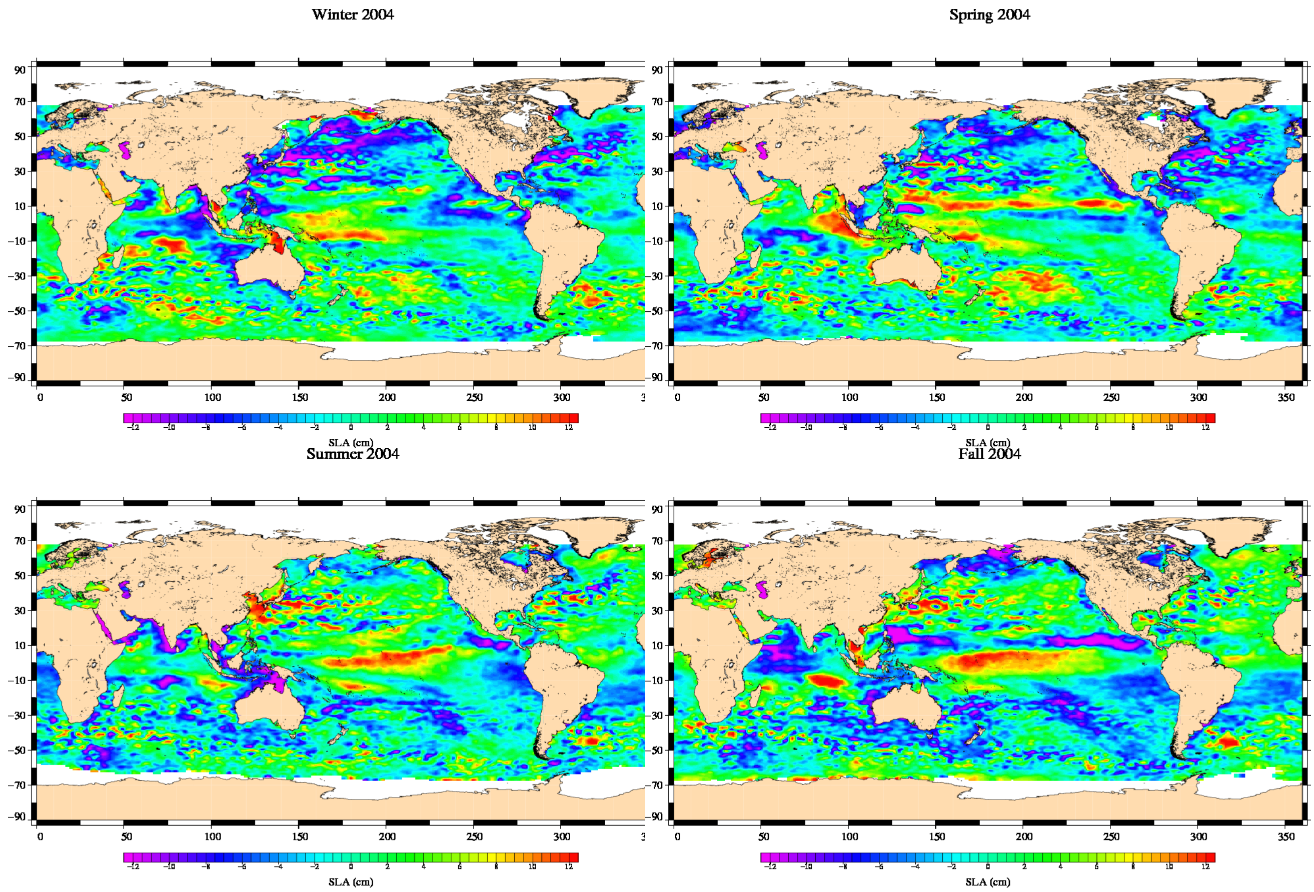

Figure 44: *Seasonal variations of Jason SLA (cm) for year 2004 relative to a MSS CLS 2001*

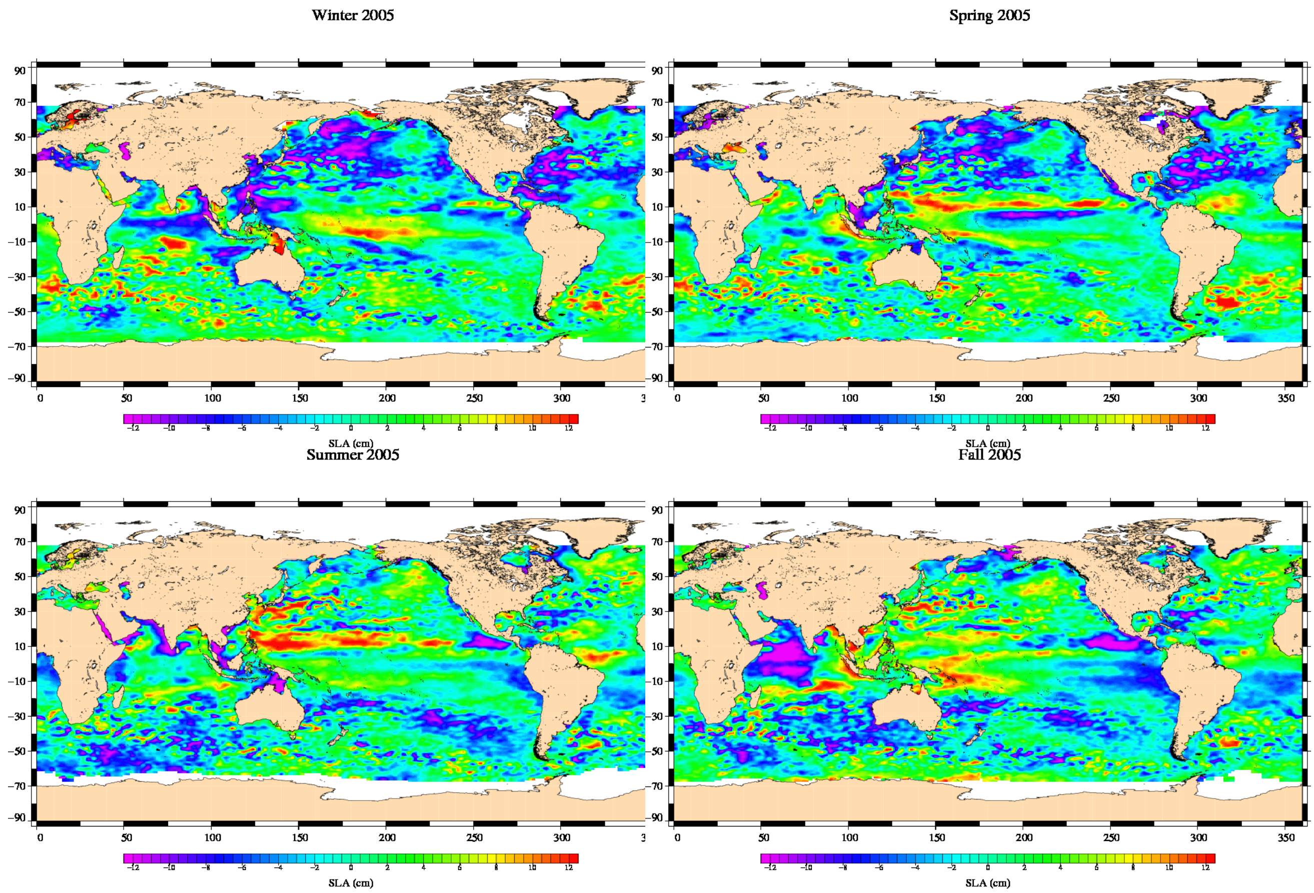

Figure 45: *Seasonal variations of Jason SLA (cm) for year 2005 relative to a MSS CLS 2001*

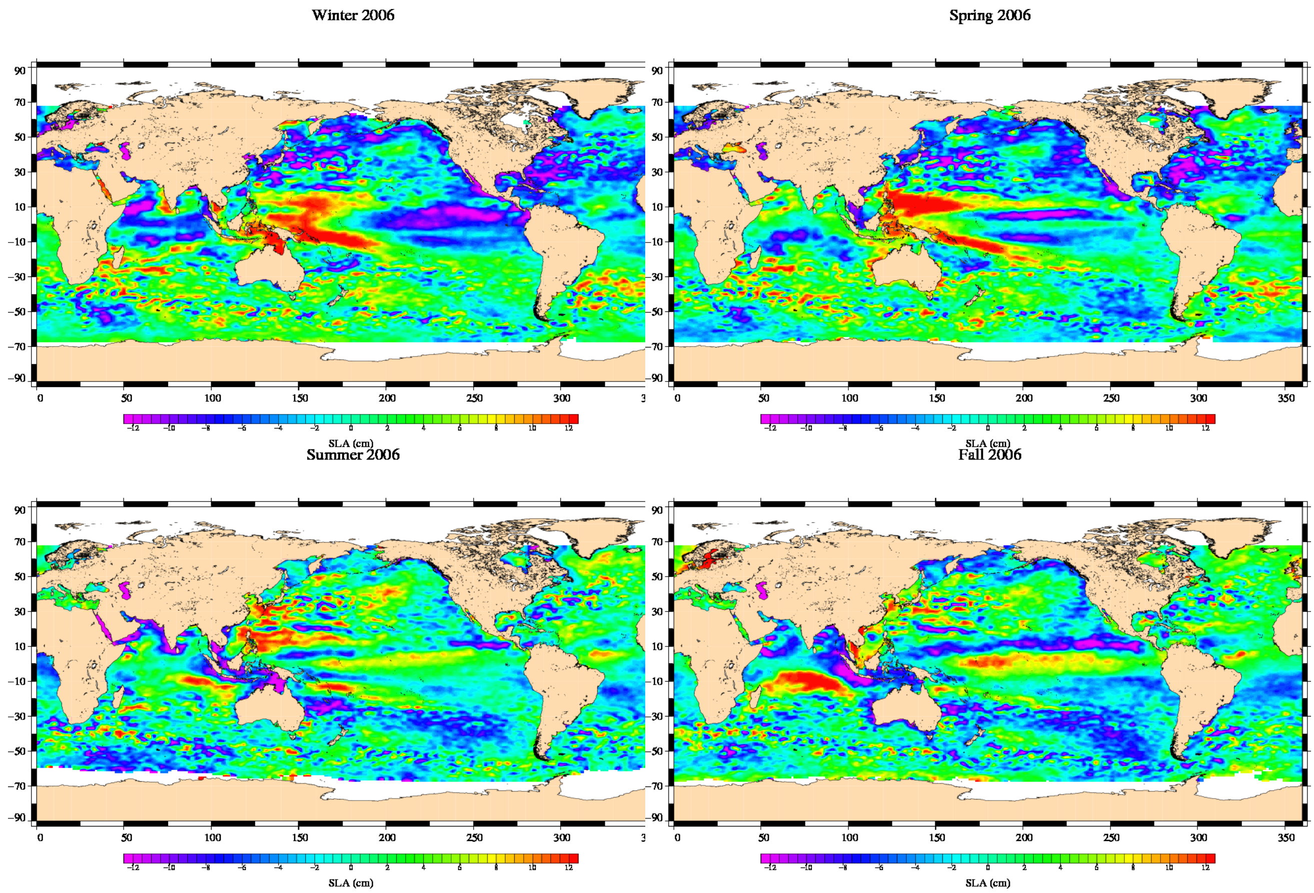

Figure 46: *Seasonal variations of Jason SLA (cm) for year 2006 relative to a MSS CLS 2001*

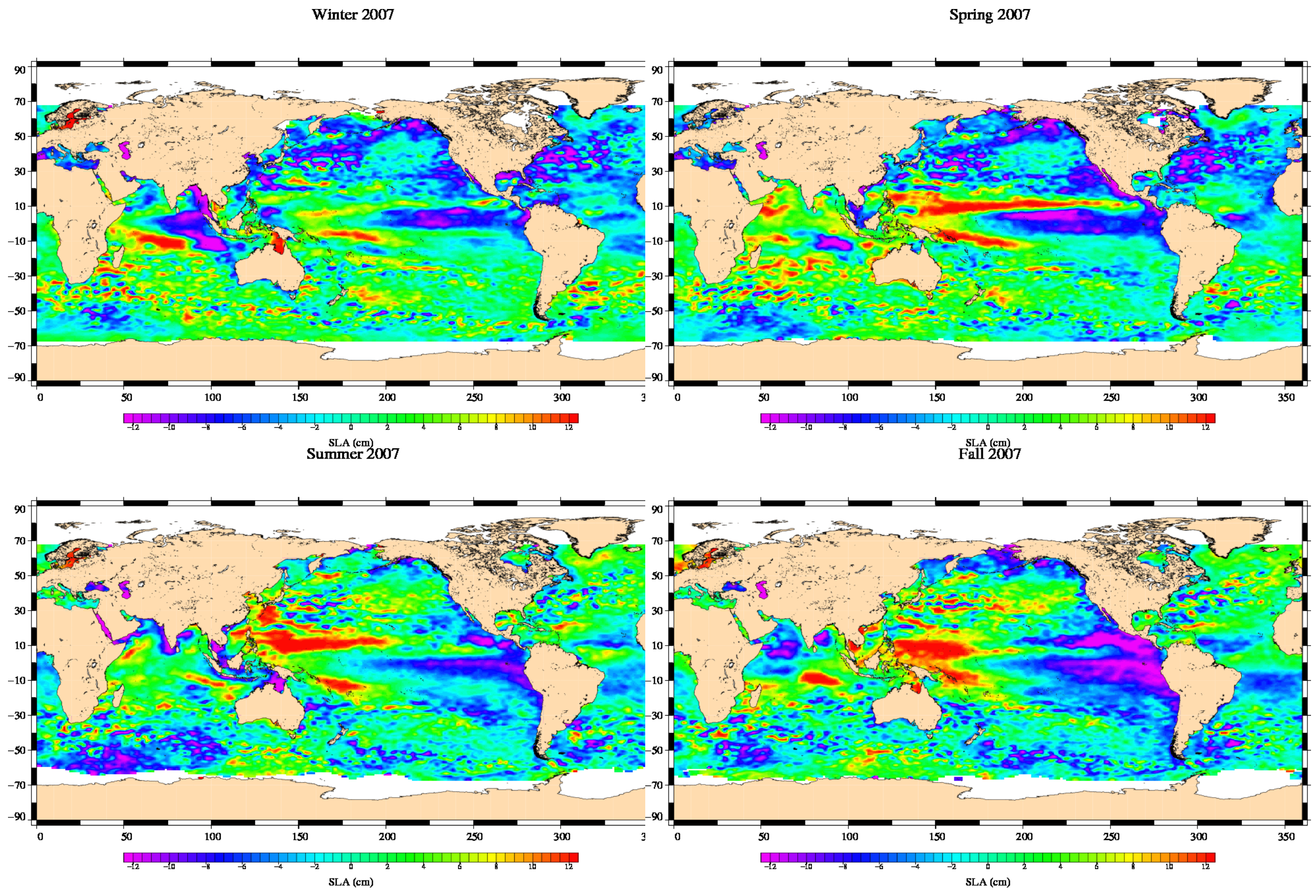

Figure 47: *Seasonal variations of Jason SLA (cm) for year 2007 relative to a MSS CLS 2001*

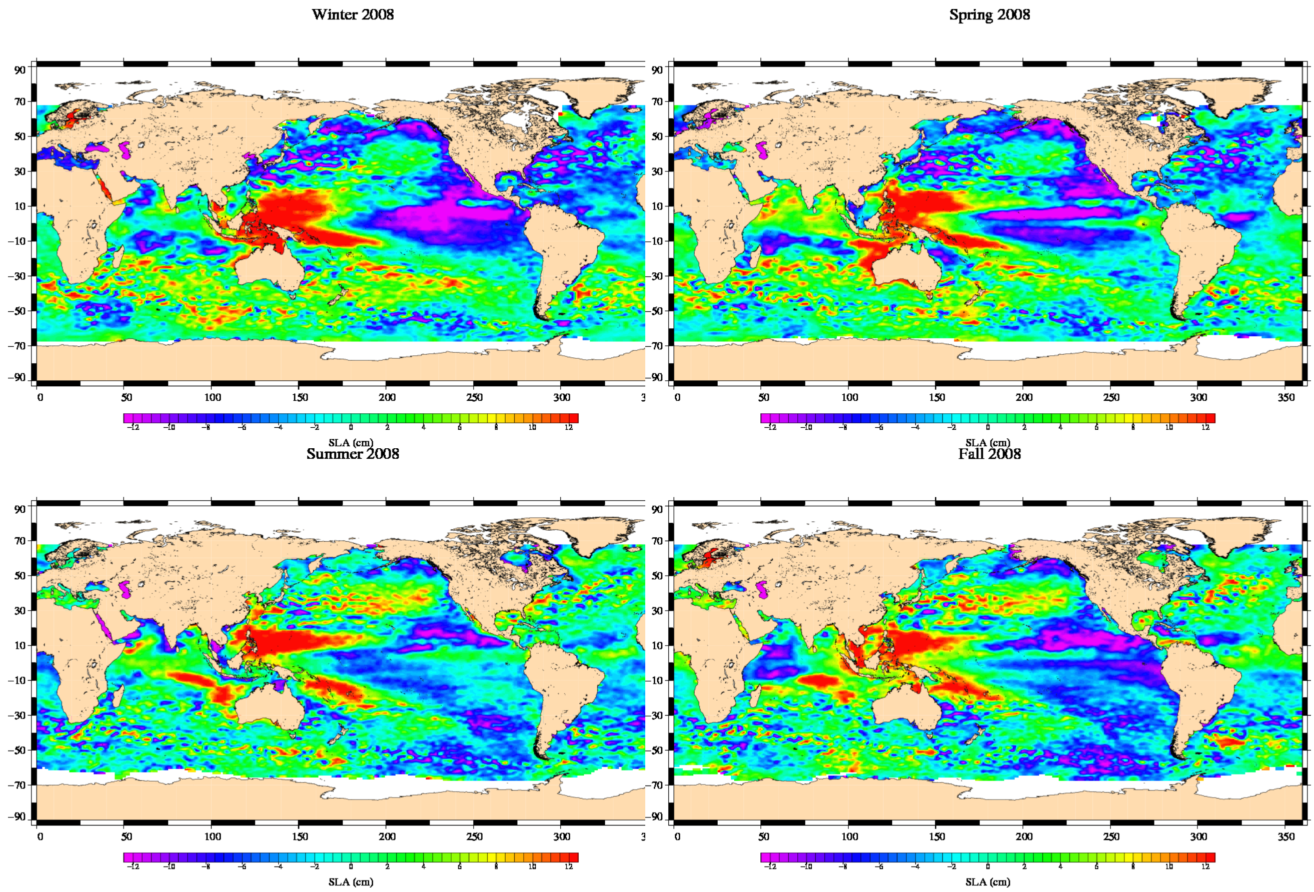

Figure 48: *Seasonal variations of Jason SLA (cm) for year 2008 relative to a MSS CLS 2001*

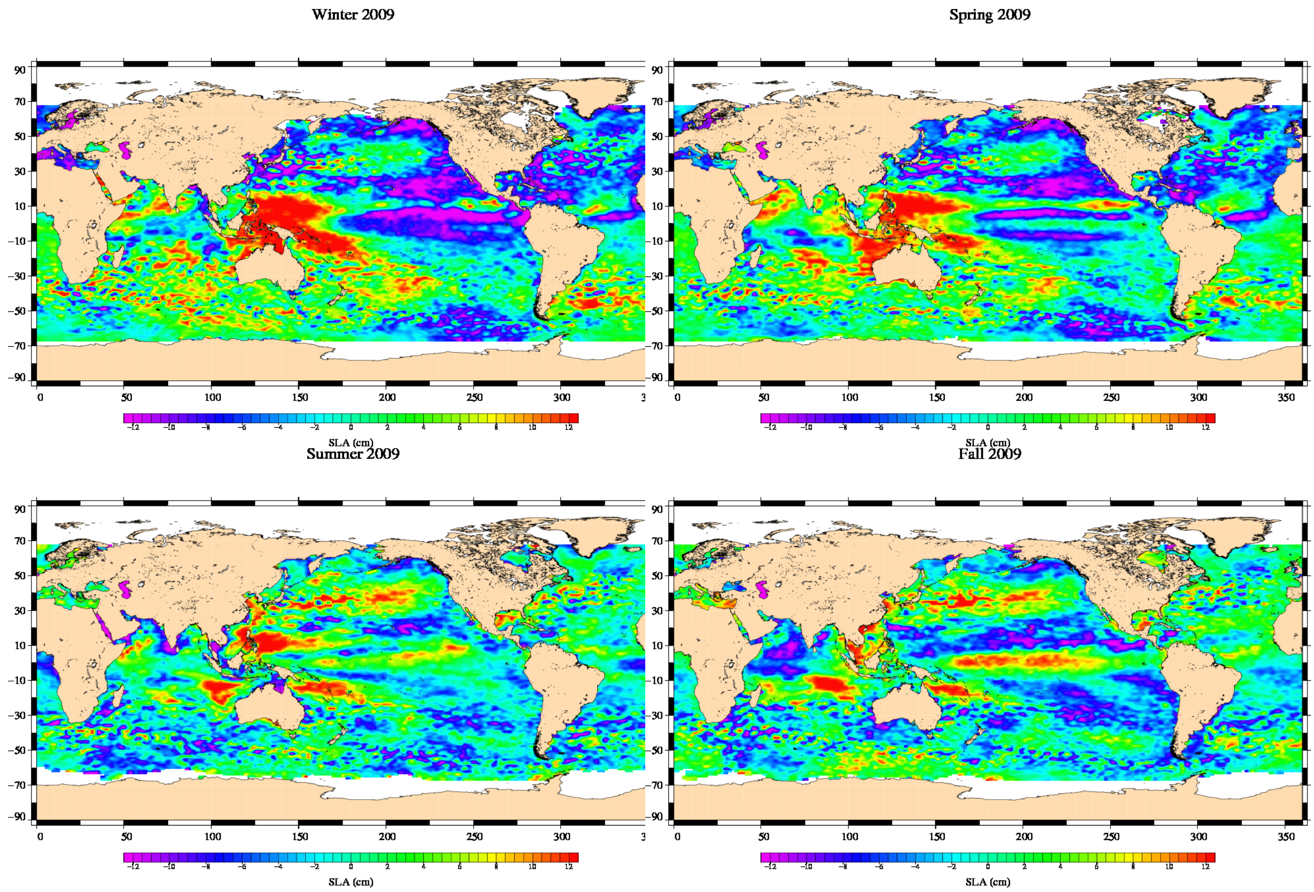

Figure 49: *Seasonal variations of Jason SLA (cm) for year 2009 relative to a MSS CLS 2001*

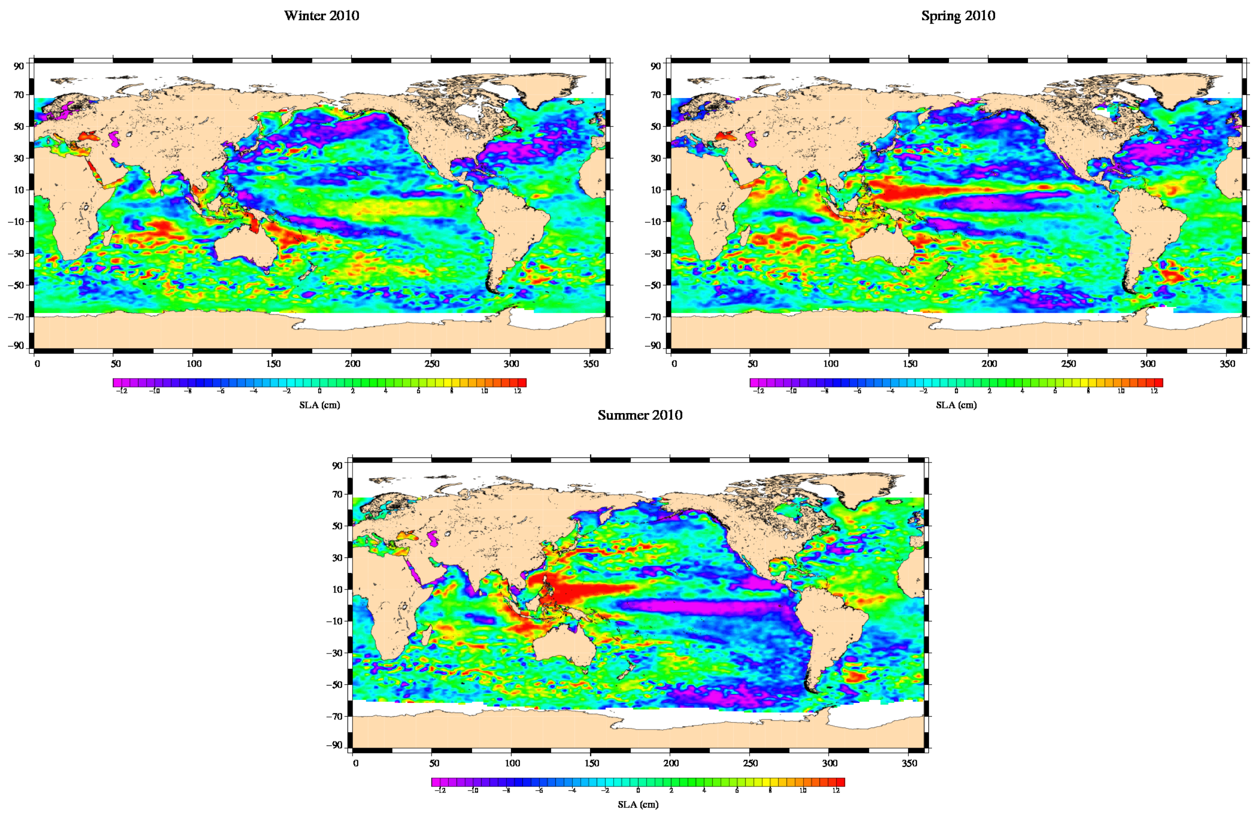

Figure 50: *Seasonal variations of Jason SLA (cm) for year 2010 relative to a MSS CLS 2001*

7. Global and regional Mean Sea Level (MSL) trends

7.1. Overview

Long-term MSL change is a variable of considerable interest in the studies of global climate change. Thus, a lot of works have been performed on the one hand to survey the mean sea level trend and on the other hand to assess the consistency between the MSL derived from all the operational altimeter missions. Besides, external data source have been used to assess the altimetric MSL evolution. The in-situ data provided by tide gauges and temperature/salinity (T/S) profiles have been used to compare the MSL. The main results derived from these works are summarized here (the complete analysis are available in the annual reports [97] and [55]). In addition, the Reynolds SST has been also monitored over the global ocean to analyze the MSL trend.

7.2. SSH applied for the MSL calculation

The SSH formula used to compute the MSL is defined for all the satellites as below :

$$SSH = Orbit - Altimeter\ Range - \sum_{i=1}^{n} Correction_i$$

with :

$$\begin{aligned}
\sum_{i=1}^{n} Correction_i \quad = \quad & Dry\ troposphere\ correction\ new\ S1\ and S2\ atmospheric\ tides\ applied \\
+ \quad & Combined\ high\ resolution\ dynamical\ atmospheric\ correction \\
+ \quad & Wet\ troposphere\ correction\ (radiometer\ or\ ECMWF\ model) \\
+ \quad & Filtered\ dual\ frequency\ ionospheric\ correction \\
+ \quad & Non\ parametric\ sea\ state\ bias\ correction \\
+ \quad & Geocentric\ ocean\ tide\ height,\ GOT\ 4.7 \\
+ \quad & Solid\ earth\ tide\ height \\
+ \quad & Geocentric\ pole\ tide\ height
\end{aligned}$$

The SSH formula has been modified or updated for each satellite in order to calculate the best MSL. Especially, stability problems of the radiometer wet troposphere correction have been taken into account :

- For Jason-1 : the radiometer wet troposphere correction is used even though 60-days signals are still detected since 2006.
- For Envisat : the ECMWF model wet troposphere correction is used to remove the effects of abnormal changes or trends observed on the radiometer wet troposphere correction, the USO

correction has been applied (drift and anomaly (see Envisat yearly report [42]). A reprocessed orbit (GdrC standard) was used.

- For T/P : the radiometer wet troposphere correction drift has been corrected with Scharroo's correction (Scharroo R., 2004 [84]), the relative bias between TOPEX and Poseidon and between TOPEX A and TOPEX B has been taken into account, the drift between the TOPEX and DORIS ionosphere corrections has been corrected for on Poseidon cycles. GSFC std0809 was used as well as a recomputed sea state bias ([92]).
- For Geosat Follow-On: the ECMWF model wet troposphere correction is used, the GIM model has been used for the ionospheric correction. Furthermore, GSFC std0809 and an updated sea state bias were used.

7.3. Analyze of the MSL trend

7.3.1. Global MSL trend derived from Jason-1 and T/P data

The global MSL trend derived from satellite altimetry - TOPEX/Poseidon, Jason-1 and Jason-2 - is now used as the reference for climate studies. A SSH bias of 8.45 cm has been applied on Jason-1 data to link it to TOPEX/Poseidon and a bias of 7.46 cm to link time series from Jason-1 and Jason-2 (see also Aviso web site http://www.aviso.oceanobs.com/en/news/ocean-indicators/mean-sea-level/). These biases have been calculated using the verification phase where Jason-1 and T/P (respectively Jason-2 and Jason-1) were on the same orbit. This allows us to compute accurately the SSH bias. This MSL plotted on figure 51 highlights a global trend of 3.28 mm/yr (post glacial rebound of -0.3 mm/yr was taken into account ([68])). However, the MSL rise is lower and very weak from the end of 2005 to the end of 2007. During this period, only Jason-1 measurements are available, thus the comparisons with T/P MSL is not possible to confirm this behavior. But the comparisons with other satellites and in-situ data as described further, do not evidence an abnormal drift on Jason-1 measurements. This MSL trend change might be explained by the very strong "La Niña" event which occurred in 2007 and beginning of 2008. Indeed, the MSL started to rise again in 2008.

7.3.2. Regional MSL trends derived from AVISO merged products

The AVISO merged products are used to compute the regional MSL trends. Thanks to the high resolution of their grids (0.5 degrees), the MSL regional trends can be calculated with a good resolution. This allows to assess very well the variability of regional slopes as plotted on map 52. Local slopes range between ±10mm/yr with large structure in main oceans, especially in Pacific Ocean. This kind of map brings a lot of information about the regional MSL evolution, which have to be analyzed in details: such as the long term evolution of oceanic circulation, such as the intensity of geostrophic currents, interannual oscillations (decadal, Madden-Julian oscillations for example).

7.4. Multi-mission comparisons of global MSL trends

The MSL has been monitored for each satellite altimeter over global ocean in order to assess the global MSL trend and also to detect any anomalies or any drifts on each MSL series. These different MSL have been plotted in figure 53, after removing annual and semi-annual signals, and filtering

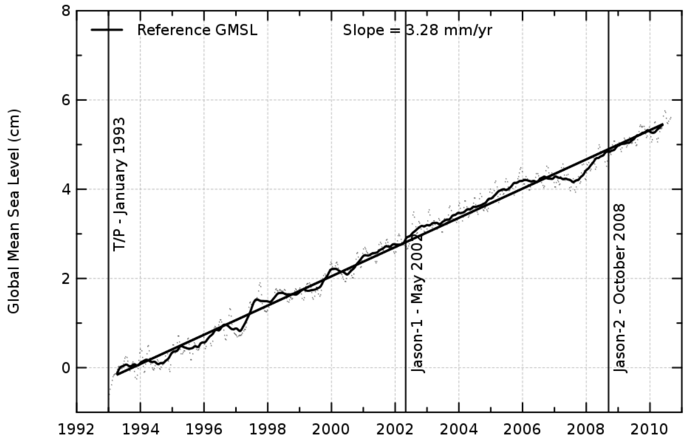

Figure 51: *Global MSL trend derived from Jason-2, Jason-1 and T/P data*

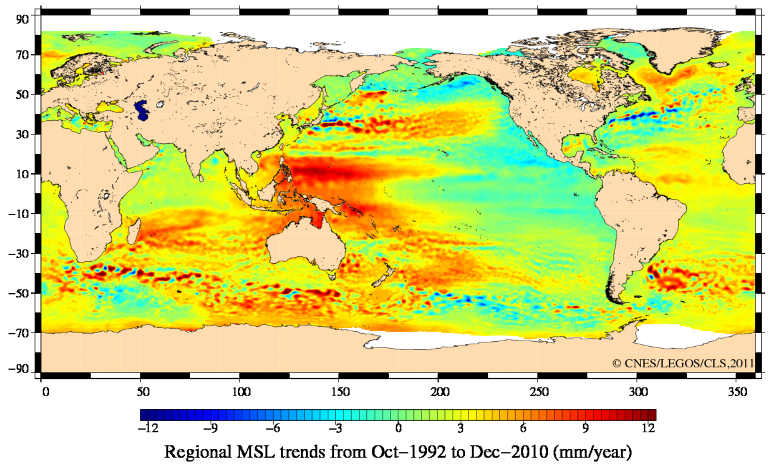

Figure 52: *Regional MSL trends derived from AVISO merged products*

out signals lower than 60 days. The T/P and Jason-1 slopes since the beginning of Jason-1 period are very close within about 0.1 mm/yr. Even though GFO slope is smaller by 0.3 mm/year over the Jason-1 period, it indicates a similar trend. Finally, only Envisat MSL shows a trend quite different with a global slope of 1.1 mm/yr. The estimation of the Envisat MSL seems impacted by an unexpected behavior on the early years. This item is described in detail in the Envisat annual report [66].

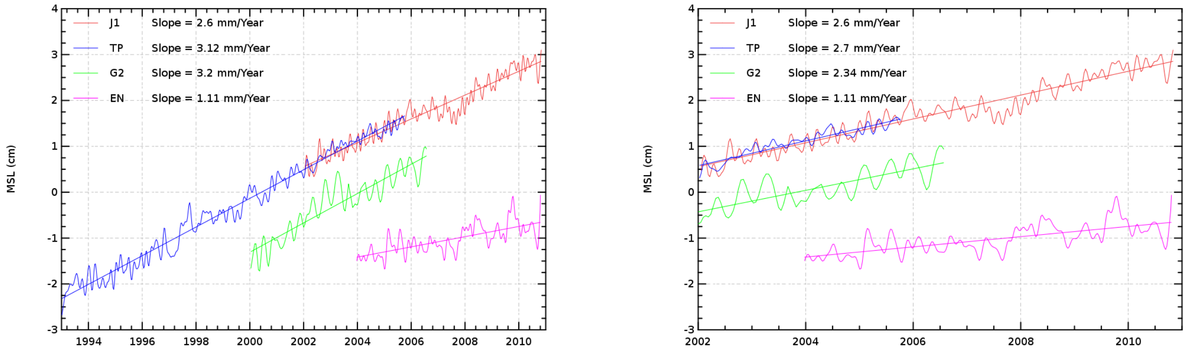

Figure 53: *Multi-mission MSL over global ocean since the beginning of T/P mission on the left and the beginning of Jason-1 mission on the right after removing annual and semi-annual signals. Post glacial rebound was not applied.*

7.5. External data comparisons

7.5.1. Tide gauges and T/S profiles

In order to assess the global MSL trend, comparisons to independent in-situ datasets are of great interest. Two methods have been developed in the frame of in-situ Cal/val and thoroughly described in annual reports ([97] and [55]). Firstly, TOPEX/Poseidon and Jason-1 altimetric data have been compared with tide gauge measurements thanks to a dedicated method which aims at detecting potential drifts in sea surface heights (SSH). The tide gauge network processed is the GLOSS/CLIVAR "fast" sea level database, formerly known as the WOCE network. Secondly, an innovating method has been developed using more than 3 000 free-drifting profiling floats of the ARGO network, which enables to assess the performance of altimetric measurements. These data have been compared to dynamic heights of the sea level computed from in-situ temperature/salinity profiles. Both methods complement each other since the first one using tide gauges only concerns coastal areas while the second one using T/S profiles is well widespread to get an assessment of the MSL in the open ocean. Nevertheless, the large coverage of T/S profiles is only available since 2004 and there is thus a non negligeable uncertainty on the estimation of the MSL trend.
From these comparison methods, SSH bias monitorings have been computed and are shown on figure 54. The upper bound of the error (LSR) on the assesment of the MSL drift computation is generally lower than 0.3 mm/yr (except for Jason-2 (0.7 mm/yr), which has only a short time serie of 2.5 years). MSL slope differences between insitu and altimeter data vary between 0 and 2.5 mm/yr and result from both the error on datasets and the intrinsic error of the method (0.5 mm/yr), partly linked to the colocation of the altimetric and in-situ measurements in space and time. Comparison with different types of in-situ data is the only way efficient enough to detect potential anomalies in altimetric records and it provides an upper bound of the error of the global MSL trend.

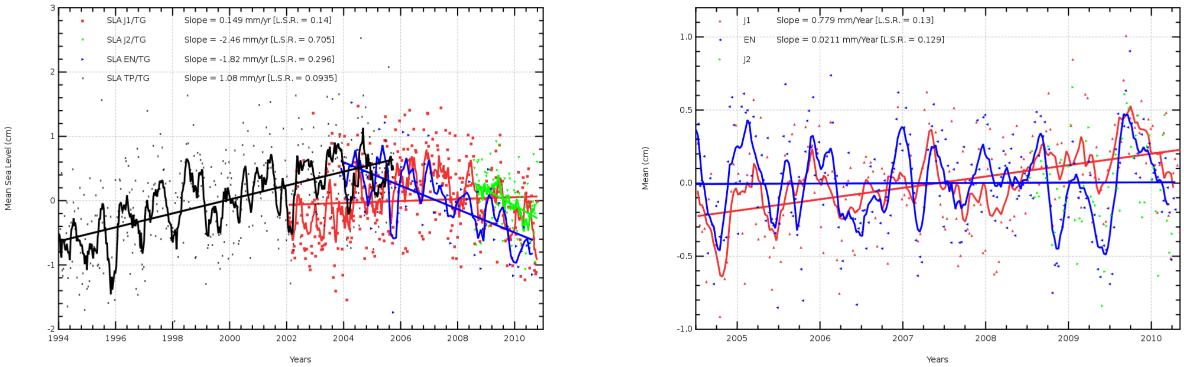

Figure 54: *Altimetric MSL drifts using tide gauges measurements (left) and T/S profiles (right)*

7.5.2. Reynolds's SST

The Reynold's SST has been monitored over the 18 year period from 1993 to 2010 along the T/P and Jason-1 tracks. It is compared with the reference MSL in figure 55, after removing annual signal and semi-annual signal. In order to compare the dynamic of the MSL and SST increases, the SST scale has been adjusted on the MSL scale so that the SST trend and the MSL trend are visually the same. The mean SST rises by less than 0.01 Celsius degree/yr with a dynamic much stronger than the MSL. In particular, the signatures of the 1998 "El Niño" and 2008 "La Niña" / ENSO events are more visible.

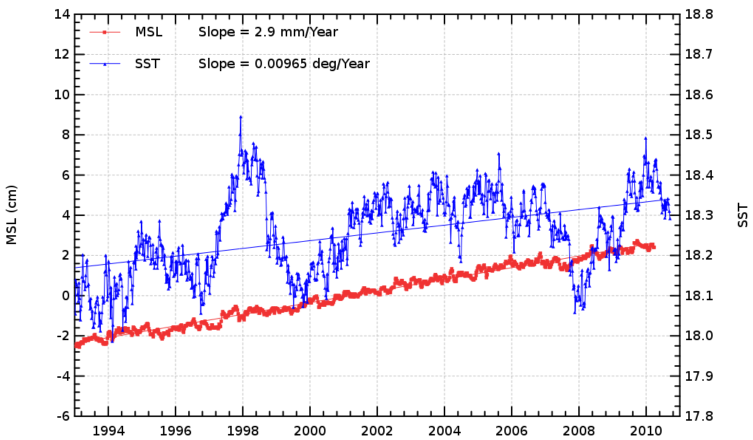

Figure 55: *Comparison of MSL and SST trend over global ocean for the Topex/Jason-1 period*

8. Particular Investigations

This sections contains some investigations led on Jason-1 data in 2010 such as the analysis of the 59-day signal on the MSL (see also [9]), the wind speed evolution over ocean (see also [10]) and the comparisons between the ITRF2005 and 2008 solutions for Jason-1&2 data.

8.1. Analysis of 58.74-day signal observed on the MSL derived from Jason-1&2 and TOPEX data

To date, the global Mean Sea Level (MSL) curve derived from Jason-1 and Jason-2 data highlights a periodic signal close to 60-days with amplitude significantly stronger than for the TOPEX MSL curve (4 mm for Jason-1 or Jason-2 and 1.5 mm for TOPEX) whereas similar altimeter standards are used for all satellites (figure 56). In fact, the exact period of this signal is 58.74 days. It corresponds to the aliasing of a semi-diurnal periodic signal (12 hours) with the ground repetitivity of Jason-1 and TOPEX missions (9.91 days).

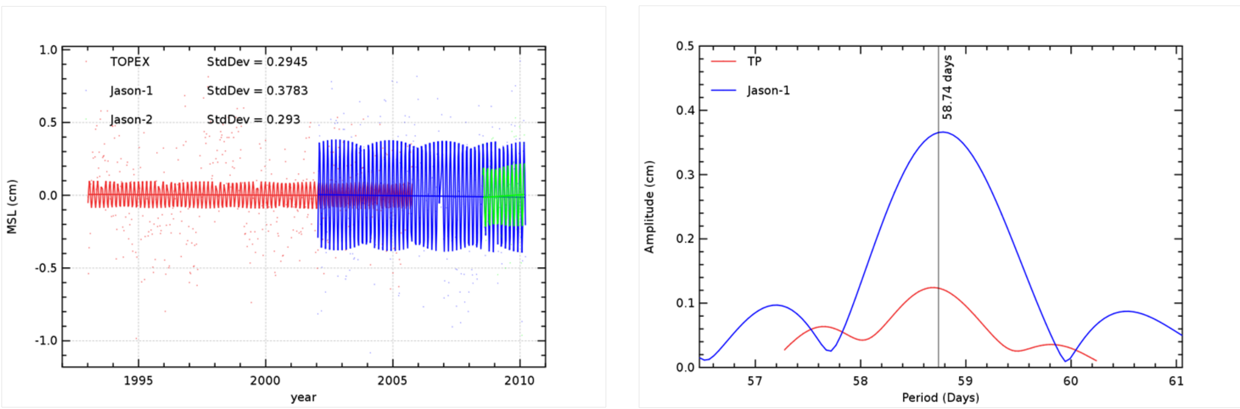

Figure 56: *Left: 58.74-day signal on global MSL after removing the global trend. Right: Periodogram on Jason-1 and TP MSL focused on 58.74-day signal.*

The first objective of this study is to describe accurately this 58.74-day signal observed on the MSL, estimating its global and local amplitudes and testing its sensitivity to the period. As shown on figure 57, the map of the 58.74 amplitude signal of the difference between Jason-1 and TOPEX shows a stronger amplitude of the signal for Jason-1 (> 5 mm) generally between -40° and 40° of latitude. Moreover, the SSH differences between altimetry and tide gauges highlight a 58.74-day signal of about 3-4 mm for Jason-1&2 and 1 mm for TOPEX. Note that similar results are obtained when comparing altimeter data with tide gauges measurements (figure 58). This result is in agreement with previous analyses and proves that the 59-day signal is not a physical signal but an error on altimetry data.

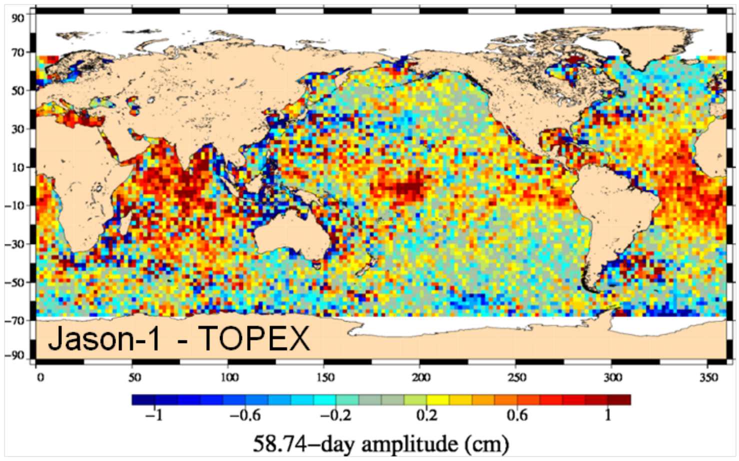

Figure 57: *Map of 58.74-day signal on the difference between Jason-1 and TOPEX.*

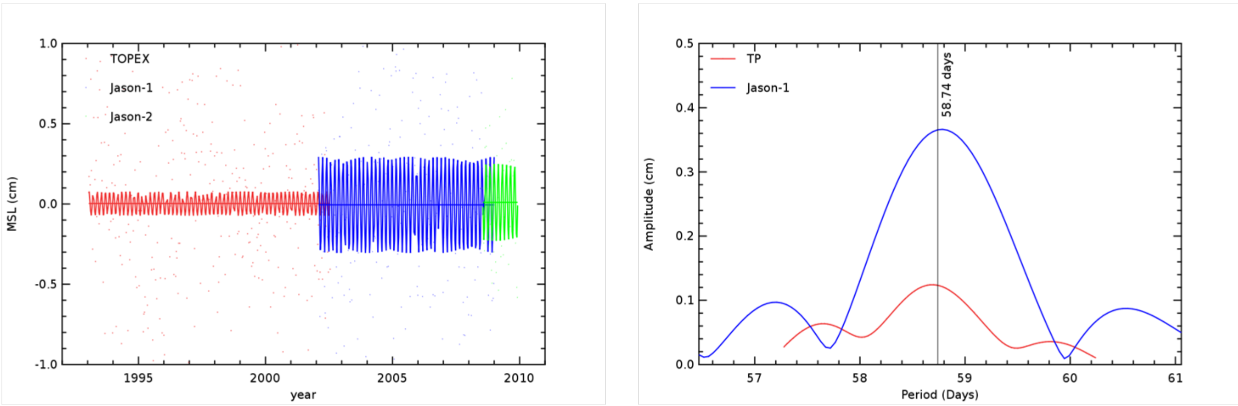

Figure 58: *Left: 58.74-day signal on altimetry/tide gauges SSH differences after removing the global trend. Right: Periodogram on altimetry/tide gauges SSH differences focused on 58.74-day signal.*

The second objective is to analyse the impact of changing corrections applied in the MSL calculation. We especially pay a great attention to oceanic tidal models which contain a strong semi-diurnal signal (S2 wave) and compare the impact of using GOT and FES tide solutions.
As shown on figure 59, the main part of the 58.74-day signal observed on the Jason-1 MSL is due to the use of GOT models in the SSH calculation while FES04 model allows us to significantly reduce down to 0.5 mm the 58.74-day signal on Jason-1 MSL.

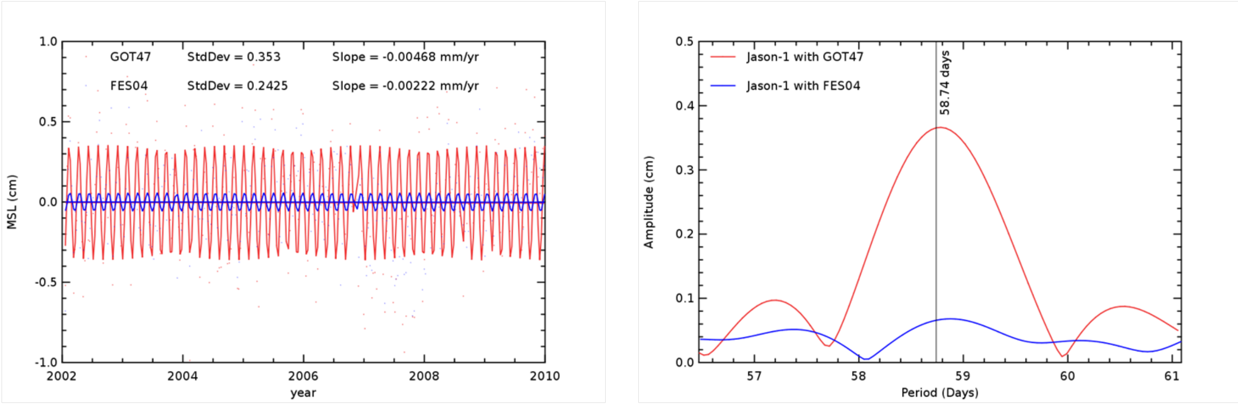

Figure 59: *Left: 58.74-day signal on Jason-1 global MSL after removing the global trend. Right: Periodogram on Jason-1 MSL focused on the 58.74-day signal.*

Using a hydrodynamical model without altimetry assimilation, a 3 mm stronger 58.74-day signal is highlighted on TOPEX MSL than in Jason-1 MSL (figure 60). The main result is that MSL errors on TOPEX for the 58.74-day signal have been likely assimilated by GOT. However, FES04 may have also assimilated TOPEX data with the same errors but this model is less sensitive to altimetry data assimilation than GOT (stochastical model), explaining its better behavior concerning the 58.74-day signal.

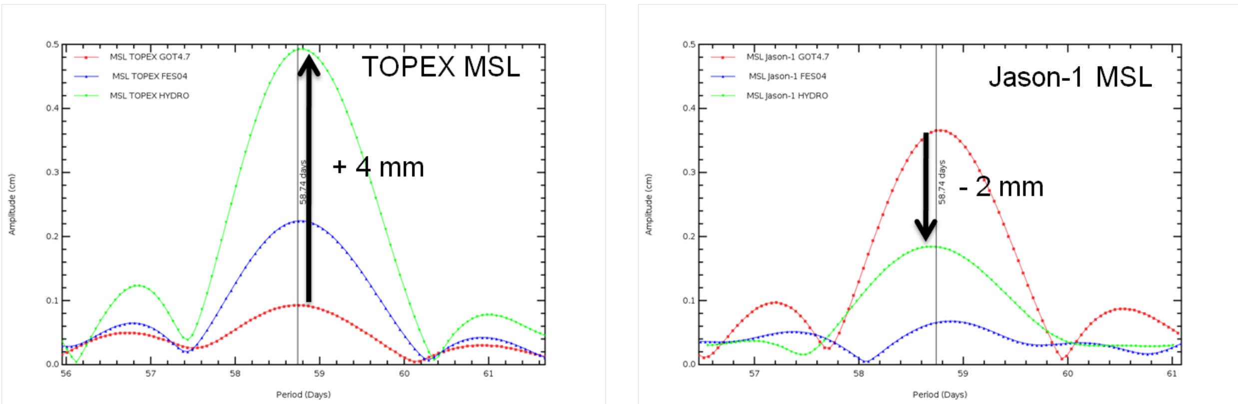

Figure 60: *Sensitivity of oceanic tide models on the 58.74-day signal. Left: TOPEX. Right: Jason-1.*

For TOPEX, a CG_RANGE_CORR correction is available in MGDR. It provides a correction to altimeter tracker range for center of mass movement caused by solar array motion and satellite roll and pitch. This correction has to be either added to the range to correct it or substracted from Sea Surface height. Figure 61 shows Orbit - range - MSS differences between Jason-1 and TOPEX during Jason-1 verification phase when direct comparison was possible. Difference is plotted in function of local time. A 12 h signal is visible. Applying the CG_RANGE_CORR correction as advised in the Handbook, increases the observed signal (blue curve), whereas applying it with the opposite sign (green curve), reduces the signal. This seemed to indicate that the CG_RANGE_CORR correction has been applied with a bad sign.
Nevertheless, at 2010 OSTST meeting, Zelensky ([104]) showed that CG_RANGE_CORR correc-

tion is valid. It might be that other thermal effects are correlated at the same frequency (12h) and are not yet corrected for.

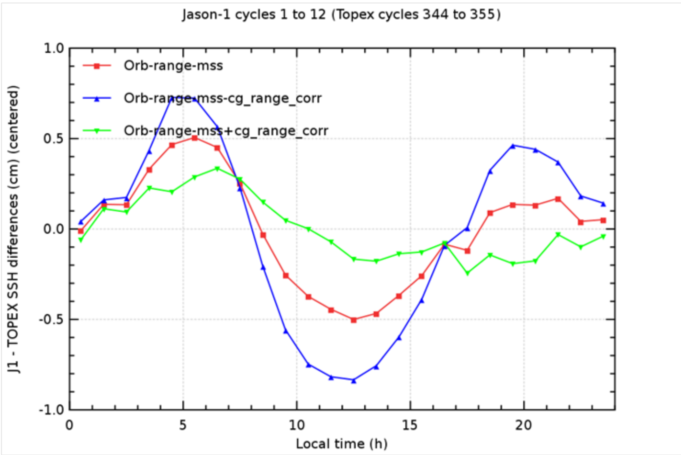

Figure 61: *[Orbit -Range -MSS] differences between Jason-1 and TOPEX applying CG_RANGE_CORR with its current sign (blue curve), its opposite sign (green curve) or without applying it (red curve).*

8.2. Analysis of wind speed evolution over ocean derived from altimeter missions and models

This study aims at analysing and comparing wind speed evolution derived from altimeter missions and different models (ECMWF, ERA-interim, NECP reanalysis) over all the altimeter period and over ocean surface. Thus the main objectives are:

- Analyzing the stability of Jason-1 and Envisat Sigma 0 thanks to wind speed cross-comparisons between both altimeters and reanalyzed models such as ERA-interim (ECMWF) and NCEP
- Extending the analysis to TOPEX, ERS-2 and Jason-2 Sigma0
- Deducing the evolution of wind speed over ocean from 1993 onwards

Note that wind speed is a product of the altimeter processing, not assimilated in models such as ECMWF for instance, mainly used to derive the SSB. But this parameter can be very important in the frame of the Climate evolution. Indeed, the ECMWF model is an operational model and it is impacted by jumps as a result of model evolutions. In addition, ERA-interim and NCEP wind speed reanalyses have not assimilated altimeter parameter, but they have both assimilated QuickSCAT data.

Moreover, concerning the computation of the wind speed of the main altimeter missions, note that:

- Envisat wind speed has been recomputed with the same algorithm (Jensen, 2006) over the whole mission period
- Jason-1 wind speed is derived from GDR-C release (Collard algorithm)
- TOPEX wind speed has been recomputed with Gourrion algorithm

As shown on figure 62, since global ocean altimeter and model wind speed are very well correlated together at small temporal scales (<1yr), it is possible to detect small jumps, oscillations or drifts. First, global ocean wind speed differences between altimeters (Jason-1, Envisat) and models (NCEP,ERA-interim) have been computed and show that the NCEP model is more consistent than ERA-interim with altimeter wind speed in terms of global annual signal. After adjusting periodic signals, drifts are highlighted on Jason-1 and Envisat wind speed by cross-comparisons with models (figure 62 top):

- For Jason-1 this drift, detected on 2005, is about 10 cm.s-1
- Concerning Envisat, the drift (about 10 cm.s-1) is detected on 2003

The global ocean wind speed differences have been calculated from TOPEX and ERS-2 wind speed too (figure 62 bottom). For TOPEX, a jump is detected in 2004 and strong oscillations are highlighted between 20 and 30 cm.s-1 between 1996 and 1999 and 2001. Indeed, a strong drift is finally observed (+2.8 cm.s-1/yr). By correcting the TOPEX-B Sigma0 by delta correction not applied in M-GDR and proposed by D.W. Lockwood (NASA, 2006), oscillations are reduced but the slope remains strong.
For ERS-2, although a strong anomaly of 40.cm.s-1 is detected in 2001, differences are more stable and do not display patterns observed with TOPEX. Thus a low negative drift is displayed.

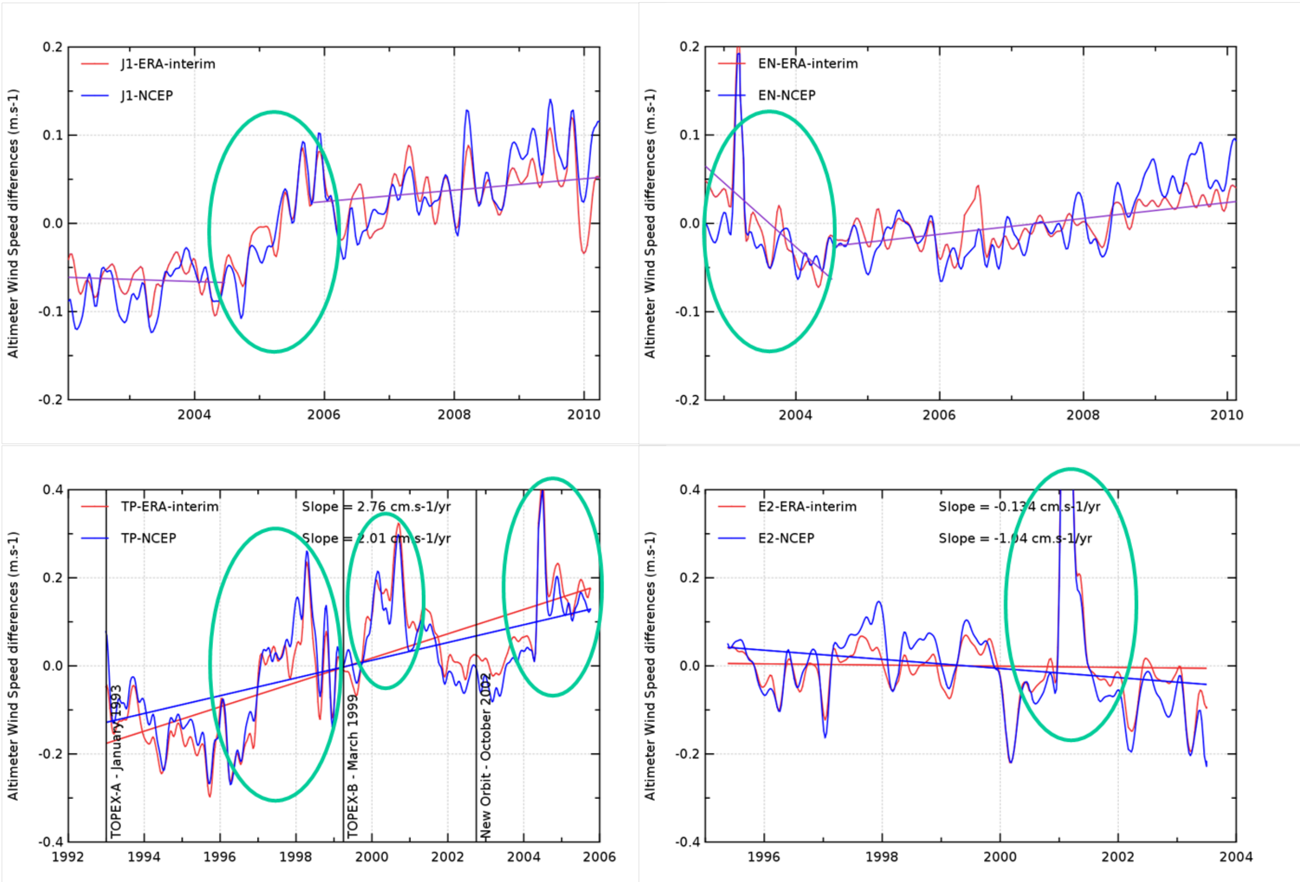

Figure 62: *Monitoring of the ocean wind speed stability on the Jason-1 (top left), Envisat (top right), TOPEX (bottom left) and ERS-2 (bottom right) time period.*

Next to these first results, it is to be noticed that a global 10 cm.s-1 wind speed jump corresponds to a 0.025 dB Sigma0 jump. Such small jumps are inside Sigma0 stability requirements but they could impact both the MSL accuracy through the SSB correction and the wind speed calculation and long-term evolution.

Concerning the MSL issue, the impact is low but not negligible. Indeed, a 10 cm.s-1 wind speed drift in 2005 on Jason-1 corresponds to a jump of +0.6 mm on the SSH. In the same way, a +2.5 cm.s-1/yr wind speed drift on TOPEX represents a drift of +0.15 mm/yr on the MSL. Moreover, these Sigma0 instabilities can also highlight instrumental anomalies impacting MSL evolution more strongly such as the end of the TOPEX-A time period or the Envisat MSL drift in 2003 for instance.

Thanks to this study, we can also characterize the ocean wind speed evolution better:

- As displayed on figure 63, a positive global trend of about +1 cm.s-1/yr seems to be emphasized from 1993 onwards

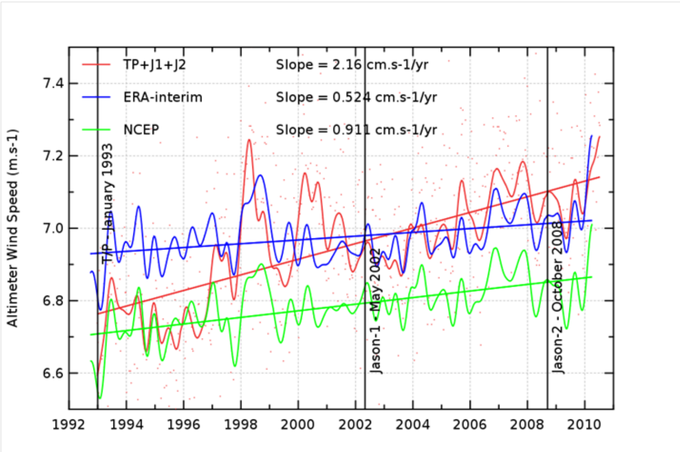

Figure 63: *Monitoring of the wind speed trends for TOPEX, Jason-1 and Jason-2 (red curve), ERA-interim model (blue curve) and NCEP model (green curve)*

- Local wind speed trends do not highlight the same spatial structures considering altimetry and models (± 5 cm.s-1/yr wind speed differences, see figure 64)

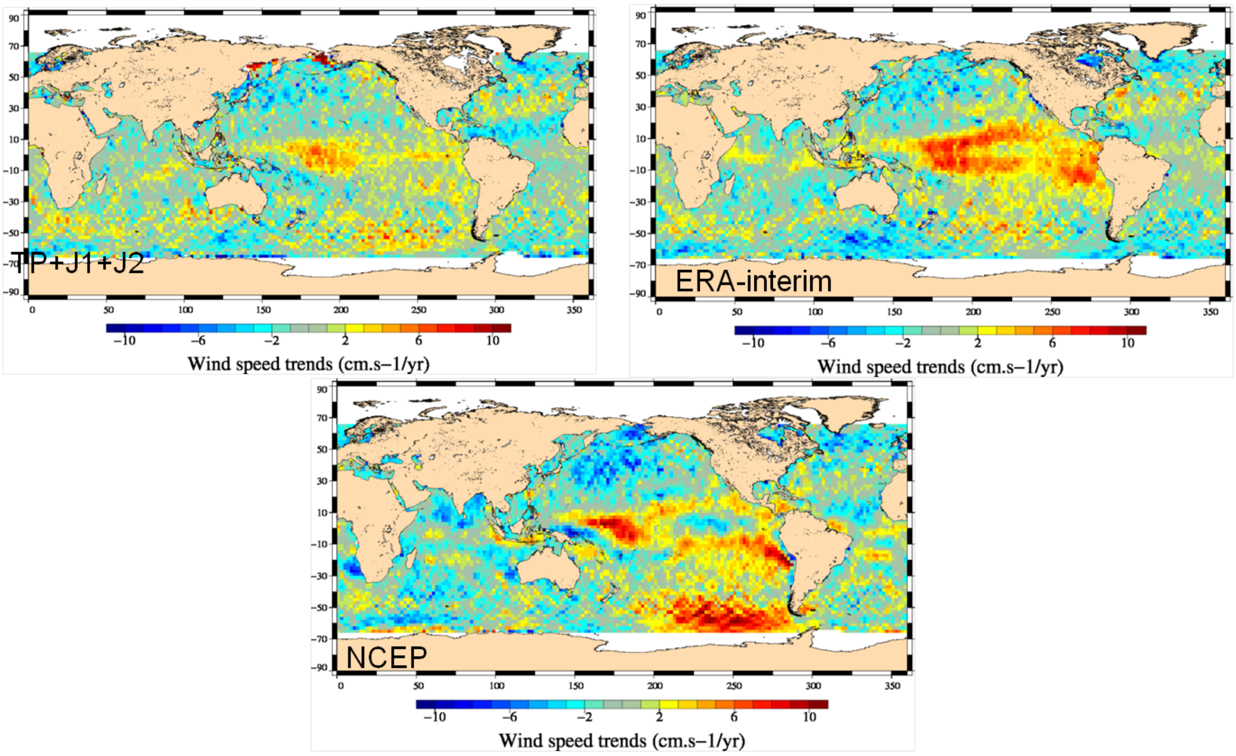

Figure 64: *Maps of the wind speed trends for TOPEX, Jason-1 and Jason-2 (top left), ERA-interim model (top right) and NCEP model (bottom)*

Finally, given these differences between models and considering the wind speed evolution as an indicator of the climate change, it seems important to improve the long-term stability of altimeter wind speed and therefore the sigma-0 parameter for climate studies.

8.3. Comparison between ITRF2005 and 2008 solutions for Jason-1 and Jason-2 orbits

Currently, POE available in GDR products uses ITRF2005 (international terrestrial reference frame). In the future, POE might use ITRF2008. CNES has produced 2 datasets of Jason-1 and Jason-2 POE orbits using Doris (Doppler Orbitography and Radiopositioning Integrated by Satellite) and SLR (Satellite Laser ranging) technics over a period of 70 cycles. Normally, for GDRs a tri-technic orbit is used (Doris, Laser and GPS). But as Jason-1 GPS receiver had reduced availability since August 2006 and finally failed to operate properly in April 2009, only Doris and Laser technics were used, in order to have a homogeneous timeserie. One set used ITRF2005, the other ITRF2008. Some results of orbit comparation can be found in [28]. In particular, [28] precises, that only the position and velocity coordinates of the DORIS and SLR stations differ between the ITRF2005 and ITRF2008 orbit solutions: the same stations and the same measurements are considered in the comparison. Hereafter, the 2 datasets are compared for Jason-1 and Jason-2 (see cycle numbers in table 5), in order to analyse the impact of the ITRF change on the sea surface height.

Mission	Orbit	Type	Cycles
Jason-1	DL_ITRF2005	Doris/Laser ITRF2005	001 - 020, 100 - 120, 200 - 220, 300 - 310
Jason-1	DL_ITRF2008	Doris/Laser ITRF2008	001 - 020, 100 - 120, 200 - 220, 300 - 310
Jason-2	DL_ITRF2005	Doris/Laser ITRF2005	001 - 068
Jason-2	DL_ITRF2008	Doris/Laser ITRF2008	001 - 068

Table 5: *O*verview of orbit types and cycle numbers used.

Mean of orbit differences (see figure 65) shows an expected north/south bias of about ± 5 mm for Jason-2 and about ± 3 mm for Jason-1. This difference might be related to different coverage of Doris network for Jason-1 and Jason-2, as well as different handling of SAA (South Atlantic Anomaly) stations.

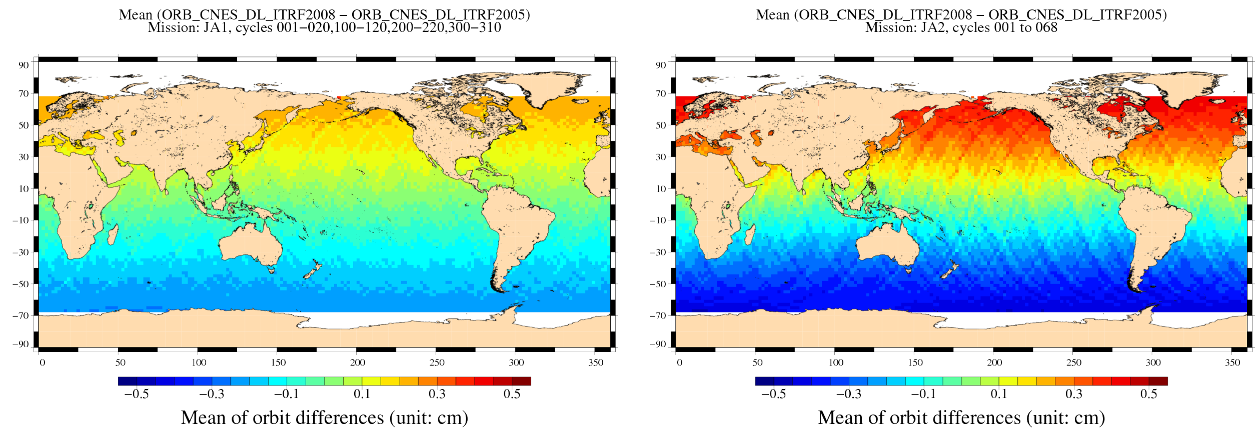

Figure 65: *Mean of orbit differences (ITRF2008 - ITRF 2005) for Jason-1 (left) and Jason-2 (right).*

Cyclic monitoring of differences of SLA variances (SLA variance using ITRF2008 orbit - SLA variance using ITRF2005 orbit) reveals an annual signal (see figure 66). It is especially well visible for Jason-2, as the study uses an uninterupted time-serie. This annual signal is not yet understood.

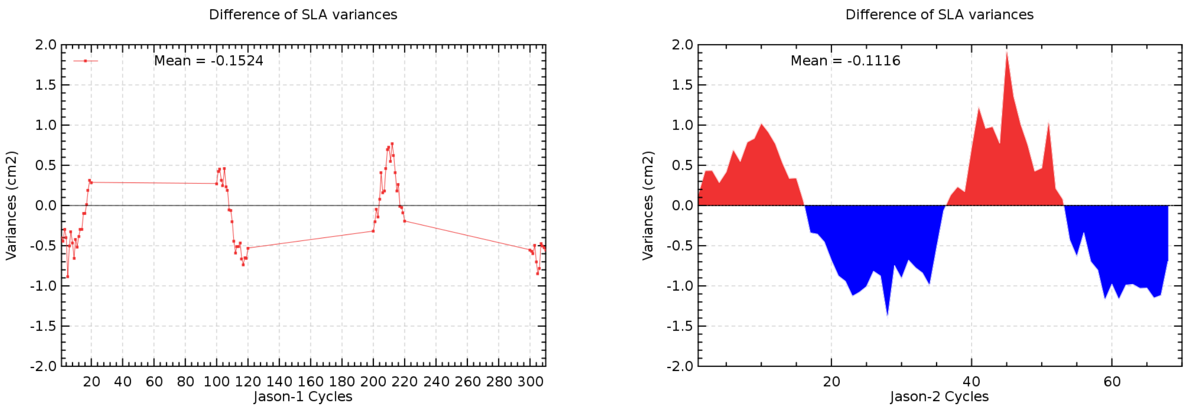

Figure 66: *Cyclic monitoring of SLA variance differences (ITRF2008 - ITRF 2005) for Jason-1 (left) and Jason-2 (right). Only data with abs(latitude) < 50°, bathymetry < -1000m and low oceanic variability were selected.*

Using either ITRF2005 or ITRF2008 orbit seems to have for Jason-1 no impact on performances of SSH differences at crossover points (see figure 67). Concerning Jason-2 a slight degradation seems to be visible. Nevertheless, the values are quite small and therefore not significant.

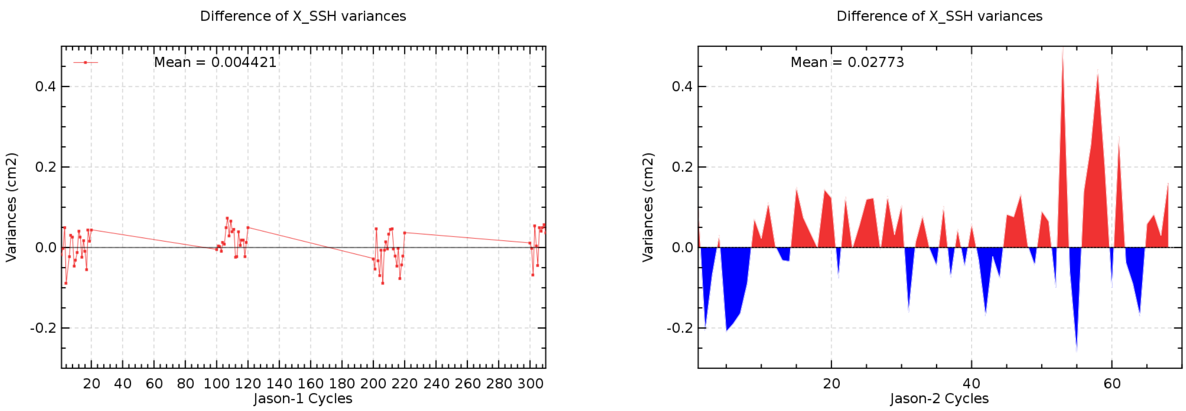

Figure 67: *Cyclic monitoring of SSH variance differences (ITRF2005 - ITRF 2008) at crossover points for Jason-1 (left) and Jason-2 (right). Only data with abs(latitude) < 50°, bathymetry < -1000m and low oceanic variablity were selected.*

Changes of ITRF version have generally an impact on MSL trend, when separating in northern and southern hemisphere. This was the case, when ITRF version changed from 2000 to 2005 (see [98]). Nevertheless, ITRF change from version 2005 to 2008 will have a very weak impact on North/South MSL trend, as shown on figure 68. MSL trend of northern or southern hemispheres are different, but using ITRF2005 or 2008 has no significant impact on the trends. Note that values from MSL trends of this study will not be the final values, as firstly the studied time series are shorter than 2 years and are even interupted for Jason-1. It is therefore difficult to adjust annual signals. Indeed, theoretical errors of the computation method are quite high, especially for the short Jason-2 period (about 1 mm/year). Secondly, the final orbits will include also GPS technic (in addition to DORIS and SLR technics).

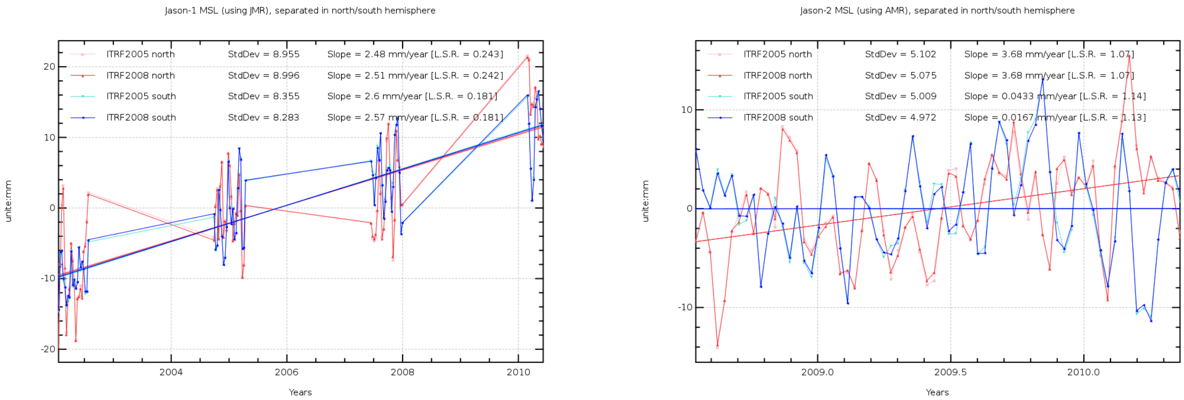

Figure 68: *Southern and northern hemisphere MSL trend using orbits based on ITRF2005 and ITRF2008 for Jason-1 (left) and Jason-2 (right). Annual and semi-annual signals are adjusted from combined Topex/Poseidon and Jason-1 time series.*

8.4. Events during 2010

During 2010, the Jason-1 satellite experienced several events, which had an impact on its data availability and quality. Several events are indicated by colored lines in figure 69.

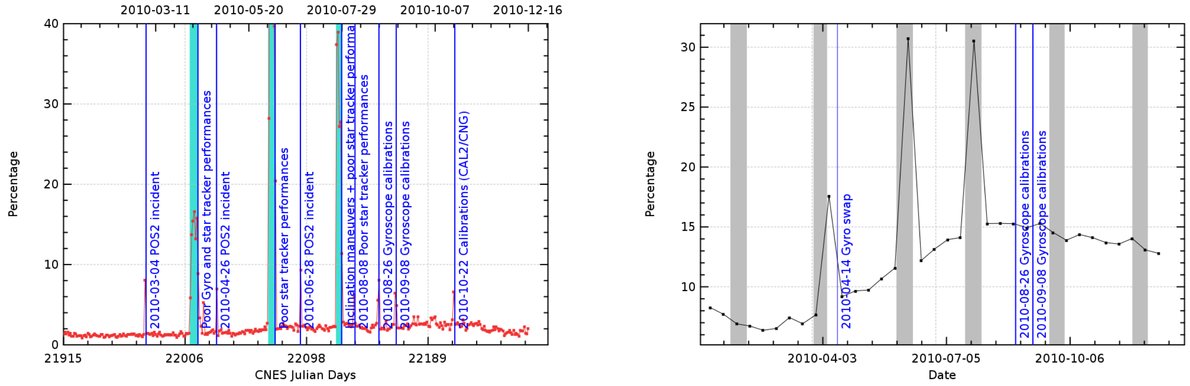

Figure 69: *Daily montitoring of missing ocean measurements (left) and cyclic monitoring of edited measurements (right) for Jason-1 during 2010. Gray stripes indicate periods, where Jason-1 is in fix mode.*

Due to poor star tracker performances related to beta angle values and also poor gyro wheel performances, Jason-1 experienced several periods of high off-nadir angles of the platform, especially when the satellite was in fixe mode (see figure 70). End of July / beginning of August, several inclination maneuvers were performed in order to deplete fuel. This had an impact on data quality, but also on data availability, as star tracker performances were poor.

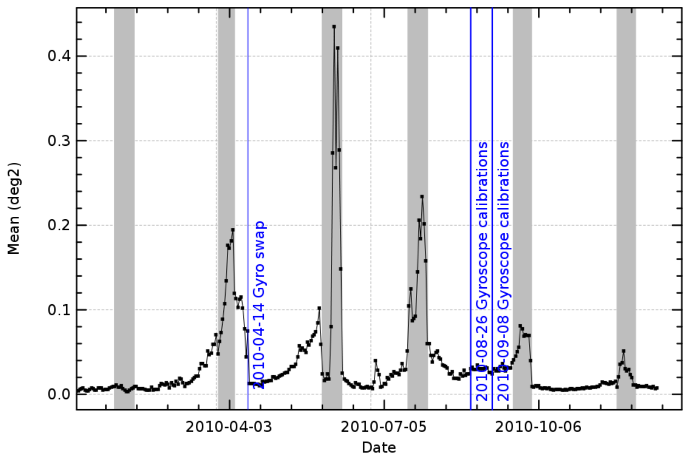

Figure 70: *Daily monitoring of Jason-1 apparent squared misponting from waveforms for 2010. Gray stripes indicate periods, where Jason-1 is in fix mode.*

8.4.1. Events of high mispointing

Since mid-march 2010, off-nadir angles of the platform were increased for Jason-1, which affected especially OSDR data, as they still use on-bord MLE3 tracking (which needs off-nadir angles < 0.4 deg). Therefore, when this threshold was exceeded, several passes had altimeter data at default value. In April (during cycle 304), off-nadir angles were such high, that altimeter lost several times tracking. Therefore, data gaps appeared, which also impacts IGDR and GDR data. Furthermore, gyroscope 1 showed poor performances during March and April. Therefore, a swap of gyroscopes was done on 2010-04-14.
Mispointing reached several times between April and October 2010 high values. During fall 2010, upload of new tables to the star trackers were done. For the last months of 2010, mispointing values were on an usual level again.

Relationship between mipointing and missing measurements, is shown for cycle 304 as an exemple. High mispointing values occured especially for local hours around 12h as shown in figure 71.

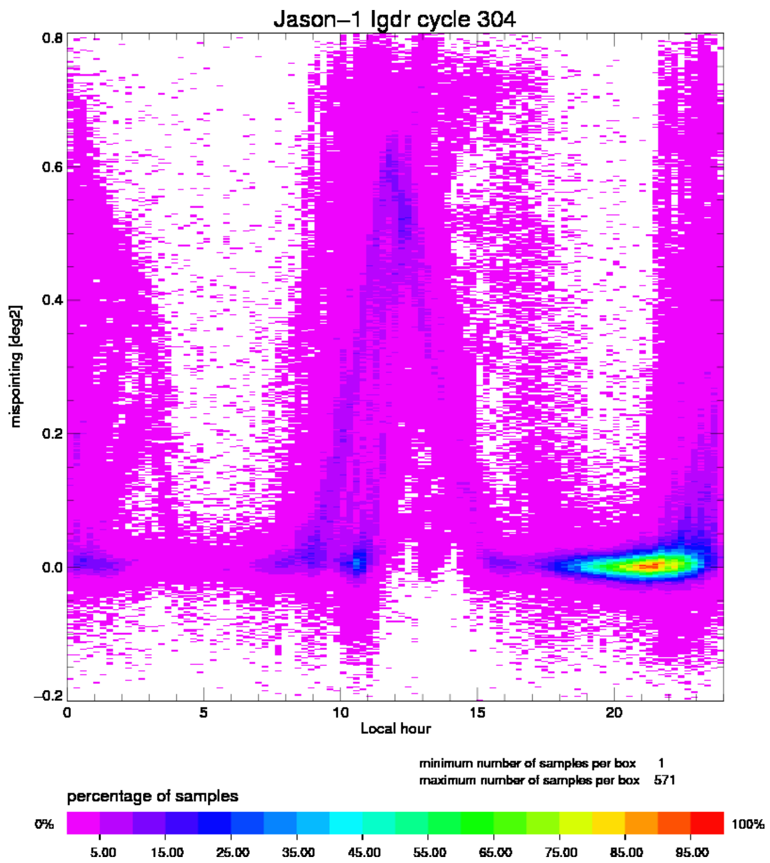

Figure 71: *Dispersion diagram between local hours and mispointing values for Jason-1 cycle 304.*

When looking at a particular pass (124), one observe, that:

- Over land (till 12h15), number of elementary range measurements and mispointing is disturbed.
- Over ocean (between approximatively 12h15 and 12h31), number of elementary range measurements is close to 20 (highest possible value) and apparent squared mispointing increases rapidely from about 0 deg2 to 0.6 deg2.

- For mispointing values higher than 0.64 deg2 (threshold for validation), data are edited. Furthermore number of elementary range measurements decreases rapidely.
- From about 12h36, mispointing values are at default value (as well as other altimeter parameters, such as range, significant wave height, backscattering coefficient), whereas number of elementary range stay at zero till 12h44. These measurements are therefore edited by the several threshold criteria.
- From 12h44 onwards, till almost the end of the pass, measurements are missing.

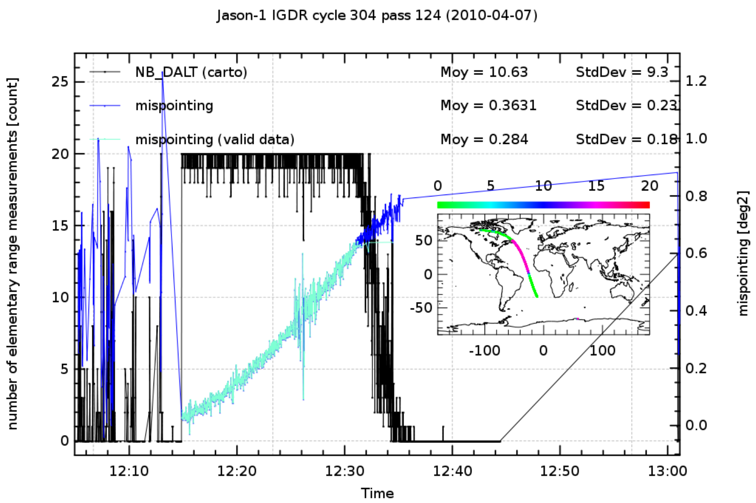

Figure 72: *Apparent squared mispointing (blue) and number of elementary Ku-band range measurements (black) for pass 124, cycle 304.*

As pass 124, many other passes of cycle 304 were impacted by high off-nadir angles. Indeed percentage of missing and edited measurements is high for this cycle, as shown on figure 73.

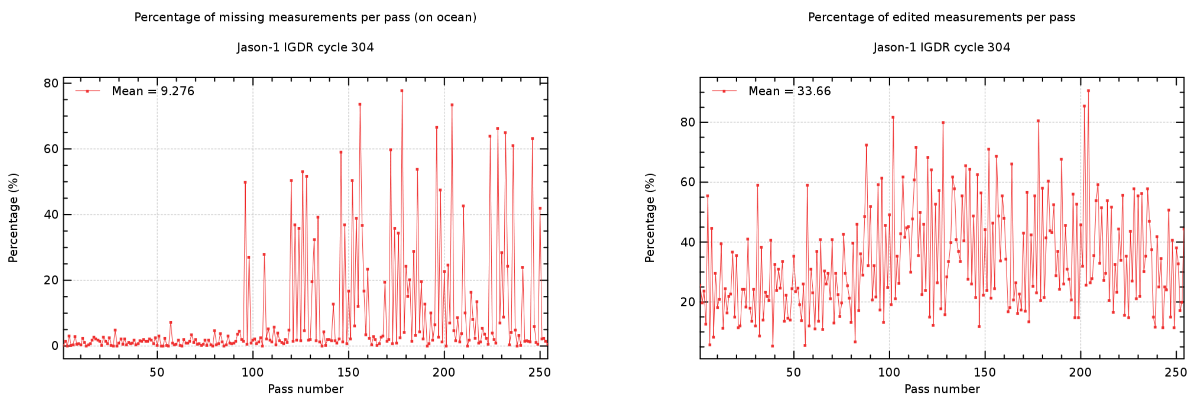

Figure 73: *Pass by pass montitoring of missing ocean measurements (left) and edited measurements (right) for Jason-1 cycle 304.*

8.4.2. Fuel depletion maneuvers

In order to reduce the risk of an explosion in the event of any type of collision, the fuel tank of Jason-1 was partially depleted. Between 10 to 12 out of plane maneuvers were planified to burn about half of remaining propellant (about 11 kg). The out of plan maneuvers began on the 20th of July around 19:00 UTC (start of cycle 315) and ended on 28th of July. The impact on the orbit inclination was 0.04° max, this changes slightly the ground track. Each maneuver consisted of 2 propulsions. One day, this modified the orbit inclination by about 0.04°, the next day the maneuvers put the orbit back to nominal inclination. During the first days of August, several OCM2 maneuvers were necessary in order to put the satellite back in its station keeping box. Finally, only 6 inclination maneuvers took place, as a problem was detected on thrust number 4.

8.4.2.1. Cross-track distance

Cross-track distance was monitored over the period of maneuvers, showing important variations to be linked with different maneuvers (figure 74). Departure up to 7 km were observed in the firsts maneuvers period. Finally cross-track distance came back to its nominal value (less than 1 km). As far as altimetry processing are concerned, the risk associated to this configuration is a degradation of the SLA from a subpar cross-track geoid gradient correction (or CTGG, see Dorandeu et al, 2003 [35]) or inadequate mean profile (time reference used for the computation of Sea Level Anomalies).

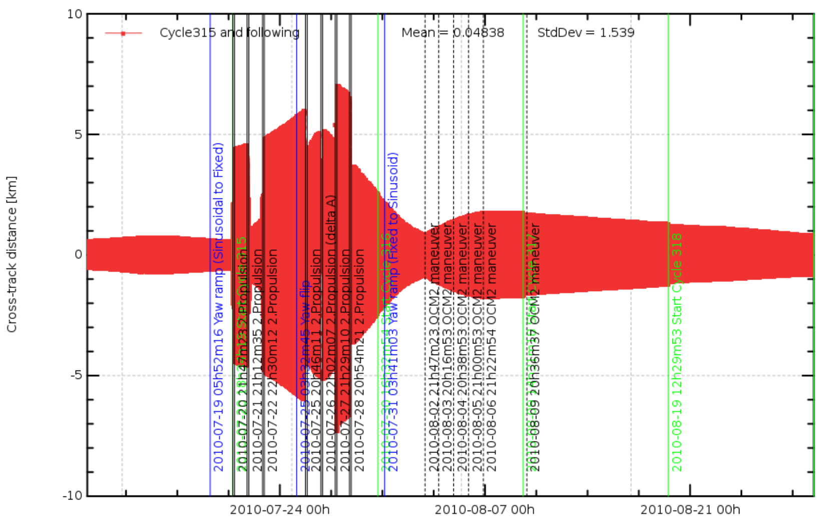

Figure 74: *Monitoring of cross-track distance from nominal ground-track for cycles 314 to 318.*

8.4.2.2. Data quality during cycle 315

During the first couples of out of plan maneuvers there were no missing measurements. But following Yaw flip maneuver, mispointing increased and several data gaps appeared, which coincide with maneuver periods (see left side of figure 75). Data during maneuver periods are edited, as orbit quality is degraded (see right side of figure 75). Following Yaw flip maneuver, number of

edited measurements increases as mispointing is very high and altimeter parameters are often at default values.
In the light of the many out of plan maneuvers (which are difficult to take into account for precise orbite computation), note that the POE for cycle 315 was not recomputed, but is an assembled MOE. Performances of SSH differences at cross-over points are therefore not as good as usual (see also figure 32).

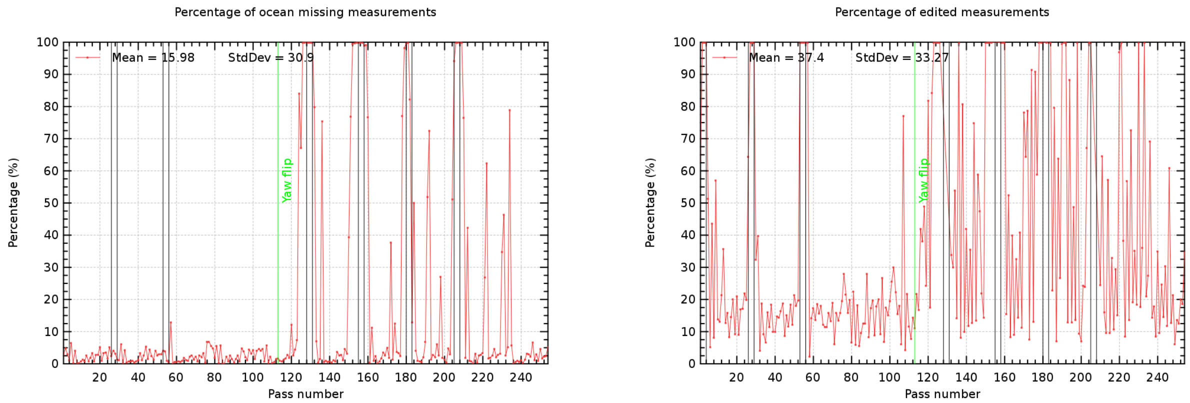

Figure 75: *Pass by pass montitoring of missing ocean measurements (left) and edited measurements (right) for Jason-1 cycle 315. Orbit maneuvers are indicated by black lines. Yaw maneuver is indicated by green line.*

9. Conclusion

Almost nine years of Jason-1 data are now available. Since the beginning of the Jason-1 mission and until the end of the T/P mission in October 2005, T/P and Jason-1 overflew the ocean over 2 parallel passes except the 21 first cycles, when they were on the same pass. Thanks to this long flight configuration, performances comparisons between both missions have been performed with success during 4 years, proving that the major objective of the Jason-1 mission to continue the T/P high precision has been reached.
The good quality of Jason-1 data has been shown in this report : the main altimeter parameters are stable and have the same behaviours as T/P ones, the crossover and along-track performances remain very good. Since mid-2008 Jason-1 flies in tandem with Jason-2. After the flight formation phase with Jason-2, Jason-1 was moved in February 2009 on its interleaved orbit. This is the same ground track as Topex/Poseidon during its tandem phase with Jason-1, but there is a time shift of 5 days. Cross-over and along-track performances remain good.

During 2010, the Jason-1 satellite experienced several events, which had an impact on its data availability. Indeed, due to poor star tracker performances related to beta angle values and also poor gyro wheel performances, Jason-1 experienced several periods of high off-nadir angles of the platform, especially when the satellite was in fix mode. This led several times to important data gaps. In spite of the pointing problems, Jason-1 continued to gather valuable data. Furthermore, end of July, several inclination maneuvers were performed in order to deplete fuel. This had an impact on data quality, but also on data availability, as star tracker performances were poor. Nevertheless a swap of gyro instrument as well as upload of tables to star trackers, improved the off-nadir angles. End of 2010, off-nadir angles were on an usual level again.

Jason-1 data were used to improve understanding of the 59-day signal visible on the MSL of TOPEX and Jason satellites. Furthermore, wind speed evolution over ocean and the comparisons between the ITRF2005 and 2008 solutions for Jason-1&2 data were studied. Also, climatic phenomena like El Niño and El Niña can be observed with Jason-1.
These studies will be continued in 2011.

Finally, since Jason-1 has be moved to an interleaved orbit with Jason-2, it continues to gather valuable altimeter data. Comparisons between both missions are consistent, which is a good indicator of the performance of both satellites.

10. References

References

[1] Abdalla, S., P. A.E.M. Janssen, and J.-R. Bidlot, 2010: Jason-2 OGDR Wind and Wave Products: Monitoring, Validation and Assimilation. *Mar. Geod.*, **33 (S1), 239-255.**

[2] Ablain, M., J. Dorandeu, Y. Faugère, F. Mertz, B. Soussi, F. Mercier, P. Vincent, and N. Picot. 2003a. SSALTO/CALVAL Jason-1 data quality assessment and Jason-1 / TOPEX cross-calibration using GDRs. *Paper presented at the Jason-1 and TOPEX/Poseidon Science Working Team Meeting, Arles (France), November.*

[3] Ablain, M., J. Dorandeu, Y. Faugere, F. Mertz, 2004. Jason-1 Validation and Cross-calibration activities Contract No 731/CNES/00/8435/00. Available at: http://www.jason.oceanobs.com/documents/calval/validation_report/j1/annual_report_j1_2004.pdf

[4] Ablain, M. and J. Dorandeu, 2005. TOPEX/Poseidon validation activities, 13 years of T/P data (GDR-Ms), Available at: http://www.jason.oceanobs.com/documents/calval/validation_report/tp/annual_report_tp_2005.pdf

[5] Ablain, M., S. Philipps, P. Thibaut, J. Dorandeu, and N. Picot 2009. Jason-1 GDR Quality Assessment Report. Cycle 273. SALP-RP-P2-EX-21072-CLS273,. http://www.jason.oceanobs.com/fileadmin/documents/calval/validation_report/J1/Bilan_Calval_J1_Cycle_273.pdf

[6] Ablain, M., S. Philipps, S. Labroue, J. Dorandeu, and N. Picot, 2007. SSALTO CALVAL Consistency assessment between Jason-1 and TOPEX. poster presented at OSTST meeting, Hobart, Australia, 12-15 march 2007. Available at: http://www.jason.oceanobs.com/documents/swt/posters2007/ablain_J1TP.pdf

[7] Ablain, M., S. Philipps, J. Dorandeu, and N. Picot, 2007. SSALTO CALVAL Performance assessment Jason-1 data. Poster presented at OSTST meeting, Hobart, Australia, 12-15 march 2007. Available at: http://www.aviso.oceanobs.com/fileadmin/documents/OSTST/2007/ablain_J1.pdf

[8] Ablain, M., S. Philipps, N. Picot, and E. Bronner (2010). Jason-2 Global Statistical Assessment and Cross-Calibration with Jason-1. *Marine Geodesy*, **33(S1), 162-185**. Available at http://pdfserve.informaworld.com/807580__925506316.pdf

[9] Ablain, M., S. Philipps, L. Carrere, G. Valladeau, J.-F. Legeais, E. Bronner, and N. Picot, 2010. Analysis of 58.74-day signal observed on the MSL derived from Jason-1&2 and TOPEX data. Oral presentation at OSTST meeting, Lisbon, Portugal, 18-20 October 2010. Available at: http://www.aviso.oceanobs.com/fileadmin/documents/OSTST/2010/oral/20_Wednesday/morning/Ablain.pdf

[10] Ablain, M., M. Urvoy, N. Tran, E. Bronner, and N. Picot, 2010. Analysis of wind speed evolution over ocean derived from altimeter missions and models. Oral presentation at OSTST meeting, Lisbon, Portugal, 18-20 October 2010. Available at: http://www.aviso.oceanobs.com/fileadmin/documents/OSTST/2010/oral/19_Tuesday/Tuesday_afternoon/ABLAIN.pdf

[11] Ablain, M., G. Valladeau, S. Philipps, P. Thibaut, and N. Picot 2010. Jason-1 GDR Quality Assessment Report. Cycle 324. SALP-RP-P2-EX-21072-CLS324,. http://www.jason.oceanobs.com/fileadmin/documents/calval/validation_report/J1/Bilan_Calval_J1_Cycle_324.pdf

[12] Ablain, M., S. Philipps, J. Dorandeu, P. Thibaut and N. Picot, 2006. SSALTO CALVAL Performance assessment Jason-1 GDR 'B'/ GDR 'A'. Poster presented at OSTST meeting, Venice, Italy, 16-18 march 2006. Available at: http://www.aviso.oceanobs.com/fileadmin/documents/OSTST/2006/ablain1.pdf

[13] Amarouche, L., P. Thibaut, O.Z. Zanife, P. Vincent, and N. Steunou. 2004. Improving the Jason-1 Ground Retracking to Better Account or Attitude Effects. *Mar. Geod.***27 (1-2): 171-197.**

[14] Arnault, S., N. Chouaib, D. Diverres, S. Jaquin, and O. Coze, 2004. Comparison of TOPEX/Poseidon and JASON Altimetry with ARAMIS In Situ Observations in the Tropical Atlantic Ocean. *Mar. Geod.***27 (1-2): 15-30.**

[15] Boy, François and Jean-Damien Desjonqueres. 2010. Note technique datation de linstant de reflexion des échos altimètres pour POSEIDON2 et POSEIDON3 *Reference: TP3-JPOS3-NT-1616-CNES*

[16] Brown G.S., "The average impulse response of a rough surface and its application", IEEE Transactions on Antenna and Propagation, Vol. AP 25, N1, pp. 67-74, Jan. 1977.

[17] Brown, S., S. Desai, W. Lu, and A. Sibthorpe. 2009. Performance Assessment of the Advanced Microwave Radiometer after 1 Year in Orbit. *Oral presentation at OSTST meeting, Seattle, USA*. Available at: http://www.aviso.oceanobs.com/fileadmin/documents/OSTST/2009/oral/Brown.pdf

[18] Callahan, Phil. electronic communication (retrk-gdr-data-rec-r10.062.pdf) send to OSTST on 13 February 2006.

[19] Carayon, G., N. Steunou, J. L. Courrière, and P. Thibaut. 2003. Poseidon 2 radar altimeter design and results of in flight performances. *Mar. Geod.***26(3-4): 159-165.**

[20] Carrère, L., and F. Lyard, Modeling the barotropic response of the global ocean to atmospheric wind and pressure forcing - comparisons with observations. 2003. Geophys. Res. Lett., 30(6), 1275, doi:10.1029/2002GL016473.

[21] Chambers, D. P., S. A. Hayes, J. C. Ries, and T. J. Urban. 2003. New TOPEX sea state bias models and their effect on global mean sea level. J. Geophys. Res. 108(C10): 3305.

[22] Chambers, D., P., J. Ries, T. Urban, and S. Hayes. 2002. Results of global intercomparison between TOPEX and Jason measurements and models. Paper presented at the Jason-1 and TOPEX/Poseidon Science Working Team Meeting, Biarritz (France), 10-12 June.

[23] Chambers, D. P. and B. D. Tapley, 1998: Reduction of Geoid Gradient Error in Ocean Variability from Satellite Altimetry. *Mar. Geod.***, 21, 25-39.**

[24] Choy, K, J. C. Ries, and B. D Tapley, 2004. Jason-1 Precision Orbit Determination by Combining SLR and DORIS with GPS Tracking Data. *Mar. Geod.***27(1-2): 319-331.**

[25] Commien, L., 2009. Différences entre l'orbite des GDR-C et GDR-B Jason-1, NT08.338

[26] Commien, L., S. Philipps, M. Ablain, and N. Picot, 2008. SSALTO CALVAL Performance assessment Jason-1 GDR "C" / GDR "B". Poster presented at OSTST meeting, Nice, France, 09-12 November 2008. Available at: http://www.aviso.oceanobs.com/fileadmin/documents/OSTST/2008/commien.pdf

[27] Commien, L. and S. Philipps, 2009 : Reprocessing of Jason-1 GDR-C, SALP-RP-MA-EA-21731-CLS

[28] Couhert, A., L. Cerri, F. Mercier, S. Houry. 2010. Status of Jason-1 and Jason-2 GDR orbits. *Talk presented at OSTST meeting, Lisbon, Portugal.* Available at: http://www.aviso.oceanobs.com/fileadmin/documents/OSTST/2010/oral/couhert.pdf

[29] Desai, S. D., and B. J. Haines, 2004. Monitoring Measurements from the Jason-1 Microwave Radiometer and Independent Validation with GPS. *Mar. Geod.***27(1-2): 221-240.**

[30] Dibarbour, G., Bruit Jason et Analyse spectrale, March 2001, CLS.ED/NT

[31] Dorandeu, J., M. H. De Launay, F. Mertz and J. Stum, 2001. AVISO/CALVAL yearly report. 8 years of TOPEX/Poseidon data (M-GDRs).

[32] Dorandeu, J. and P.Y. Le Traon, 1999: Effects of Global Atmospheric Pressure Variations on Mean Sea Level Changes from TOPEX/Poseidon. *J. Atmos. Technol.,***16, 1279-1283.**

[33] Dorandeu, J, M. Ablain, Y. Faugere, B. Soussi, and J. Stum. 2002a. Global statistical assessment of Jason-1 data and Jason-1/TOPEX/Poseiodn Cross-calibration. Paper presented at the Jason-1 and TOPEX/Poseidon Science Working Team Meeting, Biarritz (France), **10-12 June.**

[34] Dorandeu, J., P. Thibaut, O. Z. Zanife, Y. Faugère, G. Dibarboure, N. Steunou, and P. Vincent. 2002b. Poseidon-1, Poseidon-2 and TOPEX noise analysis. Paper presented at the Jason-1 and TOPEX/Poseidon Science Working Team Meeting, New-Orleans (USA), **October.**

[35] Dorandeu., J., M. Ablain, P. Y. Le Traon, 2003a. Reducing Cross-track Geoid Gradient Errors around TOPEX/Poseidon and Jason-1 Nominal Tracks. Application to Calculation of Sea Level Anomalies. *J. Atmos. Oceanic Technol.,***20, 1826-1838.**

[36] Dorandeu, J., Y. Faugère, and F. Mertz. 2003b. ENVISAT data quality: Particular investigations. Proposal for ENVISAT GDR evolutions. Paper presented at the ENVISAT Ra-2 & MWR Quality Working Group meeting. **October.**

[37] Dorandeu.,J., M. Ablain, Y. Faugère, F. Mertz, 2004 : Jason-1 global statistical evaluation and performance assessment. Calibration and cross-calibration results. *Mar. Geod.***This issue.**

[38] Durrant, T.H., J.M. Greenslade, I. Simmonds, 2009 : Validation of Jason-1 and Envisat Remotly Sensed Wave Heights. *JAOT.***26, 123-134.**

[39] Y.Faugere, J.Dorandeu, F.Lefevre, N.Picot and P.Femenias, 2005: Envisat ocean altimetry performance assessment and cross-calibration. Submitted in the special issue of SENSOR 'Satellite Altimetry: New Sensors and New Applications'

[40] Y.Faugere and J.Dorandeu, 2004: Nouvel algorithme de détection des glaces de mer pour Jason-1. SALP-PR-MA-EA-21235-CLS.

[41] Faugere Y., Estimation du bruit de mesure sur jason-1, December 2002, CLS.ED/NT.

[42] Y.Faugere, N.Granier, and A.Ollivier, 2007: Envisat validation activities. 2007 yearly report, Available at: http://www.jason.oceanobs.com/documents/calval/validation_report/en/annual_report_en_2007.pdf

[43] Förste, C., F. Flechtner, R. Schmidt, U. Meyer, R. Stubenvoll, F. Barthelmes, R. König, K.-H. Neumayer, M. Rothacher, C. Reigber, R. Biancale, S. Bruinsma, J.-M. Lemoine, and J.C. Raimondo. A New Heigh Resolution Global Gravity Field Model Derived From Combination of GRACE and CHAMP Mission and Altimetry/ Gravimetry Surface Gravity Data. *Poster presented at EGU General Assembly 2005, Vienna, Austria, 24-29 April 2005.*

[44] Fu, L. L., 2002. Minutes of the Joint Jason-1 and TOPEX/Poseidon Science Working Team Meeting, Oct. 21-23, JPL Tech. Report. JPL D-25506, edited by L. Fu, USA.

[45] Gaspar, P., S. Labroue, F. Ogor, G. Lafitte, L. Marchal and M. Rafanel, 2002: Improving non parametric estimates of the sea state bias in radar altimeter measurements of sea level. *J. Atmos. Oceanic Technol.,***19, 1690-1707.**

[46] Haines, B., Y. Bar-Sever, W. Bertiger, S. Desai, P. Willis, 2004: One-Centimeter Orbit Determination for Jason-1: New GPS-Based Strategies. *Mar. Geod.***27(1-2): 299-318.**

[47] Hamming, R. W., 1977. Digital Filter. Prentice-Hall Signal Processing Series, edited by A. V. Oppenheim Prentice-Hall, Englewood Cliffs, N. J.

[48] Hernandez, F. and P. Schaeffer, 2000: Altimetric Mean Sea Surfaces and Gravity Anomaly maps inter-comparisons AVI-NT-011-5242-CLS, 48 pp. CLS Ramonville St Agne.

[49] Hirose N., Fukumori I., Zlotnicki V., Ponte R. M. 2001: High-frequency barotropic response to atmospheric disturbances: sensitivity to forcing, topography, and friction, J. Geophys. Res. 106(C12), 30987-30996.

[50] Keihm, S. J., V. Zlotnicki, and C. S. Ruf. 2000. TOPEX Microwave Radiometer performance evaluation, 1992-1998, *IEEE Trans. Geosci. Rem. Sens.,***38(3): 1379-1386.**

[51] Labroue, S. and P. Gaspar, 2002: Comparison of non parametric estimates of the TOPEX A, TOPEX B and JASON 1 sea state bias. Paper presented at the Jason 1 and TOPEX/Poseidon SWT meeting, New-Orleans, 21-12 October.

[52] Labroue, S. P. Gaspar, J. Dorandeu, O.Z. Zanifé, P. Vincent, and D. Choquet. 2004. Non Parametric Estimates of the Sea State Bias for Jason 1 Radar Altimeter. *Mar. Geod.***This issue.**

[53] Labroue, S., Ph. Gaspar, J. Dorandeu, O.Z. Zanife. Latest Results on Jason-1 Sea State Bias with the Non-Parametric Technique. *Talk presented at OSTST meeting, Venice, Italy, 16-18 March 2006.*

[54] Legeais, J.F. and L. Carrère, July 2008, Complément de validation de la DAC_HR par rapport à la DAC , en zone côtière, Technical Note CLS.DOS/08.189.

[55] Legeais, J.F. and M. Ablain. Validation of altimetric data by comparison with in-situ T/S Argo profiles for TOPEX/Poseidon, Jason-1, Envisat and Jason-2. SALP-NT-MA-P2-21799-CLS, CLS.DOS/NT/10-308.

[56] Legeais, J.F. 2010. On the stability of the altimetric wet tropospheric correction. CLS.DOS/NT/11-033.

[57] Lemoine, F. G., S. B. Luthcke, N. P. Zelinsky, D. S. Chinn, T. A. Williams, C. M. Cox, and B. D. Beckley. 2003. An Evaluation of Recent gravity Models Wrt to Altimeter Satellite Missions.*Paper presented at the Jason-1 and TOPEX/Poseidon Science Working Team Meeting,***Arles (France), November.**

[58] Le Traon, P.-Y., J. Stum, J. Dorandeu, P. Gaspar, and P. Vincent, 1994: Global statistical analysis of TOPEX and POSEIDON data. *J. Geophys. Res.,***99, 24619-24631.**

[59] Le Traon, P. Y., and G. Dibarboure, 2004. An Illustration of the Contribution of the TOPEX/Poseidon-Jason-1 Tandem Mission to Mesoscale Variability Studies. *Mar. Geod.***27(1-2) 3-13.**

[60] Luthcke. S. B., N. P. Zelinsky, D. D. Rowlands, F. G. Lemoine, and T. A. Williams. 2003. The 1-Centimeter Orbit: jason-1 Precision Orbit Determination Using GPS, SLR, DORIS, and Altimeter Data. *Mar. Geod.***26(3-4): 399-421.**

[61] Marshall, J. A., N. P. Zelinsky, S. B. Luthcke, K. E., Rachlin, and R. G. Williamson. 1995. The temporal and spatial characterustics of TOPEX/Poseidon radial orbit error. *J. Geophys. Res.* **100(C2):25331-25352.**

[62] Martini A., 2003: Envisat RA-2 Range instrumental correction : USO clock period variation and associated auxiliary file, Technical Note ENVI-GSEG-EOPG-TN-03-0009 Available at http://earth.esa.int/pcs/envisat/ra2/articles/USO_clock_corr_aux_file.pdfhttp://earth.esa.int/pcs/envisat/ra2/auxdata/

[63] Ménard, Y. 2003. Minutes of the Joint TOPEX/Poseidon and Jason-1 Science Working Team Meeting. CNES-SALP-CR-MA-EA-15190-CN.

[64] Obligis, E, N. Tran, and L. Eymard, 2004. An assessment of Jason-1 microwave radiometer measurements and products. *Mar. Geod.***27(1-2) 255-277.**

[65] Obligis, E., L. Eymard, M. Ablain, B. Picard, J.F. Legeais, Y. Faugere and N. Picot, 2010. The wet tropospheric correction for altimetry missions: A mean sea level issue.*Oral presentation at OSTST meeting, Lisbon, Portugal.* Available at http://www.aviso.oceanobs.com/fileadmin/documents/OSTST/2010/oral/19_Tuesday/OBLIGIS.pdf.

[66] Ollivier, A., Y.Faugere and N.Granier, 2008: Envisat validation activities. 2008 yearly report, Available at: http://www.jason.oceanobs.com/documents/calval/validation_report/en/annual_report_en_2008.pdf

[67] Ollivier, A., Y.Faugere and J.Legeais, 2010: Envisat validation activities. 2010 yearly report, Available at: http://www.jason.oceanobs.com/documents/calval/validation_report/en/annual_report_en_2010.pdf

[68] Peltier, 2004, Global Glacial Isostasy And The Surface of The Ice-Age Earth: The ICE-5G (VM2) Model and GRACE. *Annual Review of Earth and Planetary Sciences*, May 2004, **Vol. 32, Pages 111-149**, doi: 10.1146/annurev.earth.32.082503.144359

[69] Picard, B., E. Obligis and S. Philipps, 2008. Monitoring of JMR secondary geophysical products, SALP-NT-MA-EA-21562-CLS.

[70] Phaden Mc.J., April2003 : Evolution of the 2002-03 El Nino, *UCLA Tropical Meteorology and Climate Newsletter,***No57**.

[71] Philipps, S. and M. Ablain,September 2007 : SALP - BC 60453-6-04: Retraitement des GDRs Jason-1 en version 'B' pour les cycles 022 à 127, SALP/BC60453-6-04.

[72] Philipps, S. and M. Ablain : Jason-2 validation and cross calibration activities 2009. SALP-RP-MA-EA-21794-CLS.

[73] Philipps, S. and M. Ablain : Jason-2 validation and cross calibration activities 2010. SALP-RP-MA-EA-21895-CLS.

[74] AVISO and PODAAC User Handbook. IGDR and GDR Jason-1 Products. Edition 4.1, October 2008. SMM-MU-M5-OP-13184-CN (AVISO), JPL D-21352 (PODAAC). Available at http://www.aviso.oceanobs.com/fileadmin/documents/data/tools/hdbk_j1_gdr.pdf.

[75] Provost., C. Arnault, N. Chouaib, A. Kartavtseff, L. Bunge, and E. Sultan, 2004. TOPEX/Poseidon and Jason Equatorial Sea Surface Slope Anomaly in the Atlantic in 2002: Comparison with Wind and Current Measurements at 23W. *Mar. Geod.***27(1-2) 31-45.**

[76] Quartly, G. D., 2004. Sea State and Rain: A Second Take on Dual-Frequency Altimetry. Mar. Geod. 27(1-2) 133-152

[77] Queffeulou, P. 2004. Long Term Validation of Wave Height Measurements from Altimeters. *Mar. Geod.***27:295-510.**

[78] Ray, R. (1999). A Global Ocean Tide Model From TOPEX/Poseidon Altimetry/ GOT99.2 - NASA/TM-1999-209478. Greenbelt, MD, Goddard Space Flight Center/NASA: 58

[79] Ray, R. D., and B. D. Beckley, 2003. Simultaneaous Ocean Wave Measurements by the Jason and Topex Satellites, with Buoy and Model Comparisons *Mar. Geod.***26(3-4): 367-382.**

[80] Ray, R. D. 2003. Benefits of the joint T/P−Jason mission for improving knowledge of coastal tides. Paper presented at the Jason-1 and TOPEX/Poseidon Science Working Team Meeting, Arles (France), November.

[81] Ray, R.D. and R.M. Ponte, Barometric tides from ECMWF operational analyses. *Annales G*, **99, 24995-25008**, 1994.

[82] Ruf C., S. Brown, S. Keihm and A. Kitiyakara, 2002a. JASON Microwave Radiometer: On Orbit Calibration, Validation and Performance, *Paper presented at the Jason-1 and TOPEX/Poseidon Science Working Team Meeting, New-Orleans (USA),***21-23 October.**

[83] Ruf. C. S., 2002b. TMR Drift - Correction to 18 GHz Brightness Temperatures, Revisited. Report to TOPEX Project, June.

[84] Scharroo R., J. L. Lillibridge, and W. H. F. Smith, Cross-Calibration and Long-term Monitoring of the Microwave Radiometers of ERS, TOPEX, GFO, Jason-1, and Envisat, **Marine Geodesy, 27:279-297**, 2004.

[85] Schaeffer, P., A. Ollivier, Y. Faugere, E. Bronner, and N. Picot. The new CNES CLS 2010 Mean Sea Surface. *Oral presentation at OSTST meeting, Lisbon, Portugal, 18-20 october 2010*. Available at http://www.aviso.oceanobs.com/fileadmin/documents/OSTST/2010/oral/19_Tuesday/Schaeffer.pdf.

[86] Tapley, B.D., M.M. Watkins, J.C. Ries, G.W. Davis, R.J. Eanes, S.R. Poole, H.J. Rim, B.E. Schultz, C.K. Shum, R.S. Nerem, F.J. Lerch, J.A. Marshall, S.M. Klosko, N.K. Pavlis, and R.G. Williamson, 1996. The Joint Gravity Model 3. *J. Geophys. Res.***101(B12): 28029-28049.**

[87] Tierney, C., J. Wahr, et al. 2000. Short-period oceanic circulation: implications for satellite altimetry. Geophysical Research Letters 27(9): 1255-1258

[88] Thibaut, P. O.Z. Zanifé, J.P. Dumont, J. Dorandeu, N. Picot, and P. Vincent, 2002. Data editing: The MQE criterion. Paper presented at the Jason-1 and TOPEX/Poseidon Science Working Team Meeting, New-Orleans (USA), 21-23 October.

[89] Thibaut, P. L. Amarouche, O.Z. Zanife, N. Steunou, P. Vincent, and P. Raizonville. 2004. Jason-1 altimeter ground processing look-up tables. *Mar. Geod.***27 (3-4), 409-432.**

[90] Tournadre, J. 2002. Validation of the rain flag. Paper presented at the Jason-1 and TOPEX/Poseidon Science Working Team Meeting, Biarritz (France), 10-12 June.

[91] Tran, N., D. W. Hancock III, G.S. Hayne. 2002. "Assessment of the cycle-per-cycle noise level of the GEOSAT Follow-On, TOPEX and POSEIDON." *J. Atmos. Oceanic Technol.,***19(12): 2095-2117.**

[92] Tran, N. , Labroue, S. , Philipps, S. , Bronner, E. and Picot, N. (2010) Overview and Update of the Sea State Bias Corrections for the Jason-2, Jason-1 and TOPEX Missions, *Marine Geodesy*,**33:1, 348 - 362**. Avialable at http://pdfserve.informaworld.com/804727__925502357.pdf

[93] World Meteorological Organization. 2008. El Nino/ La Nina Update (24 June 2008). Available at http://www.wmo.ch/pages/prog/wcp/wcasp/documents/El_Nino_Jun08_Eng.pdf.

[94] World Meteorological Organization. 2010. El Nino/ La Nina Update (30 March 2010). Available at http://www.wmo.ch/pages/prog/wcp/wcasp/documents/El_Nino_Mar10_Eng.pdf.

[95] World Meteorological Organization. 2010. El Nino/ La Nina Update (30 October 2010). Available at http://www.wmo.ch/pages/prog/wcp/wcasp/documents/El_Nino_Oct10_Eng.pdf.

[96] World Meteorological Organization. 2011. El Nino/ La Nina Update (25 January 2011). Available at http://www.wmo.ch/pages/prog/wcp/wcasp/documents/El-Nino_Jan11_Eng.pdf.

[97] Valladeau, G. and M. Ablain. Validation of altimetric data by comparison with tide gauge measurements for TOPEX/Poseidon, Jason-1, Jason-2 and Envisat. SALP-NT-MA-EA-21922-CLS, CLS.DOS/NT/10-289.

[98] Valladeau, G., S. Philipps and M. Ablain. Jason-1 Validation and cross-calibration activities (Annual report 2009). SALP-RP-MA-EA-21795-CLS, CLS.DOS/NT/10-005.

[99] Valladeau, G., S. Philipps and M. Ablain. Jason-1 validation and cross calibration activities (Annual report 2010). SALP-RP-MA-EA-21903-CLS, CLS.DOS/NT/10-332.

[100] Vincent, P., S. D. Desai, J. Dorandeu, M. Ablain, B. Soussi, P. S. Callahan, and B. J. Haines 2003a. Jason-1 Geophysical Performance Evaluation. *Mar. Geod.***26(3-4): 167-186.**

[101] Vincent, P., S. Desai, J. Dorandeu, M. Ablain, B. Soussi, Y. Faugère, B. Haines, N. Picot, K. Case, A. Badea, 2003b. Summary about Data Production and Quality. Paper presented at the Jason-1 and TOPEX/Poseidon Science Working Team Meeting, Arles (France), November

[102] Vincent, P., J.P. Dumont, N. Steunou, O.Z. Zanife, P. Thibaut, and J. Dorandeu. 2003c. Jason-1 I/GDR science processing: ground retracking improvements. Paper presented at the European Geophysical Society meeting, Nice, April.

[103] Zanife, O. Z., P. Vincent, L. Amarouche, J. P. Dumont, P. Thibaut, and S. Labroue, 2003. Comparison of the Ku-band range noise level and the relative sea-state bias of the Jason-1, TOPEX and Poseidon-1 radar altimeters. *Mar. Geod.***26(3-4): 201-238.**

[104] Zelensky, N.P., B.D. Beckley, F.G. Lemoine, S.M. Klosko, R.D. Ray, S. Holmes, D.D. Rowlands, S.B. Luthcke, D.S. Chinn, O. Bordyugov, 2010. The pussling 59-day altimeter data signal and possible causes. *Oral presentation at OSTST meeting, Lisbon, Portugal, 18-20 october 2010*. Available at http://www.aviso.oceanobs.com/fileadmin/documents/OSTST/2010/oral/20_Wednesday/morning/20_1150_zelensky_aud3.pdf.

11. Annex

11.1. Annex: Poster presented at OSTST meeting in Lisbon on October 2010

Jason-1 data quality assessment and cross-calibration with Jason-2 and TOPEX/Poseidon

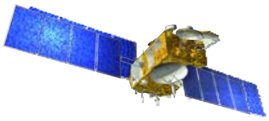

G.Valladeau[1], S.Philipps[1], M.Ablain[1], E.Bronner[2], N.Picot[2]

[1]*CLS, Space Oceanography Division, Toulouse, France*
[2]*CNES, Centre National d'Etudes Spatiales, Toulouse, France*

Overview

This study concerns global data quality assessment of the Jason-1 (JA1) altimetry system, from all GDR products available to date (GDR-C release, homogenous over all the period). This includes careful monitoring of all altimeter and radiometer parameters, performance assessment and geophysical evaluation. We also pay a particular attention to the long-term stability of the Jason-1 MSL, but also the evolution of the performances in relationship with degraded performances of star trackers and gyro wheel occurred in 2010. Moreover, comparisons with Jason-2 (JA2) SLA are performed too.

Note that between January and September 2010, the percentage of missing measurements over ocean grew up several times due to high platform mispointing (cycles 304, 310, 315) leading to altimeter lost of track (and therefore to data gaps).

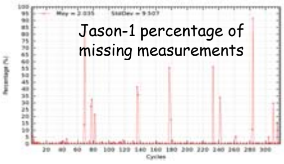

Along Track / Spatial SLA analyses

Monitoring of the Jason-1 square-off nadir

Recently, several degradations of the on-orbit performance of the star trackers and gyro wheel on JA1 has caused large off-nadir angles of the platform (see Figure 1, cycles 304,310,315). This occurs especially, when the satellite is in yaw fix mode and is related to bad beta angle environment. This leads often to edited measurements (mispointing out of thresholds, altimeter parameters at default value) and sometimes to missing measurements (altimeter lost of track).
On 2010-04-14 (cycle305), a gyro swap was performed.

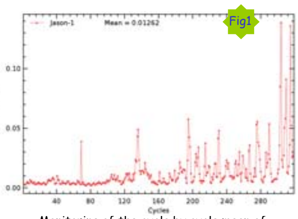

Monitoring of the cycle by cycle mean of square-off nadir on Jason-1

Jason-1 is periodically impacted by high mispointing

Jason-1/Jason-2 SSH performances at crossover

SSH performances are monitored so as to assess the global system performances since the beginning of Jason-1 and now Jason-2 altimeter mission. The GDR versions used are 'C' for Jason-1 and 'T' for Jason-2, which are comparable.
Maps of mean of SSH differences at crossovers show small geographically correlated patterns (see Figure 2). Over Jason-2 period, these structures are the same for Jason-1 and Jason-2 (see Figures 3 and 4): positive in North Atlantic, negative in South Atlantic.

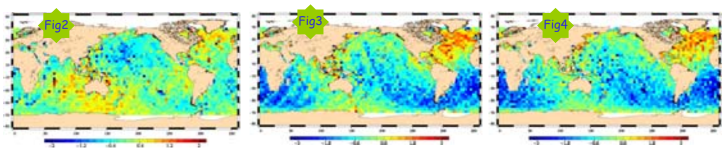

Maps of SSH at crossover. Left: Jason-1 over whole mission. Middle: Jason-1 over Jason-2 period. Right: Jason-2

The cyclic monitoring of mean of SSH differences at crossovers shows a small drift (see Figure 5), which causes discrepencies in MSL trend when seperating ascending and descending passes. During JA2 period, both satellites show similar results, though JA1 is less impacted by 120 days signals. Nevertheless, this signal is strongly reduced for JA2, when using other orbit solution (see poster « **Orbit quality assessment through SSH calculation** », S. Philipps).

Concerning the SSH standard deviation at crossover, the cyclic monitoring shows a raise which appears on both Jason-1 and Jason-2 at the beginning of 2010, around cycle 300 (see Figure 6). The high value (> 6 cm) of cycle 315, is related to fuel depletion maneuvers, as due to the numerous maneuvers, orbit is an assembled MOE, instead of POE.

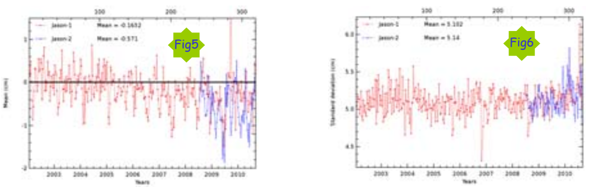

Cyclic SSH crossover differences monitoring of Jason-1 and Jason-2. Left: mean. Right: standard deviation. The following selections are used: |latitude|< 50°, Bathymetrie < -1000 m, low ocean variability (< 20 cm)

SSH performances at crossovers are good

Jason-1 Fuel depletion Maneuvers

In order to reduce the risk of an explosion in the event of anytype of collision, several inclination maneuvers were performed to deplete partially the fuel tank. They impacted most of cycle 315 (starting on 2010-07-20). In consequence, JA1 ground track departed up to +/- 7 km from its nominal ground track (see Figure 7). In the following cycles it comes gradually back to the +/- 1km.

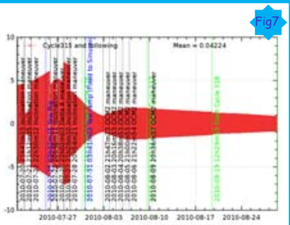

Jason-1 cross-track distance (km)

Cycle 315 should be used with caution

Conclusion

Despite the degraded performances of star trackers and the maneuvers linked to Jason-1 fuel depletion this year, results are reliable and display a good consistency with Jason-2. The long-term stability of the Jason-1 MSL is still relevant. However, recent studies on wet troposphere or wind speed corrections underline the current need to go on assessing precise altimeter and radiometer corrections in order to improve the accuracy of the estimate of the sea surface elevation and thus enhance the delivered scientific products.

References:

- Ablain, M., Cazenave, A., Valladeau, G., and Guinehut, S.: **A new assessment of the error budget of global mean sea level rate estimated by satellite altimetry over 1993-2008**, Ocean Sci., 5, 193-201, doi:10.5194/os-5-193-2009, 2009
- Philipps, S.: **Orbit quality assessment through SSH calculation**, OSTST Poster

Mean Sea Level

Global and local Mean Sea Level

Permanent monitoring of quality during the missions and studies of the necessary corrections of altimetry data regularly add to our understanding and knowledge.
With the TOPEX/Poseidon, Jason-1 and Jason-2 satellite altimetry missions, the global mean sea level (GMSL) has been calculated on a continual basis since January 1993, which results in a 3.26 mm/year global trend (see Figures 8 and 9, GIA applied).
Verification phases, during which the satellites follow each other in close succession help to link up these different missions by precisely determining any bias between them.
For further informations, please refer to the AVISO website:
http://www.aviso.oceanobs.com/en/news/ocean-indicators/mean-sea-level

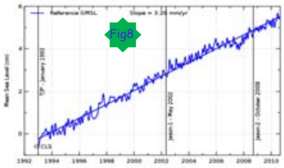

Altimetric global mean sea level 1993-2010 (TOPEX/Poseidon, Jason-1 and Jason-2)

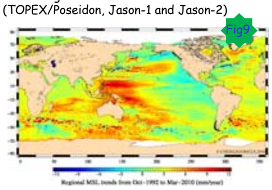

58.74-day signal on Jason-1 MSL

A 58.74 day signal is observed on MSL derived from Jason-1/Jason-2 and TOPEX data. Using GOT ocean tide models, this signal is more important for Jason-1 than TOPEX. Analysis by M. Ablain (see talk « **MSL investigations: 59-day signal differences between Jason-1&2 and TOPEX** », M. Ablain) indicates, that amplitude is dependant on tide model: using FES2004, amplitude of 58.74 day signal is higher for TOPEX than for Jason-1.

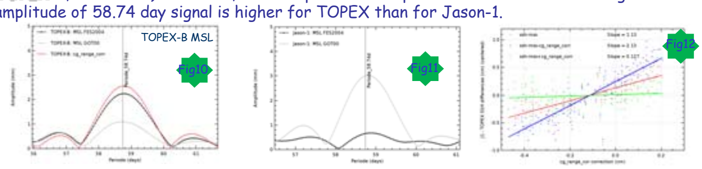

Amplitude of 58.47-day signal for MSL of TOPEX (left) and Jason-1 (middle) for different ocean tide models.
Right: Mean of cyclic J1 – TOPEX SLA differences as function of mean of TOPEX cg_range_corr. Cg_range_corr is either applied (with different signs) to TOPEX SLA or not.

It has been demonstrated that GOT models absorbed TOPEX semi-diurnal signal errors, which are therefore redistributed on Jason-1 MSL. This might be linked to the wrong sign of TOPEX mass center correction (CG_RANGE_CORR) in M-GDR products.

Particular investigations

Radiometer Wet Troposphere correction

In order to provide the best SSH assessment and thus accurately estimate climate change, altimetric and geophysical corrections have to be precisely determined. Hereafter, wet troposphere correction is analysed, as it shows different behaviour between Jason-1 (JMR), Jason-2 (AMR), Envisat (MWR) radiometer data and ECMWF model data.

A strong decrease of ~0.4 cm is observed at the beginning of 2008 with radiometer corrections (see Figures 13 and 14). This evolution could be associated with the 2008 La Nina event. Note that the correction from ECMWF model doesn't show this evolution, which would indicate that the model provides a correction which is not adapted to this period.

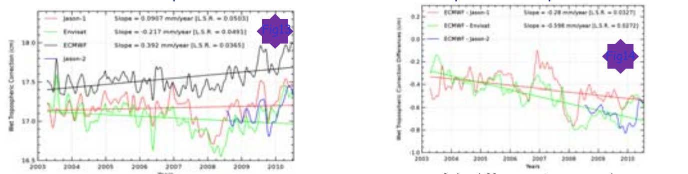

Monitoring of Jason-1, Jason-2, Envisat and ECMWF wet troposphere correction 2004-2010

Monitoring of the differences between radiometer and ECMWF model wet troposphere correction 2004-2010

This difference implies a +/- 0.3 mm/year uncertainty on the estimate of the Mean Sea Level slope. Moreover, this study demonstrates that to date the method is not adapted yet to an accurate assessment of the wet troposphere correction regarding radiometer as well as model corrections (see talk « **Trend and variability of the atmospheric water vapor: a mean sea level issue** », E. Obligis).

Ocean Wind Speed stability over the Jason-1/Envisat time period

Another specific investigation is related to the evolution of the wind speed. Wind speed cross-comparisons (altimeter and models) allows us to detect jumps or drift in altimeter wind speeds and therefore in Sigma0 parameter .
Using reanalysis, a 10 cm.s-1 wind speed jump is detected on Jason-1 in 2005 (see Figure 15) (corresponding to a 0.025 dB Sigma0 jump), which means an increase of 0.6 mm on the Mean Sea Level.

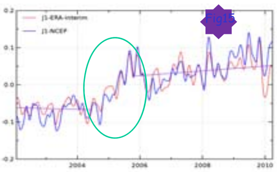

Monitoring of the difference between Jason-1 and wind speed models (ERA interim, NCEP) 1992-2010

Collecte Localisation Satellites
8-10 rue Hermes
31520 Ramonville Saint-Agne - France

OSTST
Lisbon, October 2010